Settlement Data Analysis and Prediction for Kiltunnel

Mei Yang

4813006
Geo-Engineering Section
Delft University of Technology

Settlement Data Analysis and Prediction for Kiltunnel

by

Mei Yang

to obtain the degree of Master of Geo-Engineering
at the Delft University of Technology,
to be defended publicly on Tuesday September 1, 2020 at 10:00 AM.

Student number:	4813006	
Project duration:	July 8, 2019 – Sep 1, 2020	
Thesis committee:	Dr. ir. Wout. Broere,	TU Delft, chairman
	Ir. Richard. Roggeveld,	Sweco , Supervisor
	Dr. ir. Federico. Pisano,	TU Delft , Supervisor
	Ir. Richard. De Nijs,	TU Delft , Supervisor
	Ir. Xuehui Zhang,	TU Delft , Supervisor

This thesis is confidential and cannot be made public until 1 September 2020.

Preface

This Project is the final result of the two-year master's career. In the process of completing it, not only me, but also many people worked to made a lot of effort.

Firstly, I would like to thank my committee chairman, Prof. Wout Broere. In Kiltunnel project, he gave me a lot of suggestions. Every time when I was stuck, he always put forward effective opinions to make me realize, which make a good contribution to the whole project.

Next, the sincere appreciation to Richard Roggeveld (Sweco).As one of my supervisor in company, he is responsible and professional. He is so patient to answer my questions whenever I need help.I am really thankful for his kindness.

Futhermore I extent my thanks to rest of my committee and my colleagues in Sweco.Thanks for their involvement. They gave me a lot of useful advice and offer me inspiration to improve the project.

Last but not least, I would like to thank my family and friends. Their love and support is always my strong backing, and keeps me forward without fear.

Mei Yang
Delft, May 2020

Contents

List of Figures

List of Tables

1 Introduction

1.1. Location

In the sixties of the last century, the need for a bridge or tunnel between Dordrecht and 's-Gravendeel became clear. One reason for this need stems from the closure of Haringvliet, as part of the Delta Works. As a result, the flow speed in the Dordtse Kil increased. On the other hand, due to the industrial development of the Moerdijk Port Authority, sea shipping increased considerably. As a combined result, ferry transport between Dordrecht and 's-Gravendeel became more dangerous than before. A decision to build a tunnel was taken and the Kiltunnel was constructed starting in 1974 and finished in 1977. The amount of vehicles that use the Kiltunnel is approximately 10,000 to 15,000 every day.

The Kiltunnel is located in the south-west part of Dordrecht which forms the connection of Dordrecht and 'S-Gravendeel and serves as a replacement for the ferry at 'S-Gravendeel. The tunnel connects to the A16 motorway in Dordrecht and connected to the provincial road N217 in the Hoeksche Waard. An overview of the tunnel location is shown in figure 1.1.

Figure 1.1: The location of Kiltunnel

The Kiltunnel consists of two traffic pipes with open exits. The cross-section comprises a total of 2x2 lanes for fast traffic and a lane for slow traffic and footpath on each side. The closed section is 405m long which is the combination of two parts: a land section of approximately 35m on two ends and a submerged section of approximately 335m. The submerged part consists of three elements. Each element consists of 5 sections and is 31 meters wide, 8.75 meters high, and 111.5 meters long.

1.2. Research context

Differential settlement is a big issue for an immersed tunnel. This will lead to large stress concentrations in the tunnel construction, giving rise to local cracking, failure of the construction, leakage, deterioration of exposed rebar, etc. Variety factors will influence it, like the consolidation process, the action time of different loads when construction, and the sub-soil condition, etc. To protect the integrity of the structure, settlements should be kept within limits.

Although the immersed tunnels are generally designed to withstand buoyancy by a margin of 4%, the settlements have been observed which severely exceed the predictions in the Kiltunnel. In this case, a complicating factor is a fact that the dikes on both sides have been reconstructed after immersing the elements, but not at the same location as before the immersion trench was dredged. Consolidation (at first) and creep due to this relatively new load on the subsoil can play a role as well. These aspects contribute to the problem of the differential settlements which have resulted in leaking joints and consequently increased maintenance costs. In addition, how and to what extent uneven settlement affects the structural safety of tunnels and their users, and how to reduce the durability of tunnels are unknown. As a result, it is necessary for us to do research about the settlement in Kiltunnel.

1.3. Problem

Kiltunnel consists of three elements. There are six monitoring points per element. The numbering of these points is indicated in figure 1.2. The measurement on this figure is for northern monitoring points, the point code is an odd number between 1 and 48, and the southern points should be the even number between 1 and 48. The first immersed element is TE-1 that was immersed in 18-10-1976. The second one is TE-3 on 16-11-1976, and the last is TE-2 on 6-12-1976.

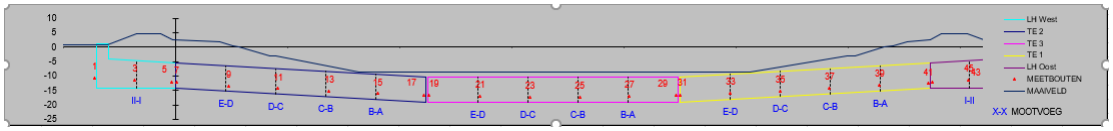

Figure 1.2: Monitoring points in Kiltunnel

The tunnel settlements have been monitored from July 1977 until now, According to the construction records and monitoring data documentary, the trend is shown in figure 1.3. The Kiltunnel experiences much large settlements than initially expected, especially in the eastern and western parts. One part of the research is to find the cause of this phenomenon. From figure 1.3, it is clearly indicated that the biggest settlement is in point 12, and big settlement difference between point 10 and point 12. Thus, why the biggest happens in point 12 and why the settlement is so big to become the problem.

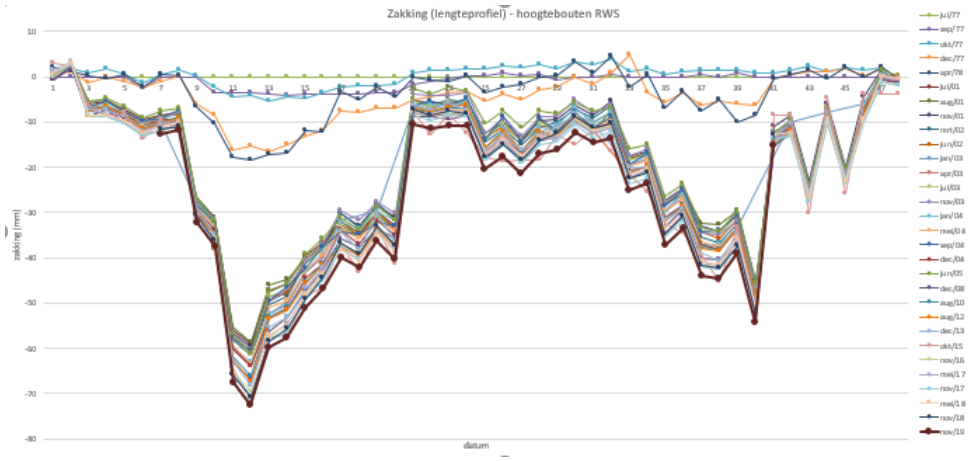

Figure 1.3: Longitudinal settlement of Kiltunnel from July 1977

In addition, there was a serious leakage that consists of sand and water inflow in 2001, and the leak point is in an expansion joint which is south part of element 2c-2d which corresponds to point 12 in the tunnel. The

details of the expansion joint are shown in Figures 1.4 and 1.5. There are two pump basements in the third tunnel element, each with its drain. The leak on the 'S-Gravendeelse entrance side gave a water inflow of 1.5 litters / sec and a sand quantity of approximately 10 liters per week. The leakage in 2001 is shown in figure 1.6. And the same leakage point in December 2019 is shown in figure 1.7. Why leakage happens and whether leakage influence the settlement are the other two questions.

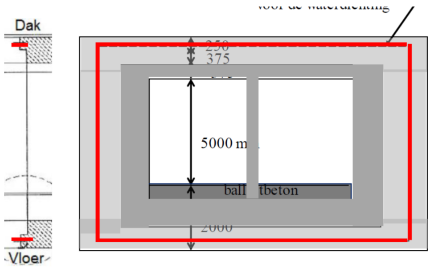

Figure 1.4: Expansion joint of tunnel elements

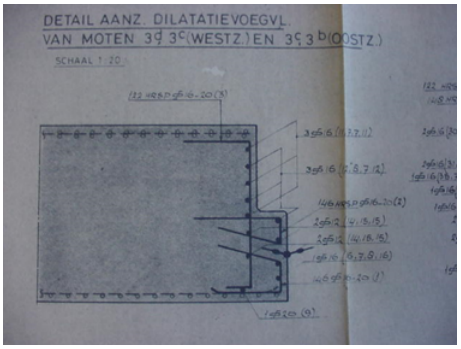

Figure 1.5: Detail of expansion joint

Figure 1.6: leaky joint with crack situation in 2001

Figure 1.7: leaky joint situation in December 2019

1.4. Objectives

The goal of this project is mainly composed of four parts:

1. Correlate numerical predictions with observed settlement data
2. Model the settlement behavior of Kiltunnel
3. Predict future expected settlements and analyze the impact on the tunnel structure
4. Compare the usefulness and accuracy of different settlement monitoring methods used at Kiltunnel

In this project, the CPT profile is important for in-situ data interpretation. The finite element method will also come to in theoretical part, finite element software can be used like PLAXIS, DianaFEM, D-Settlement. Except for the CPT profile and finite element software, the monitoring system is crucial as well. In Kiltunnel, there are several methods to combine the total monitoring system, for instance, manual measurement, inspection damage, and pilot of the OSMOS system are all applied. As a result, the real settlement data can be available. From a data perspective, the deriving trend by doing regression analysis with Python is also feasible. The expression given by python can calculate the estimated value of settlement at various time points.

Besides the data analysis, settlement prediction is an important part as well. In order to derive this aspect, the usual methods are numerical simulation and layerwise summation, numerical simulation is applied in this project, the time span for prediction is 50 year, the settlement tendency will be given. Furthermore, the result comparison in different method could be an aspect, different method might have the different emphasis, so it could be interesting to do some comparison.

1.5. Structure of investigation

In order to develop a calculation method for the issue, there must be sufficient insight into the physical processes to be presented. In the present case, it is about geology and soil condition which influence the consolidation process, causing settlement of the tunnel.

Consolidation describes the process by which a soil mass decreases in volume in response to either natural or human-made loadings. Natural loadings that induce consolidation result from geological processes such as sedimentation. In the project, there are two human-made loadings, one is for the relocation of levees that locates on the two sides of the Oude Mass river, the other is for an inflow of water and sand from outside to the inside of the tunnel. The loadings result in water dissipation and pressure variation that lead to groundwater flow and different water pressure around the tunnel. These behaviors greatly depend on soil distribution and soil properties under the tunnel.

Except for loadings, the consolidation process is also affected by time. However, it is possible to achieve this in PLAXIS 2D, as long as change the calculation mode to consolidation and define the consolidation period. In PLAXIS 2D, the time-settlement plot gives an indication to the relationship between time and corresponding settlement, which is helpful to realize what happened at a specific time.

However, CPT is a method to get in-situ properties of soil. In this case, CPT data is used as there is a lack of site investigation for a detailed numerical model. CPT based correlation methods will be used to derive soil properties. Some parameter will contribute to the sensitivity of settlement. Given the relative uncertainty as a sensitivity analysis will be performed. It is essential to understand which parameter will influence the most. One function in PLAXIS 2D makes this feasible, it allows several parameters combinations to do sensitivity analysis at the same time. Under these comparisons, it is easy to observe which one is predominant.

While researching the finite element model, there will also be some reminders from the data obtained by instrument detection. Data regression analysis is a common way to deal with a series of data. Importing data to python and using Linear regression model or logarithm regression model, not only the previous data will show, but also the settlement trend through the entire life cycle. The other potential problem is that the first measurement of settlement started seven months after the tunnel tubes were completely immersed. Data regression will help to backtrack the settlement which starts from the complete immersion. Then, comparing the results of these two methods. If there are similar, it proves that numerical simulation is suitable. Otherwise, the model needs to be improved.

The future trend is the last part that needs to pay attention to. Prediction can also be realized in PLAXIS 2D with a longitudinal direction. Once the settlement is too large, repair measures need to be taken immediately to reduce it. Normally, the consolidation process will never finish, the 99% consolidation is always a standard to achieve, but it is still time-consuming.

1.6. Reading guide

Chapter 2 contains a literature study that will be involved in this project. In chapter 3, the CPT profile and borehole which measured before the construction period are shown, besides, the soil properties are derived through the combination of table 2b of NEN9997 and Robertson's method. In Chapter 4, two assumptions for the engineering problems are proposed and some manual calculations are made for consolidation settlement. Chapter 5 and 6 contain 2 models of different directions. Chapter 5 looked into the transverse model with PLAXIS 2D, it contains the PLAXIS result analysis and the settlement prediction in next 50 years, it comes to the verification of two assumptions mentioned in chapter 4 as well. Chapter 5 also contains the monitoring data analysis with the python regression model. Chapter 6 describes the longitudinal model with PLAXIS 2D, it includes that the basic PLAXIS result and analysis for each construction stage, as well as the settlement prediction in the next 50 years. Chapter 7 concludes with the conclusions and the recommendations from this report.

2

Literature Review

2.1. Immersed tunnel

2.1.1. History

Grantz mentioned that the first immersed tunnel was built in United States in Boston in 1893 (Grantz and C, 2001). It was a sewer siphon, constructed from brick and concrete. It was 100 m long and 2.7 m in diameter. Wooden bulkheads were installed at the end of each tunnel element. After this first sewer siphon, other immersed sewer tunnels were built and the construction technique was further developed. In 1910, the first immersed rail tunnel in Detroit was built. It comprised of twin watertight steel tubes placed in a dredged trench and then surrounded by concrete. Other steel tube tunnels were built in the years that followed. In 1927 the first rectangular concrete tunnel was built.

In the thirties of last century, the first immersed tunnel in the Netherlands was designed: The Maas tunnel in Rotterdam. It was the first tunnel for road transport in the Netherlands that passed a main waterway and was constructed with the technique of prefabricated concrete elements that were constructed on a different site, towed to the tunnel location and immersed in an excavated trench in the riverbed. The construction started in the late thirties of last century and finished during the 2nd World war. The tunnel opened on 14 February 1942.

Later on in economic more prosperous times a number of other immersed tunnels followed:

1.The Coentunnel, under the North Sea canal in Amsterdam (1966)

2.The Benelux tunnel under the New Waterway in Rotterdam (1967)

3.The IJtunnel under the river IJ in Amsterdam (1968)

4.The Heinenoord tunnel under the Oude Maas (1969)

5.The Vlake tunnel in South Beveland (1975)

After 1975 every other year or two, another immersed tunnel was opened in the Netherland, until the first bored tunnel was constructed between 1996 and 1999.

2.1.2. Structure

Tunnel and bridges are the most common two ways for transportation construction method. Tunnels can be divided into immersed tunnel and bored tunnel. Figure 2.1 shows a comparison between the three types, with the immsersed tunnel lying at the bottom of the river bed. An immersed tunnel is a kind of tunnel where a trench will dug in advance at the bottom of the water, then a suitable length of tunnel section constructed a special location on the land is floated to the immersion site, sequentially immersed into the trench and connected, and then the trench is backfilled, covering the tunnel. Besides, immersed tunnel consists of prefabricated tunnel elements, the prefabricated elements will be constructed in the dock firstly and then transported to the immersion location.

Immersed tunnels are generally made up of tunnel sections connected by permanent joints. According to the different configurations of different types of joints, it can be divided into (Tang et al., 2002):

1.Flexible joints: mainly are composed by end steel shell, Gina water-stop, Omega water-stop, connection of pre-stressed steel cables, etc.

2.Semi-rigid and semi-flexible joints: main are composed by end steel shell, Gina water-stop, Omega water-stop, corrugated steel plate connector, horizontal shear key and vertical shear key, etc.

3.Semi-rigid joints, and rigid joints: mainly are composed by end steel shell, Gina water-stop, connecting steel plate, joint concrete, etc.

4.Rigid joint: is formed by pouring concrete underwater, and the joint stiffness is basically the same as the body of the immersed tube

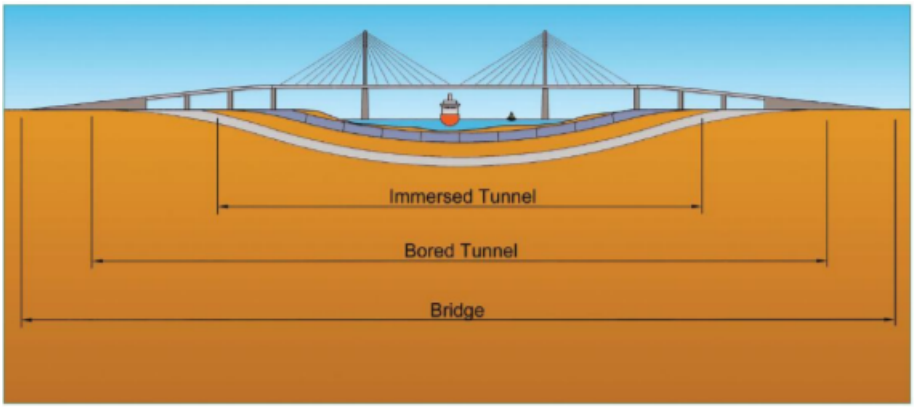

Figure 2.1: Comparison between three methods to cross waterway

Tunnel elements consists of segments with rigid joints between them. However, the connection between the elements is flexible joint (see figure 2.2). The most critical part in element joints are Gina and Omega (see figure 2.3 and 2.4). The connection process is shown in Figure 2.5.

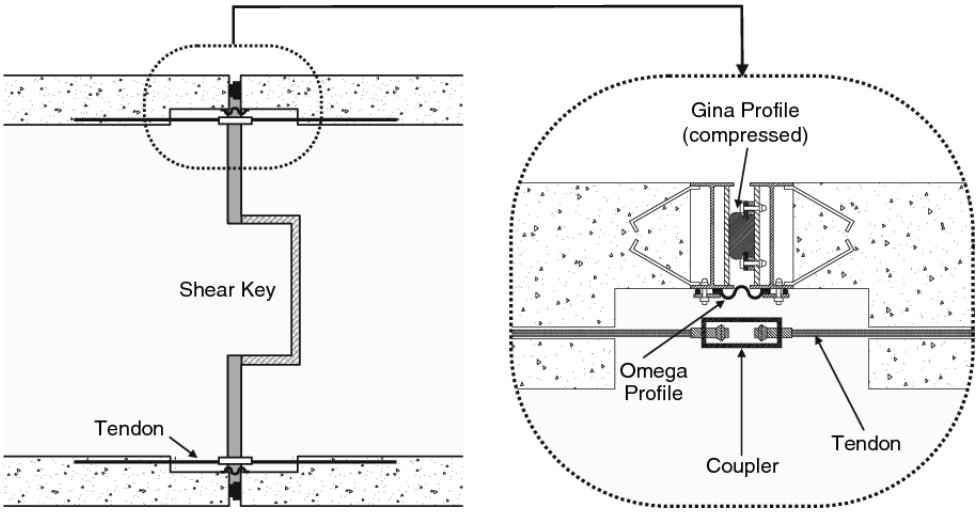

Figure 2.2: Flexible joint composition

For an immersed tunnel, the following construction phases can be roughly distinguished, figure 2.6 gives an overview (Grantz and C, 2001):

1. Construction of the access roads and the approach structure.
2. Construction of the tunnel elements in a dry dock, casting factory or ship yard.
3. Dredging the trench.
4. Floating the elements to the final location.
5. Immersing and linking the tunnel elements.
6. Under filling the tunnel element with sand (If a sand bed foundation is chosen) and backfilling the trench.
7. Finishing work such as walls, road furnishing, installing of the tunnel's technical installations.

2.1.3. Advantage and disadvantage of immersed tunnel

Compared to bored tunnel and bridge, immersed tunnel has the following advantages:

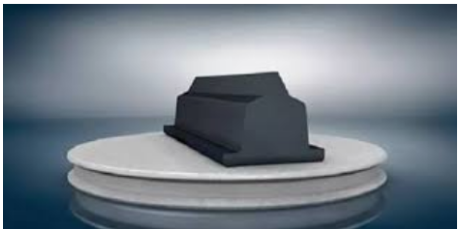

Figure 2.3: Gina Gasket

Figure 2.4: Omega Seal

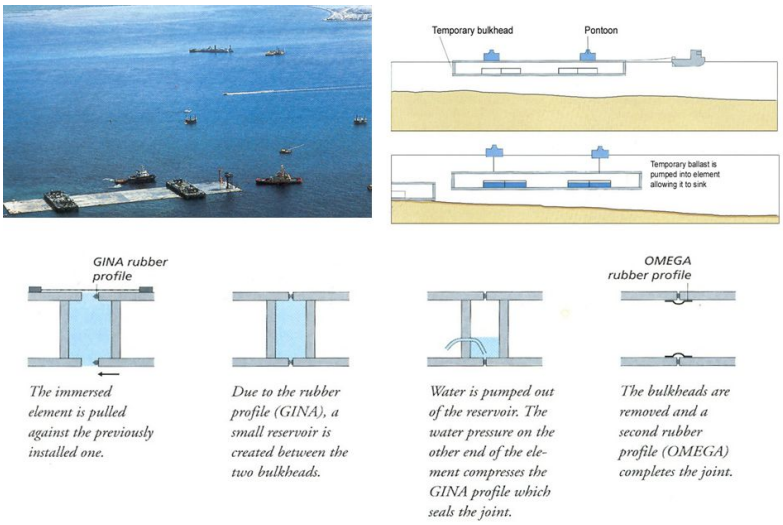

Figure 2.5: Joint connection process between elements

1. Strong adaptability to geology and hydrology: Due to the shallow excavation in the foundation trench, the construction technique of excavation and foundation treatment is relatively simple. Due to the buoyancy of the immersed elements, the load on the foundation is small. Because the pipe section adopts the construction process of prefabrication and then floating and sinking, which avoids difficult underwater operations, it can be constructed in deep water, and has strong adaptability to tidal range and water velocity.

2. Shallow burial can be easily connected with the roads on both sides of the strait: Compared with shield tunnels with large burial depth, the pavement elevation of the immersed tube tunnel can be raised, and it is easy to connect with the onshore road tunnel

3. Good waterproof performance: each prefabricated pipe section is very long, generally about 100m, and the ring width of the precast segment of the shield tunnel is only 1m, so the number of joints in the immersed tunnel is small.

4. The construction period of the immersed tube tunnel is short: due to the long length of each prefabricated tube section, an immersed tube tunnel can be completed with only a few precast tube sections. Excavation of the precast tube section and the foundation trench can be performed simultaneously, and the precast tube section is not at the tunnel site. Short interference time

5. Low cost of immersed tube tunnel: less earthwork excavation for underground trenches, lower unit price than underground excavation, compared with the prefabrication of the pipe section and the shield, the required cost is lower.

6. Good construction conditions: In the construction of immersed tube tunnels, most of the main processes such as prefabrication and floatation and sinking of pipe sections are performed on water, and there are very few underwater operations. Except for a few divers, workers are working on water without the need for Work under pressure.

7. Immersed elements can be made into large sections and multiple lanes: a tunnel cross section can accommodate 4 to 8 lanes at the same time. The structure size is not limited. Shields are limited in size and

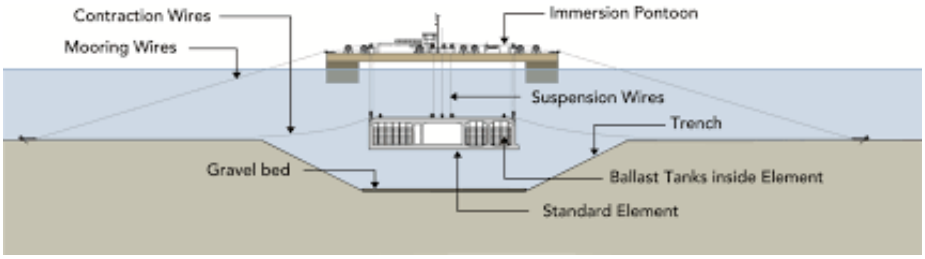

Figure 2.6: Immersion process

generally have only two lanes.

However, immersed tunnels also have the following disadvantages: The construction site needed is larger, which can interference with navigation, and construction is greatly affected by natural conditions such as weather and hydrology(Liu, 2017).

2.2. Settlement of immersed tunnel

There are a number of factors that cause settlement of immersed tunnel over time, including loads and operation etc.

2.2.1. Loads

The loads acting on the tunnel can be divided into construcion loads and dynamic loads(Gang et al., 2012).

Construction loads is the additional load. Weight of construction appliances, grouting load and etc all belong to construction load. Foundation layer is the predominant factor to effect settlement during the construction. As a result, compressibility of the foundation layer will be very different when the foundation treatment change. Siltation is also an important factor to influence settlement in construction phase. This is especially troublesome in the case of tunnel elements supported on jacks prior to installing a jetted sand or sand flow foundation where the interface becomes inaccessible. Oversiltation will cause immersion to be unsafe and inaccurate. Besides, original soil and the foundation will be disturbed by cyclic silting and dredging.

Dynamic loading includes tidal action, earthquake loading, vehicle and pedestrians load etc. Tidal action leads to cyclic behaviour of the soil which cause original soil fluctuate and produce settlement, especially in weak layers like silt or clay layer. If the sand-flow foundation is not compacted enough, sand will suffer scour. Under certain circumstances, large amplitude tidal variation or wave action may cause settlement of sands caused by their gradual compaction due to daily oscillations in pore pressure. If covered by a clay layer that slows the relief of pore pressures, the upper layers of sand may cause oscillation of the supporting ground(Grantz and C, 2001). Earthquake loading is not usual but can result in great harm. Shock and vibration may cause liquefication of the sand flow foundation. For sand, it is easier to liquefied and the substantial settlememt happens. However, liquefication will cause pore water pressure increase and accelerate consolidation settlement in soft soils. Vehicle and pedestrian load are the most common form for load. Overload vehicle is the main problem to cause settlement. For example: due to overload vehicle, the Tingstad tunnel in Gothenburg Sweden which constructed in 1968 suffered a largest settlement 50 mm.

2.2.2. Recompressive deformation of foundation soil

Immersed tunnels are usually put at the bottom of the riverbed. In this way, for the soil layer at the bottom of the tunnel, a self-weight load of an overlying soil layer of about 10 m was applied to these soil layers before the tunnel construction. Due to the excavation of the trench, the soil layer at this location was unloaded which will cause rebound deformation. After the tunnel section was immersed, the tunnel section and the overburden load caused the natural foundation soil layer to be compressed again and lead to recompression deformation. Therefore, the deformation of the natural foundation soil layer is a process of unloading and rebounding, and then compression deformation.

2.2.3. Compression Deformation of Tunnel foundation Layer

The important feature of the immersed tube tunnel is its light weight and strong adaptability to various geological conditions. In this way, the foundation treatment of the immersed tunnel is not to solve the prob-

lems of the strength and deformation of the foundation soil, but mainly to make the gap between the tunnel and the foundation dense. Foundation treatment of immersed tube tunnels generally includes first laying method, back filling method and pile foundation. The first laying method is to place a sand and gravel cushion in the super-digged base trench before laying the tunnel section, and then flatten it with a scraper, then sink the tunnel section, and fill the pipe section with water or sand to form an overload to make the pad The layers are fully compacted. The latter filling method is to excavate the foundation trench by about lm first, and install a temporary support at the bottom of the trench. After the tunnel element is stabilized on the support, then pass through the sides of the tunnel section or the reserved holes in the element to element backfilling of bottom space. Post-filling methods mainly include sand blasting, sand pressing and grouting. If the foundation soil at the bottom of the tunnel is particularly weak and the bearing capacity is very small, the pile foundation or foundation reinforcement method will also be used.

Regardless of whether it is the first-lay method or the back-fill method, since it is performed underwater, it is not easy to make the gap between the tunnel and the foundation dense. Even for immersed tunnels with pile foundations, due to the compression and deformation of the joints between the pile top and the tunnel pipe section, some settlement will occur after the completion of the immersed tunnel. For example, the Tingstad tunnel in Sweden uses a pile foundation. After the completion of the tunnel, a settlement of 40 mm to 50 mm occurred. In this way, the compression of the foundation layer is also an important part of the settlement of the immersed tube tunnel (Shao and Li, 2005).

2.3. Compression and consolidation of soil

2.3.1. Compression

Compressibility of soil is the property through which particles of soil are brought closer to each other, due to escapage of air and/or water from voids under the effect of an applied pressure. The compressibility of soils under one-dimension compression can be described from the decrease of volume of voids with the increase of the effective stress. The relationship of void ratio and the effective stress can be depicted as semi-log plot (see figure 2.7).

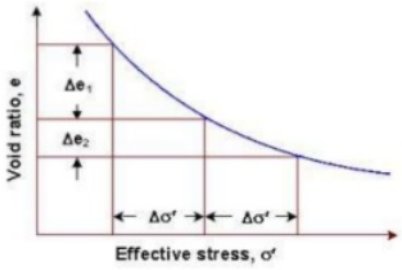

Figure 2.7: The relationship between voids and effective stress

a_v is the coefficient of compressibility which means the rate of change of void ratio (e) with respect to the applied effective pressure (p) during compression.

$$a_v = \Delta e \div \Delta p \tag{2.1}$$

where:
e_0 = initial void ratio
p_0 = initial effective stress
e_1 = final void ratio
p_1 = final effective stress

$$\Delta e = e_1 - e_0$$

$$\Delta p = p_1 - p_0$$

In compression of soil, coefficient of volume compressibility m_v is the volume decrease of a unit volume of soil per unit increase of effective pressure during compression. The relationship between this and effective stress increase and corresponding strain are in equation 2.2. And m_v can be linked with coefficient of

compressibility which shows in equation 2.3.

$$\Delta\varepsilon_v = m_v \times \Delta\sigma_v^{'} \tag{2.2}$$

$$m_v = \left(\frac{1}{(1+e_0)}\right) \times \left(\frac{\Delta e}{\Delta p}\right) = \frac{a_v}{(1+e_0)} \tag{2.3}$$

2.3.2. Consolidation

Consolidation refers to the process in which soft soil is compressed and dehydrated under the action of external forces and gradually becomes dense. Consolidation always induce settlement, consolidation settlement refers to the settlement caused by the deformation of the soil skeleton under the foundation load, and with the dissipation of the excess pore water pressure. The rate of consolidation settlement depends on the rate of pore water discharge.

Some assumptions are made for theory of consolidation, they are:

- Clay is homogeneous, isotropic and saturated.
- The clay layer is laterally confined.
- Consolidation parameters from test applies to clay layer from which sample for test was taken.
- Water and clay particles are incompressible.
- Darcy's law is valid.
- One-dimensional compression, and one-dimensional flow
- Soil properties are constant with time.

For saturated soil, increased vertical stress cause pore pressure to increase immediately. For sand, pore pressure increase dissipates rapidly due to high permeability. However, for clay, pore pressure dissipates slow due to low permeability.

If time is considered,the whole process will be divided into 3 phases:

1. At the time of initial loading (t = 0):

There is no drainage and pore water takes initial change in vertical loading since water is incompressible. And soil skeleton does not take the initial loading. The relationship is showns below (see figure 2.8).

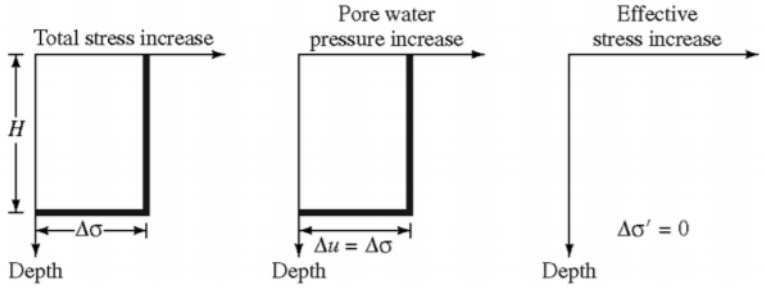

Figure 2.8: relationship in different pressure under t = 0

2. Between t = 0 to t = ∞ :

The water is allowed to drain and excess water pressure decreases due to initial loading dissipates, and soil skeleton takes loading as pore pressure decrease (see figure 2.9).

3. At time t = ∞ :

Excess water pressure decreases until to zero due to the initial loading dissipates, and soil skeleton takes the whole loading. Effective stress increase equals the vertical stress increase (see figure 2.10).

The one-dimensional consolidation testing procedure was first suggested by Terzaghi. This test is performed in a oedometer. The schematic diagram of a oedometer is shown in figure 2.11. Figure 2.12 shows a photograph of an oedometer. The soil specimen is placed inside a metal ring with two porous stones, one at the top of the specimen and another at the bottom. The specimens are usually 64 mm in diameter and 2-5mm thick. The load on the specimen is applied through a lever arm, and compression is measured by a micrometer dial gauge. The specimen is kept underwater during the test. Each load is usually kept for 24 hours. After that, the load is usually doubled, which doubles the pressure on the specimen. And the compression measurement is continued. At the end of the test, the dry weight of the test specimen is determined. Figure 2.13 shows a consolidation test in progress. In 1D consolidation test, there are three stages to show. Stage 1

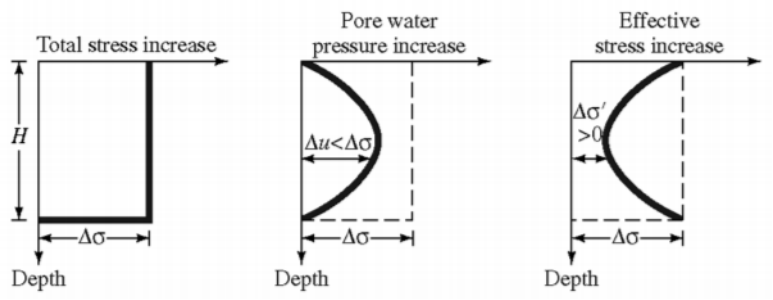

Figure 2.9: relationship in different pressure under t = 0 to t = ∞

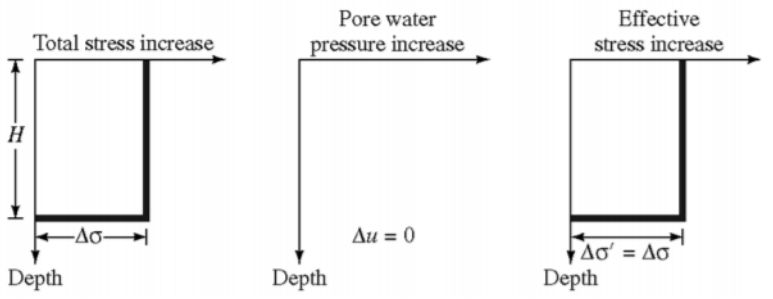

Figure 2.10: relationship in different pressure under t = ∞

is initial compression which primarily caused by pre-loading. Stage 2 is primary consolidation which excess pore water pressure dissipation and corresponding soil volume change. Stage 3 is secondary consolidation which occurs after excess pore water pressure dissipation and due to plastic deformation readjustment of soil particles.

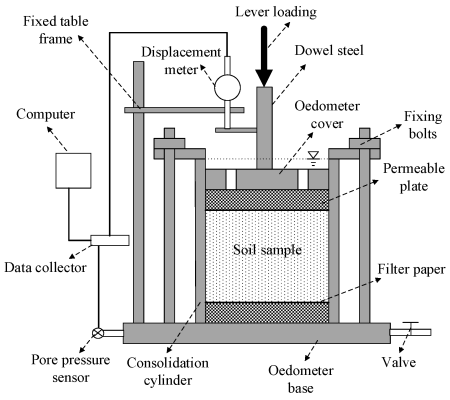

Figure 2.11: oedometer test profile

Figure 2.12: oedometer device details

The clay under consolidation can be divided into two types, they are:

- Normally consolidated clay: clay that has never been loaded in the past by more than the existing effective overburden pressure

$$P_c = P_0$$

- Overconsolidated clay: due to pre-existing structures or erosion of overburden, clay has been loaded by more than the existing effective overburden pressure $P_c > P_0$. Overconsolidation ratio is defined as the ratio of past maximum stress and present existing stress.

$$OCR = \frac{P_c}{P_0} \tag{2.4}$$

However, when the load increases more than once, the curve changes completely. The following plot (figure 2.14) is the curve consists of results of numerous load and unload increments. It is very obvious to observe

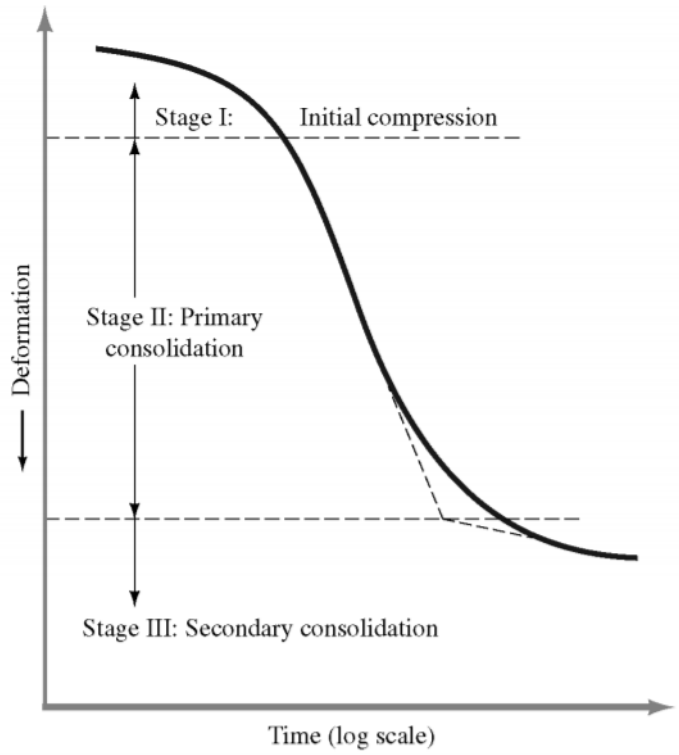

Figure 2.13: 1D consolidation test plot

that there is a unloading-reloading loop between different loading. These loops are commonly explained by the soil viscosity effect. Clayey soils have larger loops because of their relatively higher viscosity, and sandy soils have narrow loops because of their low viscosity, silty soils being in between(Cui et al., 2013).

For normally consolidated clays, compression index Cc can be calculated as follows:

$$C_c = \frac{\Delta e}{\Delta log(p)} \tag{2.5}$$

From e-log(p) curve, the re-compression index (Cr) is the slope of the equivalent linear portion of the unloading/reloading curve.

$$C_r = \frac{\Delta e}{\Delta log(p)} \tag{2.6}$$

The indication for C_c and C_r is on the figure 2.15.

Consolidation settlement of normally consolidated clay layer can be represented in equation 2.7.

$$S = \frac{C_c}{(1+e_0)} \times H \times \log \frac{P_1}{P_0} \tag{2.7}$$

For overconsolidated clay, two possible way will happen:

1. when (P_0 and P_1) < P_c, the plot is shown in figure 2.16. And the settlement is calculated in equation 2.8.

$$S = \frac{C_c}{(1+e_0)} \times H \times \log \frac{P_1}{P_0} \tag{2.8}$$

2. when $P_0 < P_c$ and $P_1 > P_c$, the plot is shown in figure 2.17. And the settlement is calculated in equation 2.9.

$$S = \frac{C_c}{(1+e_0)} \times H \times \log \frac{P_c}{P_0} + \frac{C_c}{(1+e_0)} \times H \times \log \frac{P_1}{P_c} \tag{2.9}$$

Another terms contributes to consolidation process are coefficient of consolidation C_v and time factor T_v

$$C_v = \frac{K}{m_v \gamma_w} \tag{2.10}$$

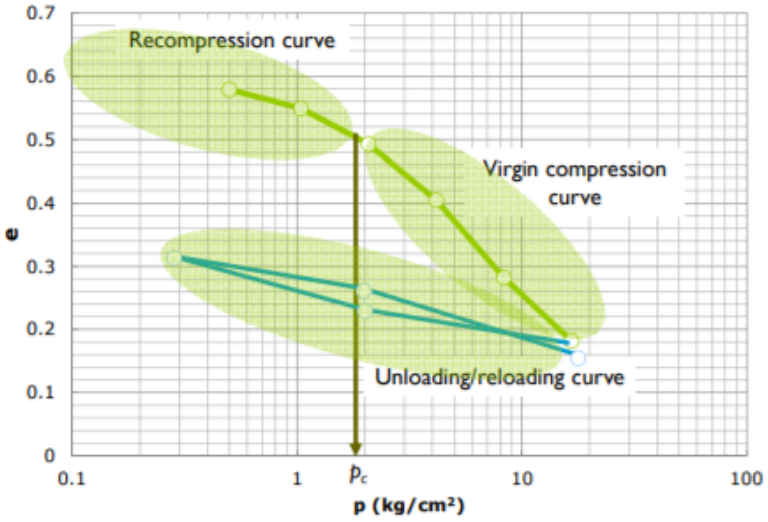

Figure 2.14: unloading-reloading curve

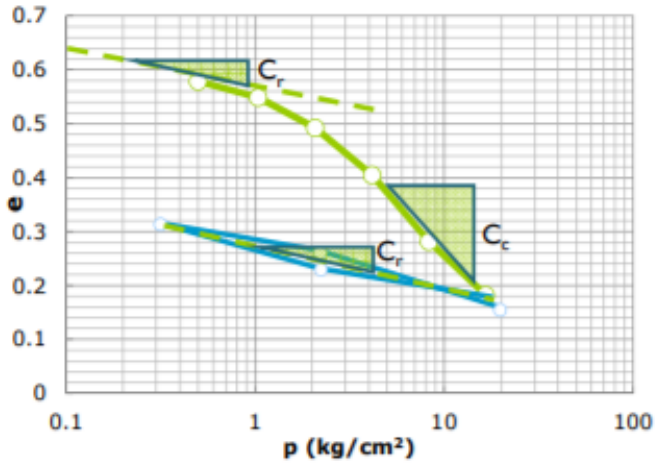

Figure 2.15: Indication of C_c and C_r

$$T_v = \frac{C_v t}{H^2} \tag{2.11}$$

where:

- k = soil permeability
- m_v = coefficient of volume compressibility
- H = longest drainage path within clay layer

According to the above terms, the degree of consolidation will be deducted fro empirical chart (see figure 2.18)

At time t and depth z, the distribution of each stress part is on figure 2.19. Degree of consolidation is expressed as a percentage of the amount of consolidation at a given time within a soil mass to the total amount of consolidation obtainable under a given stress condition. The degree of consolidation at any time (t) is the percentage of settlement that took place at this time with respect to to ultimate consolidation settlement. It is an important parameter to calculate consolidation settlement. The equation is as follows:

$$U_{tz} = \frac{\Delta\sigma'}{\Delta p} = \frac{\Delta p - \Delta u}{\Delta p} = 1 - \frac{\Delta u}{\Delta p} \tag{2.12}$$

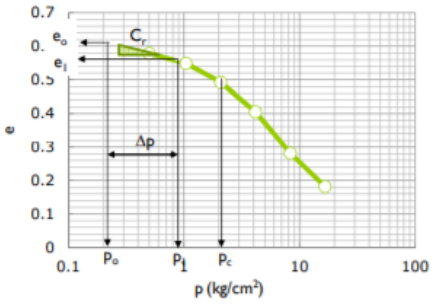

Figure 2.16: distribution when (P_0 and P_1) < P_c

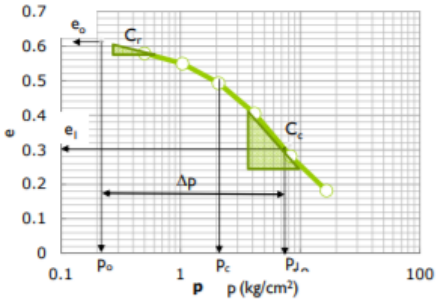

Figure 2.17: distribution when (P_0 < P_c) and P_1 > P_c

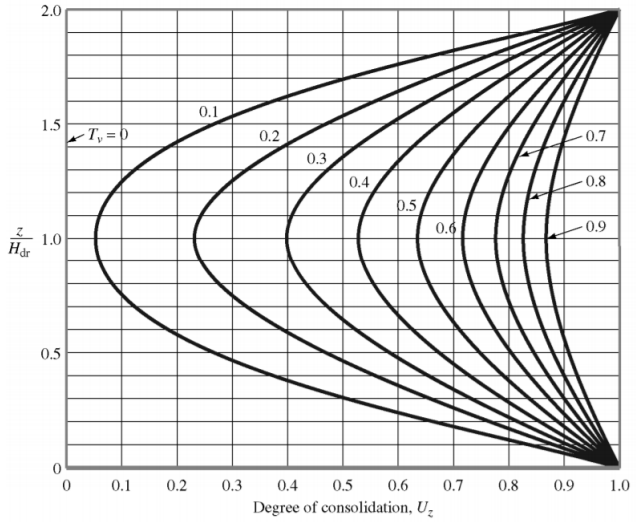

Figure 2.18: time rate of consolidation settlement

Average degree of consolidation (U_t) for the clay layer at time "t":

$$U_t = 2\int_0^H U_{tz}dz \tag{2.13}$$

Settlement of clay layer of thickness 2H at time t = ∞:

$$S_{ultimate} = m_v \Delta p(2H) \tag{2.14}$$

Settlement of clay layer of thickness 2H at time t=t:

$$S_t = m_v \Delta\sigma'(2H) = m_v(\Delta p U_t)(2H) = U_t S_{ultimate} \tag{2.15}$$

Average degree of consolidation (U_t) at time "t":

$$U_t = \frac{S_t}{S_{ultimate}} \tag{2.16}$$

2.4. Finite element model

2.4.1. Failure criteria of soils

Morh-Coulomb failure criteria

The Mohr–Coulomb (MC) failure criterion is a set of linear equations in principal stress space describing the conditions for which an isotropic material will fail, with any effect from the intermediate principal stress $\sigma 2$ being neglected. Because the compression is negative, the normally order for principal stress is that $\sigma 1$ is the

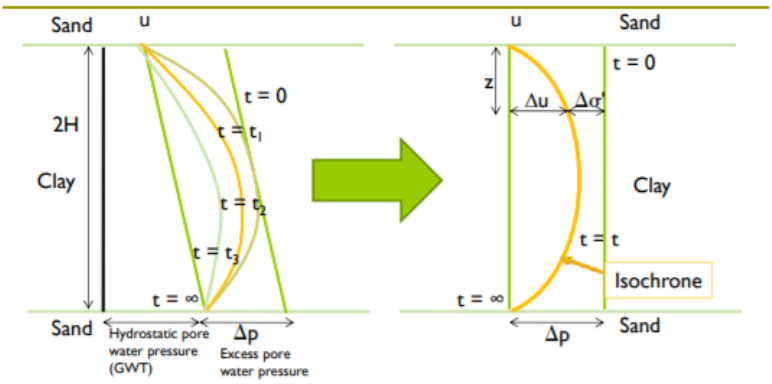

Figure 2.19: stress distribution when t = t at depth z

most negative principal stress and $\sigma 3$ is the least negative principal stress. The formula for Morh-Coulomb criteria can be expressed as follows:

$$t^* \leq c' \cos\phi' - s^* \sin\varphi' \tag{2.17}$$

$$t^* = \frac{1}{2}(\sigma_3' - \sigma_1') \tag{2.18}$$

$$s^* = \frac{1}{2}(\sigma_3' + \sigma_1') \tag{2.19}$$

$$\frac{1}{2}(\sigma_3' - \sigma_1') \leq c' \cos\varphi' - \frac{1}{2}(\sigma_3' + \sigma_1') \sin\phi' \tag{2.20}$$

$$-\sigma_1' \leq \frac{2c' \cos\varphi'}{1-\sin\varphi'} - \frac{1+\sin\varphi'}{1-\sin\varphi'}\sigma_3' \tag{2.21}$$

The Morh-Coulomb criterion can be visualised in different stress diagrams. In addition to the shear-normal stress diagram, the principal stress diagram can be indicated in figure 2.20. The inclination of the failure line which is indicated by parameter b is defined as $\frac{1+\sin\varphi'}{1-\sin\varphi'}$ and the intersection at the σ_1-axis which is indicated by parameter a is $\frac{2c' \cos\varphi'}{1-\sin\varphi'}$. The latter term is the unconfined compressive strength or uniaxial compressive strength. Besides the parameters a and b, the parameters c and d can also be defined, which are the maximum vertical stress and the maximum principal stress difference in a triaxial test, respectively(Brinkgreve, 2018a). And the corresponding expressions are:

$$c_* = a - b\sigma_3' = \frac{2c' \cos\varphi' - \sigma_3'(1+\sin\varphi')}{1-\sin\varphi'} \tag{2.22}$$

$$d = \left|\sigma_1' - \sigma_3'\right|_{max} = \frac{2c' \cos\varphi' - \sigma_{cel} \sin\varphi'}{1-\sin\varphi'} \tag{2.23}$$

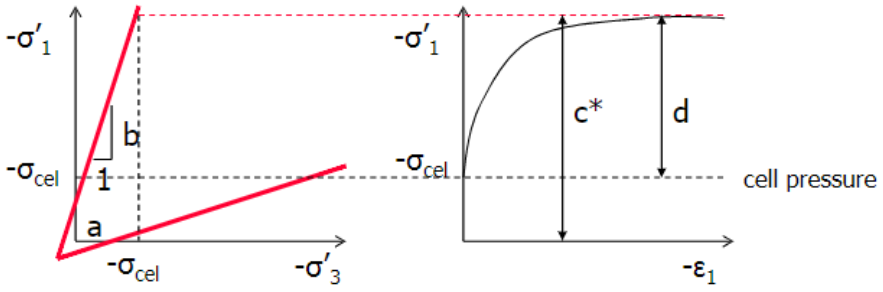

Figure 2.20: Mohr-Coulomb Criterion in a Principal Stress diagram

The Mohr-Coulomb criterion can be formulated for all combinations of principal stresses, which is relevant if the principal stresses are not ordered. This leads to the full Mohr-Coulomb failure contour consisting of six failure surfaces which form a 'hexagonal cone' in the three-dimensional principal stress space (see figure 2.21). Deviator plane is a cross-section which is taken in perpendicular to the isotropic stress axis in principal stress space at a particular value of isotropic stress and look towards the origin (see figure 2.22). The shapes of deviator plane depends on friction angle. For $\varphi = 0$, the contour is a regular hexagonal. There are two types of point on the irregular hexagon:

- Compression point: this is on the sharp corners. These points that are reached when following the stress path in a triaxial compression test.

- Extension point: this is on the 'obtuse' corners. These points that are reached when following the stress path in a triaxial extension test.

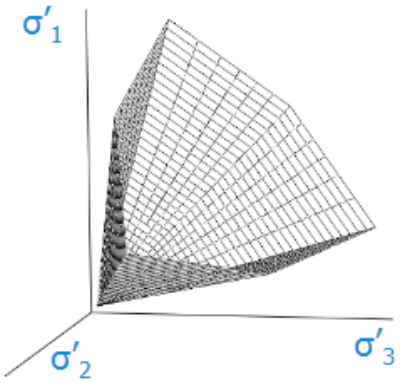

Figure 2.21: /Mohr-Coulomb failure contour

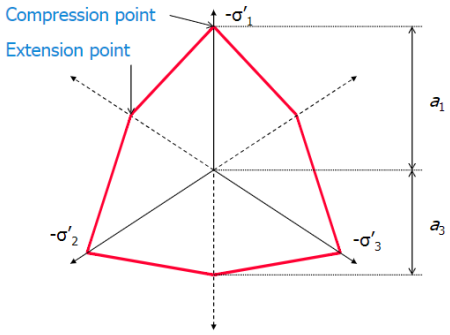

Figure 2.22: Mohr-Coulomb in deviator planne

Tresca criterion

Friction angle decide the shape of deviator plane. For $\varphi = 0$, the contour is a regular hexagonal. This is a special case of Mohr-Coulomb criterion, which is called Tresca Criterion (see figure 2.23). One preferred situation for applying Tresca criterion is to define the strength of clays in terms of undrained shear strength. In this case, cohesion parameter c takes up the role of undrained shear strength s_u. The relationship between principal stress and cohesion is:

$$(\sigma_3^{'} - \sigma_1^{'}) \leq 2c \tag{2.24}$$

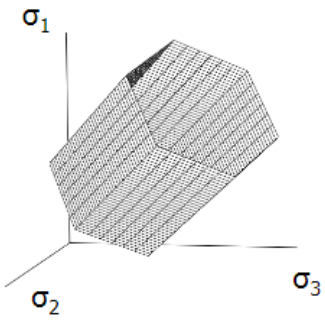

Figure 2.23: Tresca Criterion

Drucker-Prager criterion

Drucker-Prager criterion is derived from Mohr-Coulomb criterion and with shape as a circular cone (see figure 2.25). The criterion can generally be formulated in $q \leq \alpha p + K^*$. Owing to the match for some points between Drucker-Prager criterion and Mohr-Coulomb criterion, the expression of them consists of the following:

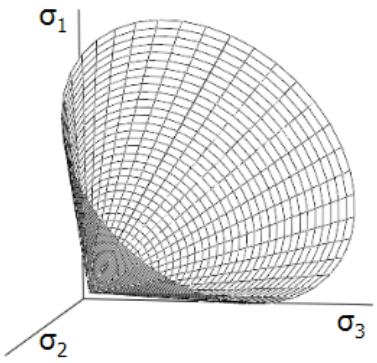

Figure 2.24: Druker-Prager criterion

In compression point:

$$\alpha = \frac{6\sin\varphi'}{3-\sin\varphi'} \tag{2.25}$$

$$K^* = \frac{6c\cos\varphi'}{3-\sin\varphi'} \tag{2.26}$$

In extension point:

$$\alpha = \frac{6\sin\varphi'}{3+\sin\varphi'} \tag{2.27}$$

$$K^* = \frac{6c\cos\varphi'}{3+\sin\varphi'} \tag{2.28}$$

Von Mises criterion
For $\alpha = 0$, Druker-Prager criterion contour becomes a circular tube, and this is the special case for Druker-Prager criterion which is known as the Von Mises criterion (see figure 2.25). However, this failure criterion is not suitable for soil but for steel.

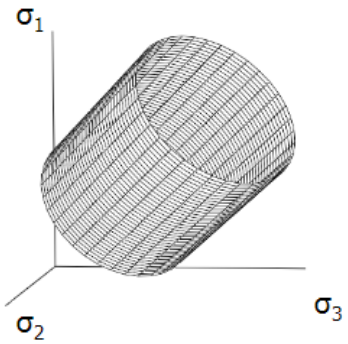

Figure 2.25: Von Mises criterion

Matsuoka-Nakai and Lade criterion
The Matsuoka-Nakai criterion matches Mohr-Coulomb criterion in compression point as well as extension point. Comparing to Mohr-Coulomb criterion, the contour of Matsuoka-Nakai criterion is more smooth and goes outside Mohr-Coulomb in other than compression and extension points. Lade criterion goes a bit outside Mohr-Coulomb in extension points as well if the compression point matches Mohr-Coulomb. The compression in these three criterions are in figure 2.26. Matsuoka-Nakai criterion is considered to be slightly better for shear failure in soils, and Lade is considered to be slightly better for shear failure in sandy types of soil.

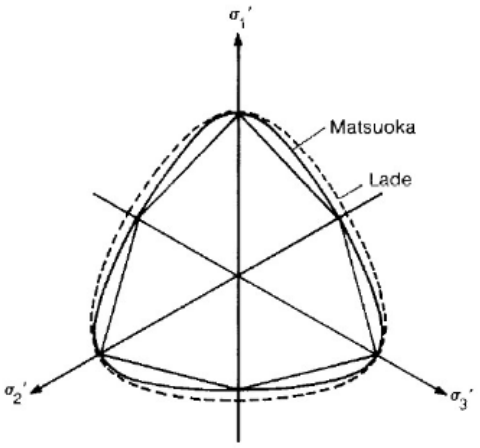

Figure 2.26: Comparison between Mohr-Coulomb , Matsuoka-Nakai and Lade

2.4.2. Plasticity theory

The linear elasticity theory is effective for modelling materials which undergo small deformations and which return to their original configuration upon removal of load. However, almost all real materials will undergo some permanent deformation, which still remains after removal of load. When the stress reaches some critical value, significant permanent deformations will usually occur, this material property is called the yield stress. The basic principle of elastoplastic is that toal strains and strain rate are divided into an elastic component and a plastic component. The classical theory of plasticity is concerned with materials which initially deform elastically, but which deform plastically upon reaching a yield stress. The fundamental calculation method for plastic strain rate is flow rule. The term 'flow' describes that plastic strains are associated with 'flow' of materials. In sands and other granular materials plastic flow is due both to the irreversible rearrangement of individual particles and to the irreversible crushing of individual particles. And the assumptions for plastic theory are (L et al., 1973):

- the response is independent of rate effects
- the material is incompressible in the plastic range
- there is no Bauschinger effect
- the yield stress is independent of hydrostatic pressure
- the material is isotropic

There are four types of simple models which shown in figure 2.27-30. In Linear Elastic-Plastic model both the elastic and plastic curves are assumed linear. In Elastic/Perfectly-Plastic model, work-hardening is neglected and the yield stress is constant after initial yield. The elastic strains can be neglected altogether as in the Rigid/Linear Hardening and Rigid-Perfectly-Plastic model. The Rigid-Perfectly-Plastic model is the crudest of all and hence in many ways the most useful.

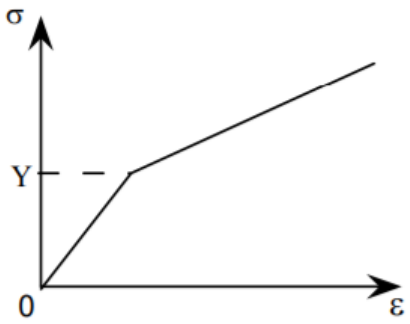

Figure 2.27: /Linear Elastic-Plastic Model

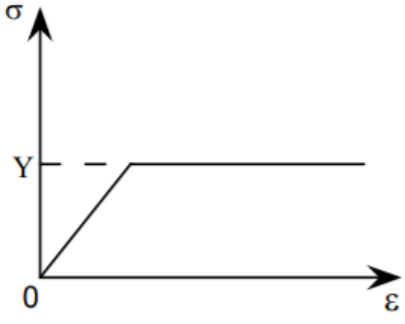

Figure 2.28: Elastic/Perfectly-Plastic Model

The flow rule is defined by the so-called plastic potential function g. The relationships of each part are

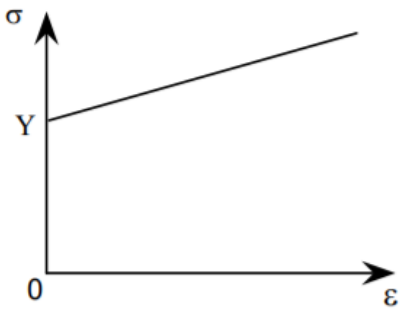

Figure 2.29: /Rigid/Linear Hardening Model

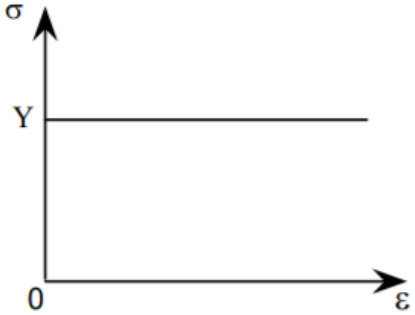

Figure 2.30: Rigid-Perfectly-Plastic Model

indicates below:

$$\epsilon_{ij} = \epsilon^e_{ij} + \epsilon^p_{ij} \qquad \text{(total strain)} \tag{2.29}$$

$$d\epsilon_{ij} = d\epsilon^e_{ij} + d\epsilon^p_{ij} \qquad \text{(strain rates)} \tag{2.30}$$

And for plastic strain rates:

$$d\epsilon^p_{ij} = d\lambda \frac{\partial g}{\partial \sigma'_{ij}} \tag{2.31}$$

Where:

- $d\lambda$ = scalar; magnitude of plastic strains
- $\frac{dg}{d\sigma}$ = vector; direction of plastic strains
- g = plastic potential functions

The determination of occurrence for plasticity is based on yield function. The yield function is a function of the stress state and often indicated by the symbol f. Stress and optionally strain and other parameters are all the components. The expression is $f = f(\sigma', \epsilon)$. Evaluating the function f when some action takes place, the outcome will determine whether or not the plastic strain occur:

- $f \leq 0$, pure elastic behaviour occurs;
- $f = 0$ and $df \leq 0$, the condition becomes unloading from a plastic state, which is also elastic behaviour;
- $f = 0$ and $df = 0$, elastoplastic behaviour occurs.

All stress combinations with $f = 0$ can be regarded as a border in the stress space which is yield contour or yield surface. Yield contour can be visualised in a stress diagram (see figure 2.31). On the yield contour, $f = 0$, within the contour, f is less than 0 and outside the yield contour f would be larger than 0. However, the third situation is impossible, because stress states in this condition do not exist.

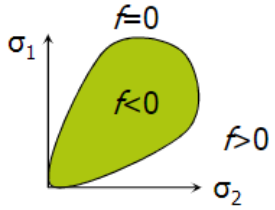

Figure 2.31: yield contour for plasticity

2.4.3. Hardening and softening

When the material yields to a certain degree, the internal structure of the material is readjusted after the crystal position is changed, so that it regains its ability to continue to resist external loads. After continuing to load, the stress-strain curve continues to rise after yielding, indicating that after the material yields, the stress must be increased to match new plastic deformation, which is called hardening. When the stress-strain curve reaches its peak, the load decreases until it breaks. This phenomenon of increasing stress and strain is called softening. The yield function for hardening and softening is not only a function of stress, but also of a state parameter which indicated by the symbol κ. And κ is generally expressed as a function of the plastic strain.

This is the so-called hardening rule or softening rule. Comparing to the yield contour for plasticity, yield contour for hardening and softening is flexible, and different contour may exist for different values of κ(see figure 2.32). In case the yield contour expands, hardening occurs, and in case the yield contour shrinks, it is softening behaviour. Softening behaviour is related to the strength reduction.

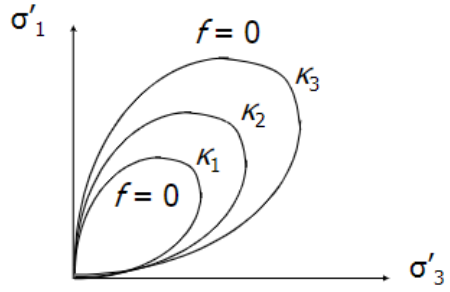

Figure 2.32: Hardening and softening yield contour

Compared to plastic theory, the variables in yield function of hardening and softening are not only the stress anymore, but also the state parameter κ, which is a function of plastic strain ϵ^p. Under this circumstance, hardening parameter must be considered as well when use the chain rule of partial differentiation. The sress-strain relationship is(Brinkgreve, 2018b):

$$\frac{\partial f^T}{\partial \underline{\sigma'}} d\underline{\sigma'} + \frac{\partial f}{\partial \kappa} \frac{\partial \kappa^T}{\partial \underline{\epsilon^p}} d\underline{\epsilon'} = 0 \tag{2.32}$$

Compaction hardening is one type of strain hardening. Compaction hardening occur if the yield contour is closed around the p-axis and this yield contour is called a cap. Besides, compaction hardening is beneficial to model plastic strains that are generated during primary compression, which is the concept of pre-consolidation. By introducing 'soft' boundaries in the stress diagram at the level at which the soil is pre-loaded, the pre-consolidation stress σ_c can be set, figure 2.33 illustrate it. Compressive stress paths below the pre-consolidation stress will only cause elastic strains, but if the stress paths tends to go beyond the boundary, corresponding yield contour will be pushed out. As a result, plastic volumetric strains generates so that the 'softer' response is observed during primary loading. The contour can be curved to instead of straight lines, which is more realistic for a cap-type yield contour (see figure 2.34).

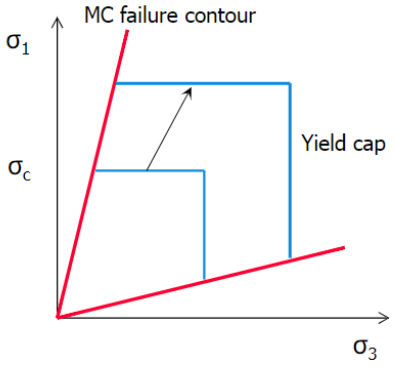

Figure 2.33: /Rigid/Yield contour for pre-consolidation

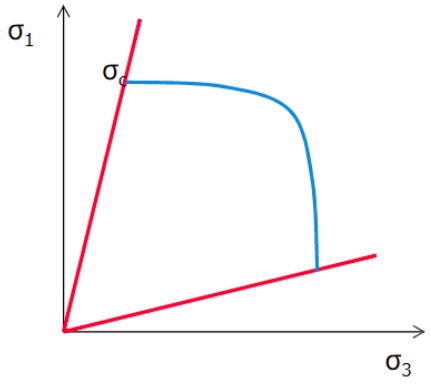

Figure 2.34: Yield contour with curve for pre-consolidation

2.4.4. Hardening soil Model

The Hardening Soil is an advanced model for simulating the behaviour of different types of soil, both soft soils and stiff soils. When subjected to primary deviatoric loading, soil shows a decreasing stiffness and simutaneously irreversible plastic strains develop. In the special case of a drained triaxial test, the observed relationship between the axial strain and the deviatoric stress can be well approximated by a hyperbola. Such a relationship was first formulated by Kondner (1963) and later used in the well-known Duncan Chang Model.

The Hardening Soil Model, however, supersedes the hyperbolic model by far.On the one hand, using the theory of plasticity rather than the theory of elasticity, on the other hand,by including soil dilatancy and introducing a yield cap. For Hardening Soil, the influence of the increase in modulus during the reloading phase after unloading can be considered, which is particularly suitable for analyzing the unloading and reloading problems after excavation (Fu and Jiang). The basic parameters of HS Model are:

- m: Stress dependent stiffness according to a power law
- E_{50}^{ref}: Plastic straining due to primary deviatoric loading
- E_{oed}^{ref}: Plastic straining due to primary compression
- E_{ur}^{ref} , ν_{ur}: Elastic unloading reloading
- c, φ, ψ: Failure according to the Mohr-Coulomb failure criterion

The characteristics of HS Model are indicates (Brinkgreve, 2018b):

- Stress-dependent stiffness behavior according to a power law
- Hyperbolic stress-strain relationship in axial compression
- Plastic strain by mobilizing friction (shear hardening)
- Plastic strain by primary compression (compaction hardening)
- Elastic unloading/reloading
- Failure behavior according to the Mohr-Coulomb criterion
- Small-strain stiffness (HSsmall model only)

Stress dependency of soil stiffness is the basic feature of the present Hardening Soil Model. For oedometer conditions of stress and strain, the model implies for example the relationship $E_{oed} = E_{oed}^{ref}(\frac{\sigma}{P^{ref}})^m$. In the special case of soft soils, it is realistic to use m = 1. In one-dimensional rebound recompression experiment and CPTu end-resistance derivation method, the expressions are:

$$E_{oed}^{ref} = \frac{2.3(1+e_0)}{C_c} P^{ref} \qquad \text{clay/silt} \tag{2.33}$$

$$E_{oed}^{ref} = mp^{ref} \qquad \text{sand} \tag{2.34}$$

$$E_{50}^{ref} = \frac{E_{50}^{ref}}{3} \tag{2.35}$$

$$E_{ur}^{ref} = \frac{3(1+e_0)(1-2\nu_{ur})(1+\nu_{ur})}{1.3C_{ur}(1-\nu_{ur})} P^{ref} \qquad \text{clay/silt} \tag{2.36}$$

$$E_{ur}^{ref} = \frac{(1-2\nu_{ur})(1+\nu_{ur})}{(1-\nu_{ur})} P^{ref} m_r K_0^{-(t-1)} \tag{2.37}$$

For normally consolidated clays, $m = 1$, the expressions are:

$$E_{oed}^{ref} = 0.5 E_{50}^{ref} \tag{2.38}$$

$$E_{oed}^{ref} = \frac{50000kpa}{I_p} \qquad \text{(correlation with } I_p \text{ for } P^{ref} = 100kpa) \tag{2.39}$$

For sand, $m = 0.5$, the expressions are:

$$E_{oed}^{ref} = E_{50}^{ref} \tag{2.40}$$

$$E_{oed}^{ref} = RD \cdot 60Mpa \tag{2.41}$$

In PLAXIS, the relationship between three young's modulus is

$$E_{ref}^{oed} = E_{50}^{ref} = 3E_{ur}^{ref}$$

The default setting $P_{ref} = 100Kpa$. $R_f = 0.9$ is also the default. When undrained behavior is considered in the Hardening Soil model, the drainage type should preferable be set to Undrained (A). Alternatively, Undrained (B) could use in the situation that effective strength properties are not known or Undrained (A) cannot describe shear strength very well. Undrained (C) is not possible since the model is essentially formulated as an effective stress model. In Hardening Soil Model, the V_{ur} is a pure elastic parameter (Bentely, 2019). The following figures are the parameters of present hardening model. The soil stiffness is the most important one in the model,and some parameters can be adopted with default values like m and poisson's ratio.

Failure parameters as in Mohr-Coulomb model (see Section 3.3):

c	:	(Effective) cohesion	[kN/m^2]
φ	:	(Effective) angle of internal friction	[°]
ψ	:	Angle of dilatancy	[°]
σ_t	:	Tension cut-off and tensile strength	[kN/m^2]

Basic parameters for soil stiffness:

E_{50}^{ref}	:	Secant stiffness in standard drained triaxial test	[kN/m^2]
E_{oed}^{ref}	:	Tangent stiffness for primary oedometer loading	[kN/m^2]
E_{ur}^{ref}	:	Unloading / reloading stiffness (default $E_{ur}^{ref} = 3E_{50}^{ref}$)	[kN/m^2]
m	:	Power for stress-level dependency of stiffness	[-]

Advanced parameters (it is advised to use the default setting):

ν_{ur}	:	Poisson's ratio for unloading-reloading (default ν_{ur} = 0.2)	[-]
p^{ref}	:	Reference stress for stiffnesses (default p^{ref} = 100 kN/m^2)	[kN/m^2]
K_0^{nc}	:	K_0-value for normal consolidation (default $K_0^{nc} = 1 - \sin\varphi$)	[-]
R_f	:	Failure ratio q_f / q_a (default R_f = 0.9) (see Figure 6.1)	[-]
$\sigma_{tension}$	:	Tensile strength (default $\sigma_{tension}$ = 0 stress units)	[kN/m^2]

Figure 2.35: Hardening Soil Model parameters

c_{inc}	:	As in Mohr-Coulomb model (default c_{inc} = 0)	[kN/m^3]

Instead of entering the basic parameters for soil stiffness, alternative parameters can be entered. These parameters are listed below:

C_c	:	Compression index	[-]
C_s	:	Swelling index or reloading index	[-]
e_{init}	:	Initial void ratio	[-]

Figure 2.36: Hardening Soil Model parameters

3

Subsoil condition analysis

This chapter examines how to classify the available subsoil data and determine the required geo-technical parameters for the calculations to be made.

3.1. Soil layer interpretation

3.1.1. Available data

Before the construction of the Kiltunnel, soil conditions were investigated along the tunnel. However, due to limiting factors, the existing underground soil layer data of the Kiltunnel is insufficiently detailed to allow a detailed finite element model to be constructed. According to Dinoloket, there are some extra borehole which can supplement the available data set from the construction period. For the sake of convenience, each hole has been numbered, and the following figure shows a detailed distribution (see figure 3.1).

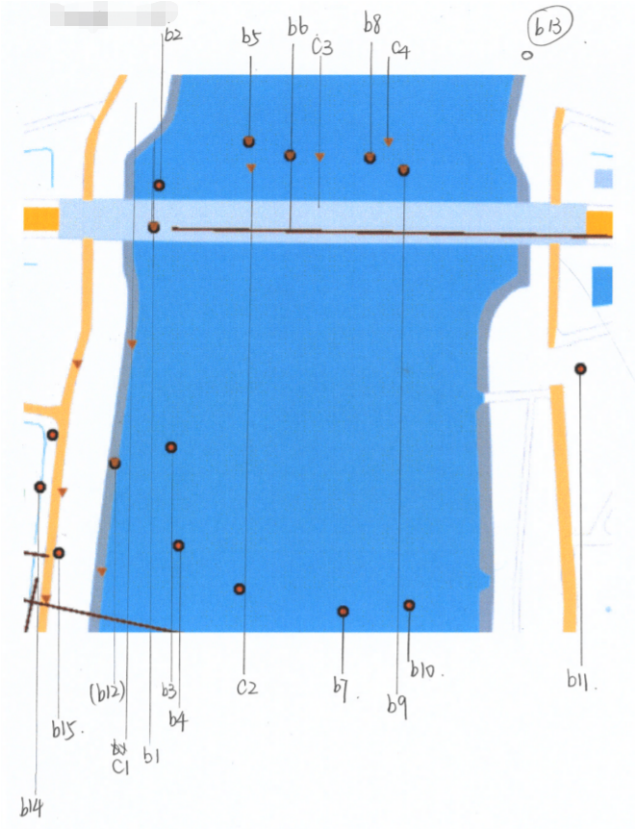

Figure 3.1: Numbers for the distribution of boreholes

Some CPT data can still be obtained from the construction documentation records at the time. The figures below are the whole CPT data for Kiltunnel and the corresponding numbers in the river are b5, b6, c3, b8, c4, b9, respectively.

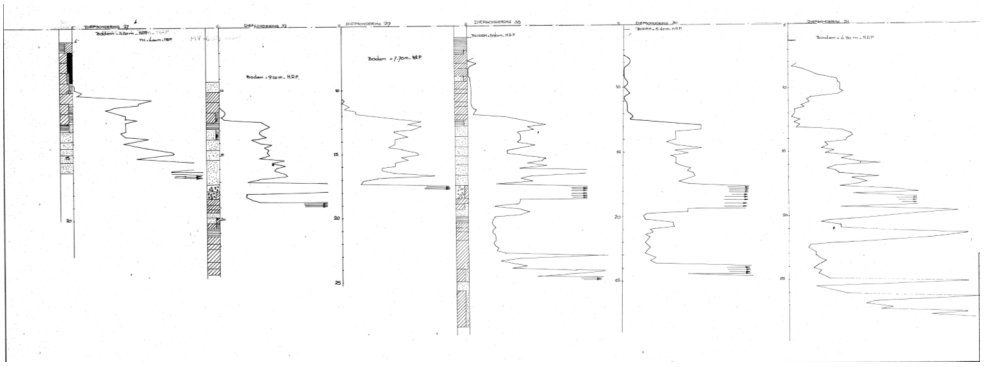

Figure 3.2: CPT profile for the boreholes across the river

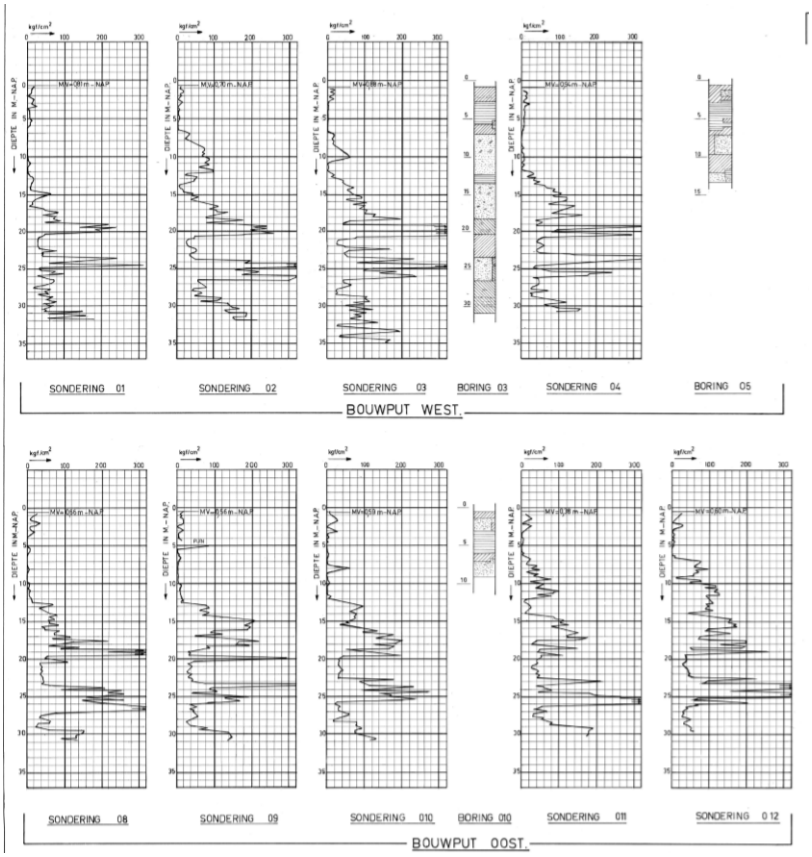

Figure 3.3: CPT profile for two sides

In addition to sub-soil layer information given by the CPT, the settlement data obtained by the monitoring system is also known, which provides a reference for the largest settlement and most dangerous cross-section in the tunnel(see figure 1.3).

3.1.2. Longitudinal direction

The sub-soil condition for the longitudinal direction can be simplified in the light of CPT profile on the river. However, the maximum depth of the sub-soil layer on the CPT profile reached only NAP -28m, which is insufficient for building finite element model. From the Dinoloket, additional information can be obtained as

the compensation. Figure 3.4 is the cross section of soil layer within 0.5km extension of East and West ends of tunnel. The three tunnel elements locates from 0.6km to 0.9 km. Soil data stretches to NAP -50m, and the soil are all sandy clay below NAP -28m.

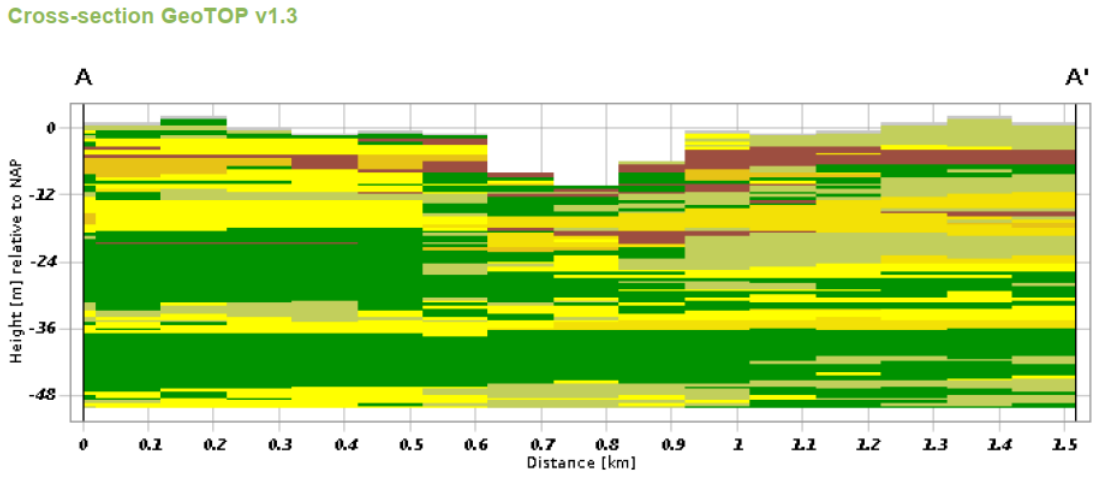

Figure 3.4: Soil layer compensation for longitudinal direction

Because the borehole logs, lab testing or samples are all missing in this project, reasonable assumptions have to be made for clarifying the soil type. On the one hand, there is large diversity for the soil layers above the tunnel; on the other hand, the soil under the tunnel contributes to settlement most. Therefore, the soil interpretation starts at NAP -10m, the parts above it are negligible when interpreting the effect on tunnel settlements. The final distribution is on table 3.1.

Depth (NAP -)	Type
10m – 11.5m	Moderate organic clay
11.5m – 12m	Pre-loaded peat
12m – 18.5m	Moderate clean sand
18.5m-37m	Medium sandy clay
37m - 48m	Moderate clean clay
48m – 50m	Medium sandy clay

Table 3.1: Longitudinal Subsoil interpretation

In terms of the profile, depth starts on 10m – 11.5m with moderately organic clay. In the specific explanation from Dinoloket, the soil type belongs to clay. But CPT data indicates that it is also mixed with peat. The objective of the study is the accuracy determine ongoing settlements, and moderately organic clay is expected to result in more future settlements than a weak organic clay, as it is expected that for weak organic clay all deformations already have finished. Therefore, moderately organic clay is selected fro this layer.

At 11.5m – 12m, a consolidaed peat is detected. Figure 3.6 shows the relocation position of the levee. And it is obvious that the point 12 marked with a black dot corresponds to the relatively high point of the levee which means the heaviest load before construction. Futhermore, preloading-unloading-reloading process existed, and pre-loaded peat is the more conservative choice in this situation.

At 12m – 18.5m, the soil type is chosen as moderate clean sand. Based on the detailed explanation on Dinoloket, the layer are mixed with very coarse sand, very fine sand, very medium coarse sand and also gravel and debris, but most are medium coarse sand. Taking the an average, the moderate clean sand is chosen.

When interpreting the subsoil profile, all the boreholes located on the river present a relatively homogeneity. Owing to the lack of other borehole data, soil profile of depth at NAP -(18.5m – 28.5m) remains the same with soil type of b8. Dependent on the explanation of dinoloket, most are medium sandy clay, therefore, moderate sandy clay is the best option.

The soil type of 37m – 50m follows with the cross section on figure 3.5 which is obtained from Dinoloket.

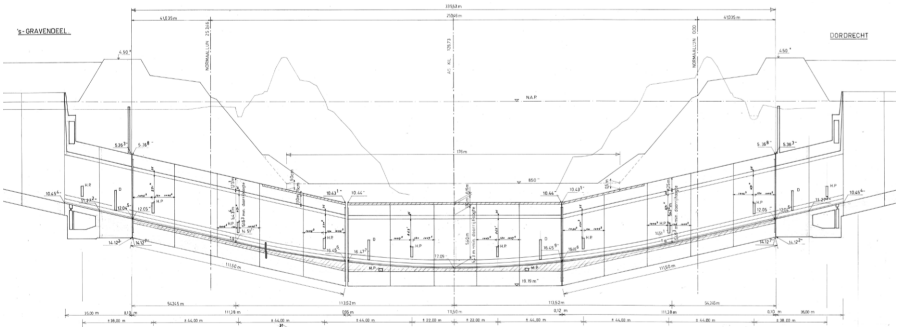

Figure 3.5: Longitudinal profile with point 12

3.1.3. Transverse direction subsoil

Through comparison, the most probable soil layer profile for point 12 is at b4. The water level is at NAP -0.8m. The cross-section profile can be obtained from Dinoloket. The maximum depth is at NAP -51m, the supplementary information are as the graph shows (see figure 3.6). In figure 3.6, the tunnel structure is between 0.675 - 0.75 in x-axis. The borehole profile can be simplified as indicates on table 3.2.

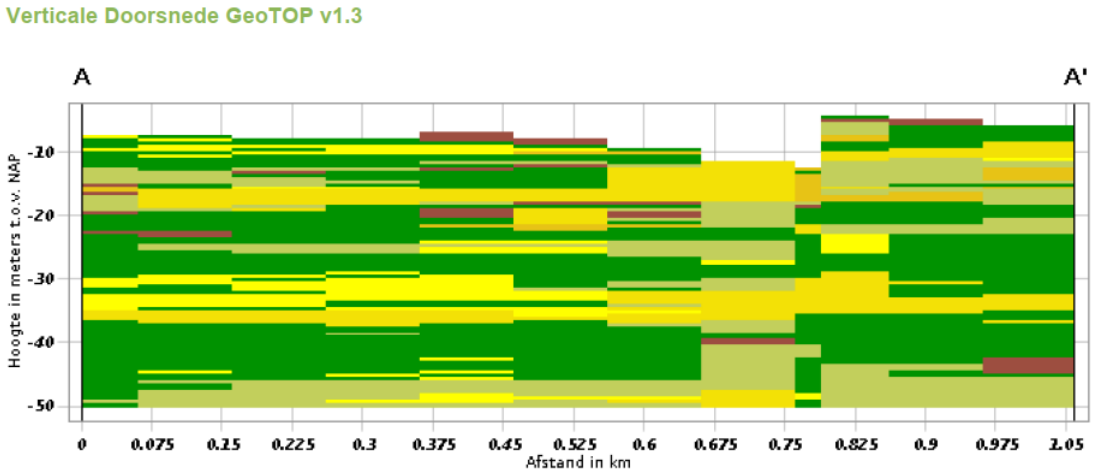

Figure 3.6: Soil layer compensation for transverse direction

Depth (NAP -)	Type
0.8m – 2.3m	Clay, medium humic, slightly sandy
2.3m – 3.05m	Sand, very fine, silty
3.05m – 6.05m	Clay, humic
6.05m - 15.8m	Sand, medium coarse, slightly humic
15.8m - 24.8m	Sandy clay
24.8m – 25.8m	Very fine sand
25.8m – 29.8m	Clay sandy, slightly silty
29.8m – 34.8m	Sand, medium fine
34.8m – 37.8m	Clay, moderate silty
37.8m - 38.8m	Peat
38.8m - 45.8m	Sandy clay
45.8m – 50.8m	Sand, medium fine

Table 3.2: Transverse Subsoil interpretation

The information given in the table above was obtained before the construction of the tunnel. Water level changed to NAP -5.5m after the construction. Besides, soil layer has partially overlap in both transverse and

longitudinal direction. This leads to soil distribution under the tunnel which is at approximately NAP -19m has to be matched in these two directions. Due to the lack of soil layer data, a lot of assumptions are made. The main principle of these assumptions is to be conservative which means that if the most dangerous situation can meet the requirements, then the actual situation can meet the requirements as well cause the actual situation is not as bad as the supposed dangerous situation. In order to meet general requirement for modeling, the depth of soil layer is extended to 60m. Combining CPT profile and Dinoloket information, an assumption is made that the rest part is be sandy clay. Integrating multiple information to finalize the transverse soil layer as shown in table 3.3.

Depth [m NAP -]	Type
0m – 5.5m	water
5.5m – 8.0m	Humic clay moderate
8.0m - 15.8m	Weak silty sand
15.8m - 29.8m	Medium sandy clay
29.8m – 37.8m	Fine sand
37.8m – 60.8m	Medium sandy clay

Table 3.3: Final transverse Subsoil interpretation

In order to keep uniform layers in two direction, the subsoil condition under the tunnel must be the same although there is big variety above. Table 3.4 shows the final profile of longitudinal subsoil.

Depth [m NAP -]	Type
0m – 1.6m	Medium sandy clay
1.6m – 3.6m	Peat
3.6m - 7.5m	Sandy clay
7.5m – 12.3m	Moderate organic clay (humic clay)
12.3m - 13m	Preloaded peat
13m - 18.5m	Moderate clean sand
18.5m – 30m	Sandy clay
30m – 38m	Fine sand
38m – 60m	Sandy clay

Table 3.4: Final longitudinal subsoil interpretation

3.2. Soil Properties interpretation

Soil is made up of different-sized particles. All soils contain mineral particles, organic matter, water and air. The combinations of these determine the soil's properties – its texture, structure, porosity, chemistry and colour.

In finite element model, strength parameters and stiffness parameters are crucial. Soil strength (S) is described as the function of three major parameters including effective normal stress or net force per unit area acting perpendicular to a slip surface $\sigma^{'}$ cohesion c, and internal-friction angle θ of the slope material. The predominant equation indicates below:

$$\tau = \sigma^{'} \tan\theta + c \tag{3.1}$$

Soil stiffness constitutive model parameters are required when investigating and/or modeling stress-related deformations in G-technical problems. Typical inputs to these models include stiffness parameters of subsurface soils that are defined using variants of Young's (elastic) modulus, E. Elastic modulus variants such as secant modulus in drained triaxial test (E50), tangent modulus for primary oedometer loading (Eoed), as well as unloading/reloading modulus (Eur), are often requested inputs in numerical analyses.

The identification of the soil was carried out based on the method of Robertson and the method of NEN 9997-1 table 2b. In this case, the available data only contain cone resistance, and void ratio doesn't indicate in table 2b. These two methods cannot be used separatelybut the combination of these two methods are the best option. Thus, soil strength and stiffness parameters will derived from the method of NEN 9997-1 table 2b and the void ratio and permeability which are not on table 2b will be deducted from the method of Robertson.

3.2.1. Method of NEN 9997-1 table 2b

Unlike the Robertson interpretation method, only the cone resistors is important when applying the NEN 9997-1 method. And it is a more conservative method. There are relationships between qc in real measurement and qc in table 2b. The conversion are:

$$C_{qc} = (\frac{100}{\sigma_0^{'}})^{0.67} \tag{3.2}$$

$$q_{c,table} = C_{qc} * q_c \tag{3.3}$$

For soft soil, cohesion is an important parameter but for sand, it is almost zero. In order to avoid internal calculation mistake of software itself, the cohesion for sand set as 1 Kpa. Once the qc is available, interpolation method will be applied to calculate corresponding values. The interpretation of soil strength and stiffness parameters in transverse and direction are given in table 3.5 and 3.6.

Type	$\gamma^{'}$ (KN/m^2)	h (m)	$\sigma^{'}$ (KN/m^2)	qc (MPa)	C_{qc}	$q_{c,table}$ (MPa)
Humic clay	6	2.5	75.3	0.5	1.21	0.6047
Weak silty sand	11	7.8	161.1	10	0.7265	7.2652
Sandy clay	8	14	273.1	7.3	0.5101	3.7238
Fine sand	10	8	353.1	15	0.4294	6.4417
Sandy clay	8	23	537.1	7.3	0.3242	2.3669

Table 3.5: Soil parameters in transverse direction

Type	E_{100} (MPa)	ϕ	c (KPa)
Humic clay	1.1798	15	15.7965
Weak silty sand	18.8259	27.0867	1
Sandy clay	7.4476	33.619	22.7905
Fine sand	45	32.5	1
Humic clay	14.4012	24.6673	12.8024

Table 3.6: Soil parameters in transverse direction

- $\gamma^{'}$ = effective weight of soil
- h = thickness of soil layer
- $\sigma^{'}$ = cumulative effective stress
- qc = measured cone resistance
- C_{qc} = turnover factor to ground tension of 100
- $q_{c,table}$ = corresponding cone resistance in table 2b
- E_{100} = modulus of elasticity standardized for an effective soil stress of 100 kPa.
- ϕ = friction angle
- c = cohesion

Due to the continuity of the model soil layer in different directions, the soil is necessary to keep uniform under the tunnel. The parameters of the last three soil layers will remain the same. In addition, the top layers are not saturated, but the total weight will be taken as the effective weight in all calculations. And the final indication of soil parameters in longitudinal direction are on table 3.7 and 3.8.

3.2.2. Robertson's method

Method Robertson (1990) is used in the interpretation of CPTs. The corrected values of the cone resistance qt and friction number Rf are used as input parameters. The cone resistance qc corrected for pore water effects. Rf is the ratio, expressed as a percentage, of the sleeve friction resistance fs, to the cone resistance qt, both measured at the same depth.

$$qt = qc + u2(1 - a) \tag{3.4}$$

$$Rf = \frac{fs}{qt} \times 100\% \tag{3.5}$$

Type	$\gamma^{'}$ (KN/m^2)	Thickness (m)	$\sigma^{'}$ (KN/m^2)	qc (MPa)	C_{qc}	$q_{c,table}$ (MPa)
Medium sandy clay	18	1.6	28.8	1	2.3025	2.3025
Peat	13	2	54.8	0.15	1.4963	0.2244
Sandy clay	18	3.9	125	0.8	0.8611	0.6889
Moderate organic clay	16	4.8	201.8	0.5	0.6247	0.3124
Preloaded peat	12	0.7	210.2	1.7	0.6079	1.0334
Moderate clean sand	9	5	254.8778	12	0.5343	6.4112
Sandy clay	8	12	351.1642	7.3	0.5101	3.7238
Fine sand	10	8	431.1642	15	0.4294	6.4417
Sandy clay	8	22	608.7642	7.3	0.3242	2.3669

Table 3.7: Soil parameters in longitudinal direction

Type	E_{100} (MPa)	ϕ	c (KPa)
Medium sandy clay	6.6114	24.5064	12.2229
Peat	0.8417	15	4.2083
Sandy clay	1.5	22.5	1
Moderate organic clay	0.9495	15	15
Preloaded peat	3.8625	15	19.3688
Moderate clean sand	19.2336	31.1758	1
Sandy clay	7.4476	33.619	22.7908
Fine sand	45	32.5	1
Humic clay	14.4012	24.6673	12.8024

Table 3.8: Soil parameters in longitudinal direction

However, pore pressure and sleeve friction resistance are missing in this case. As mentioned above, it is impossible to obtain the soil strength and stiffness parameters from the Robertson's method. But relative density can be calculated from the equation 3.6 from Robertson's method. And relative density is related to void ratio. Thus, void ratio can be derived from this series of parameters.

$$D_r^2 = \frac{Q_{cn}}{305 Q_C Q_{OCR} Q_A} \tag{3.6}$$

where

- $Q_n = \frac{qc/pa}{(\sigma^{'}_{v0}/pa)^{0.5}}$
- pa = Reference pressure of 100kpa, in same unit as qc and $\sigma^{'}_{v0}$
- Q_c = Compressibility factor range from 0.9 (low compressibility) to 1.1 (high compressibility)
- Q_{OCR} = Overconsolidation factor = $OCR^{0.18}$
- Q_A = Aging fator = $1.2 + 0.05\log(t/100)$

$$D_r = \frac{e - e_{min}}{e_{max} - e_{min}} \tag{3.7}$$

where

- e_{min} = minimum void ratio
- e_{max} = maximum void ratio

In Kiltunnel, the soil is normally consolidated so that the OCR is 1. And the time lasts for 42 years after the total construction. For sand, the normal range for void ratio is 0.3 - 0.6, and 0.5 - 1 for clay. However, USCS is another measurement for void ratio range. The USCS is arranged so that most soils may be classified into at least the three primary groups (coarse grained, fine grained, and highly organic) by means of visual examination and simple field tests. The shortcoming of USCS is the range for clay indicates unclear, so that USCS applies more on sand. USCS charts are on figure 3.7.

The resulting parameters and final void ratios in both two directions are in following tables.

All values that derived from table 2b and other methods are theoretical values. In the practical modeling, the parameters may be modified according to the actual situation and monitoring data.

Depth[m NAP-]	Type	Qcn	Qc	Qa	Dr^2	Dr
5.5 - 8	Humic clay	5.7620	1.1	1.1801	0.01455	0.1206
8 - 15.8	Weak silty sand	78.7866	1.1	1.1801	0.1990	0.4461
15.8 - 29.8	Sandy clay	44.1735	1.1	1.1801	0.1116	0.3340
29.8 - 37.8	Fine sand	79.8256	1.1	1.1801	0.2016	0.4490
37.8 - 60.8	Sandy clay	31.4989	1.1	1.1801	0.0796	0.2821

Table 3.9: Relative density for transverse direction

Type	Rough range			USCS range		
	e_{max}	e_{max}	e	e_{max}	e_{max}	e
Humic clay	1	0.5	0.9397	-	-	-
Weak silty sand	0.6	0.3	0.4662	0.98	0.33	0.6900
Sandy clay	1	0.5	0.8330	-	-	-
Fine sand	0.6	0.3	0.4653	0.85	0.4	0.6479
Sandy clay	1	0.5	0.8590	-	-	-

Table 3.10: Void ratio for each layer in transverse direction

Description	USCS	Void ratio [-]		
		min	max	Specific value
Well graded gravel, sandy gravel, with little or no fines	GW	0.26	0.46	
Poorly graded gravel, sandy gravel, with little or no fines	GP	0.26	0.46	
Silty gravels, silty sandy gravels	GM	0.18	0.28	
Gravel	(GW-GP)	0.30	0.60	
Clayey gravels, clayey sandy gravels	GC	0.21	0.37	
Glatial till, very mixed grained	(GC)	-	-	0.25
Well graded sands, gravelly sands, with little or no fines	SW	0.29	0.74	
Coarse sand	(SW)	0.35	0.75	
Fine sand	(SW)	0.40	0.85	
Poorly graded sands, gravelly sands, with little or no fines	SP	0.30	0.75	
Silty sands	SM	0.33	0.98	
Clayey sands	SC	0.17	0.59	
Inorganic silts, silty or clayey fine sands, with slight plasticity	ML	0.26	1.28	
Uniform inorganic silt	(ML)	0.40	1.10	
Inorganic clays, silty clays, sandy clays of low plasticity	CL	0.41	0.69	
Organic silts and organic silty clays of low plasticity	OL	0.74	2.26	
Silty or sandy clay	(CL-OL)	0.25	1.80	
Inorganic silts of high plasticity	MH	1.14	2.10	
Inorganic clays of high plasticity	CH	0.63	1.45	
Soft glacial clay	-	-	-	1.20
Stiff glacial clay	-	-	-	0.60
Organic clays of high plasticity	OH	1.06	3.34	
Soft slightly organic clay	(OH-OL)	-	-	1.90
Peat and other highly organic soils	Pt	-	-	
soft very organic clay	(Pt)	-	-	3.00

Figure 3.7: USCS void ratio range

Depth [m NPA-]	Type	Qcn	Qc	Qa	Dr^2	Dr
0 - 1.6	Medium sandy clay	18.6339	1.1	1,1801	0.04706	0.2169
1.6 - 3.6	Peat	2.0263	1.1	1,1801	0.005118	0.07154
3.6 - 7.5	Sandy clay	7.1554	1.1	1,1801	0.01807	0.1344
7.5 - 12.3	Moderate organic clay	3.5197	1.1	1,1801	0.00889	0.0943
12.3 - 13	Preloaded peat	11.7255	1.1	1,1801	0.0296	0.1721
13 - 18	Moderate clean sand	75.1649	1.1	1,1801	0.1898	0.4357
18 - 30	Sandy clay	44.1735	1.1	1.1801	0.1116	0.3340
30 - 38	Fine sand	79.8256	1.1	1.1801	0.2016	0.4490
38 - 60	Sandy clay	31.4989	1.1	1.1801	0.0796	0.2821

Table 3.11: Relative density for longitudinal direction

Type	Rough range			USCS range		
	e_{max}	e_{max}	e	e_{max}	e_{max}	e
Medium sandy clay	1	0.5	0.8915	-	-	-
Peat	1	0.5	0.9643	-	-	-
Sandy clay	1	0.5	0.9328	-	-	-
Moderate organic clay	1	0.5	0.9529	-	-	-
Preloaded peat	1	0.5	0.9140	-	-	-
Moderate clean sand	0.6	0.3	0.4693	0.75	0.35	0.5757
Sandy clay	1	0.5	0.8330	-	-	-
Fine sand	0.6	0.3	0.4653	0.85	0.4	0.6479
Sandy clay	1	0.5	0.8590	-	-	-

Table 3.12: Void ratio for each layer in longitudinal direction

Except void ratio, permeability is crucial for the result of model as well. An approximate estimation of soil hydraulic conductivity or coefficient of permeability, k, can be made from an estimate of soil behavior type using the CPT SBT charts. On the basis of following chart (see figure 3.9), the middle value of each range is chosen to test firstly, then it will be adjusted in the model according to the obtained results. The value of preset permeability coefficient for each soil is on table 3.13.

SBT Zone	SBT	Range of k (m/s)	SBT_n I_c
1	Sensitive fine-grained	$3x10^{-10}$ to $3x10^{-8}$	*NA*
2	Organic soils - clay	$1x10^{-10}$ to $1x10^{-8}$	$I_c > 3.60$
3	Clay	$1x10^{-10}$ to $1x10^{-9}$	$2.95 < I_c < 3.60$
4	Silt mixture	$3x10^{-9}$ to $1x10^{-7}$	$2.60 < I_c < 2.95$
5	Sand mixture	$1x10^{-7}$ to $1x10^{-5}$	$2.05 < I_c < 2.60$
6	Sand	$1x10^{-5}$ to $1x10^{-3}$	$1.31 < I_c < 2.05$
7	Dense sand to gravelly sand	$1x10^{-3}$ to 1	$I_c < 1.31$
8	*Very dense/ stiff soil	$1x10^{-8}$ to $1x10^{-3}$	*NA*
9	*Very stiff fine-grained soil	$1x10^{-9}$ to $1x10^{-7}$	*NA*

**Overconsolidated and/or cemented*

Figure 3.8: Estimated soil permeability (k) based on the CPT SBT chart by Robertson (2010)

In addition to the parameters of the soil layer, the material used for backfilling in Kiltunnel is silex instead of the commonly used sand. Silex is a human-made material that is a formed from a mixture of clay, limestone and silica. The thickness of the backfilled silex is 0.5m. Sand-flow foundation is chosen as the foundation method. However, the sand-flow foundation is not compacted enough when constructed. Therefore, the category is equivalent to loose clean sand when dealing with basic related parameters. The thickness of foundation is 0.5m as well. The parameters for these two are on table 3.14.

All the above data are calculated based on table 2b of NEN9997 and Robertson's method, and these parameters are the data basis for the model built afterwards as well. However, in the actual model, the data is often impossible to match at the beginning, so slight adjustment may also be involved in the modeling

Type	Permeability [m/s]
Humic clay	5×10^{-9}
Weak silty sand	1×10^{-6}
Sandy clay	5×10^{-6}
Fine sand	5×10^{-4}
Sandy clay	5×10^{-6}
Peat	5×10^{-9}

Table 3.13: Permeability for each soil type

Type	γ'	E_{100} (MPa)	ϕ	c (KPa)	e	k [m/s]
Silex	9	50	32.5	1	0.2149	0.01
Loose clean sand	9	15	30	1	0.6	1×10^{-3}

Table 3.14: Supplementary materials parameters

process.

4

Description of the assumptions and first approximation calculation

This chapter aims to propose two main assumptions to cause the serious settlement and leakage, and the relevant general calculation of estimated settlement. Assumptions will be verified in PLAXIS model, see chapter 5 for specific elaboration.

4.1. Assumption

According to the physical circumstance, there are two assumptions possiblly explain the occurrence of settlement and leakage. And they will be verified in following chapter.

Assumption 1

In 2001 a serious leak occurred in an expansion joint in tunnel element 2. The water drainage flows directly into the sewer. Leaks in tunnels are not special and occur in several tunnels, but have never had sand-carrying leaks before. The original source of sand is doubtful aspect, and it is not sure where it come from. In point 12, the soil profile near the tunnel drainage collector is sandy clay and the soil layer above is weak silty sand. The backfilled material is silex. Besides, the foundation is loose sand pancake with density 500 KN/m^3.

The settlement data of this leakage gives a least impression of approximately 7 m^3 of sand loss. From the angular rotation of the tunnel section, it emerges that the underside of element 2c-2d is 14 mm open. The settlement has a volume of approximately 72 m3 of sand over a tunnel width of 30 m. The leak on the entrance side of the 's-Graving part gives a water volume of 1.5 liter / sec (= 5.4 m^3 / hour) and a sand volume of approx. 10 liters per week.

However, the original source of the leaked sand still remains a problem. The geological profile drawing shows that the weak slity sand layer has little possibility to inflow. Considering this aspect, the undercurrent of sand flow foundation is the most likely cause. The loss of sand foundation cause uneven settlement, then induce the crack of expansion joint, so that leak happened. This could be the first assumption.

In addition to undercurrent, whether the water and sand leaked into the tunnel will affect the tunnel is also a question, so the impact of the inflow will also be discussed in the next chapter.

Assumption 2

Due to the relocation of the levee, the soil under element 1 and 2 suffered from loading-unloading-reloading process. According to the profile, the levee on both the east and west sides moved further east and west, widening the existing river channels. As a result, the load on the tunnel element 1 and 2 reduced.

Soft clayey soil may experience cycles of unloading-reloading over decades for several reasons, such as pre-loading, staged construction or natural phenomena. Settlement is one of the problems which induced by the ongoing consolidation of these soft clayey soil. The plastic deformation occurs when the consolidation stress is greater than the pre-consolidation stress for natural clays (Habibbeygi and Nikraz, 2018).

It is obvious that the current loading on the tunnel is less than the previous loading, which means that the current circumstance of the soil under tunnel is in reloading process with the vertical effective stress is

Depth	Type	Unit Weight [KN/m^3]	Stress [KN/m^2]
+0.95 - -1.2	sandy clay	18	38.7
-1.2 - -2.45	Fine sand	21	26.25
-2.45 - -3.2	Peat	12	9
-3.2 - -6.2	Humic clay	16	48
-6.2 - -8.5	sand, coarse category	19	43.7
Total (KPa)	165.65		

Table 4.1: Top load before relocation

less than maximum applied consolidation stress before unloading. Besides, the excavation of trench and put tunnel element are unloading-reloading process as well, making soil suffer some plastic deformation.

Considering the impact of the relocation of the two sides of the levee on the overall soil layer, and the process of loading-unloading-reloading for several times, which may cause a large settlement. This is the assumption for the cause of the settlements in this case.

4.2. Structure analysis for leakage

The above two assumptions are derived from the soil layer. This section focuses on the structure. Under normal circumstances, the main cause of cracks in engineering structure is deformation, which accounts for more than 80% of all cracks. For tunnels, crack width is generally required to be controlled between 0.15-0.2mm. The uneven settlement results in the longitudinal bending of the tunnel. Generally speaking, when the internal force exceeds the ultimate tensile strength of the tunnel structure, cracks will occur. Some examples show that differential settlement of 50 mm has been able to produce transverse cracks in the whole tube section, which may also penetrate the full thickness of the base concrete plate. Besides, for the immersed tunnel with large bottom width, after the completion of tube hauling, immersion and connection, the foundation treatment is generally carried out by means of sand pouring, sand blasting, grouting, grouting and other methods to eliminate the harmful void under the tunnel. During foundation treatment, under the action of slurry or water sand mixed liquid pressure, the tunnel section tends to bulge and bend.

According to the leakage report, on the expansion joints of the outer walls locations in 2c-d, measuring strips are mounted below and above stainless steel strips with a gap of 10 mm. After 6 weeks, the north wall was measured above 10.2 mm, below 10.5 mm. On the south wall above 10.1 mm and below 10.4 mm. In addtion, the differencial settlement between point 12, and settlements of nearby western and eastern section joint are 35.4mm and 60mm, thus, the settlement difference between point 12 and the adjacent section joint on the west side is 36.1mm, and the settlement difference with the adjacent joint on the east side is 12.5mm, which gives the roughly rotation angle θ of 0.1 and -0.03 degree if clockwise is positive direction. As a result, the outer wall is under tremendous tension, while the inner wall is under tremendous compression at point 12. On the tunnel cross-section of point 12, according to the monitoring recording, it is found that the difference between the north and south settlements does not exceed 5mm, so there will be no further torsion at this maximum settlement point.

4.3. Pre-overburden Pressure

Before the construction of Kiltunnel, the levee had been relocated in order to broaden the river. This influences the stress state. Comparing to previous load, the load on the top was reduced. Pre-overburden pressure is the stress difference between previous load and current load. The borehole information which was detected before construction of the tunnel is used to calculate the load before relocation. KT-107-a indicates the position before and after relocation. Specific thickness in model will be calculated with the relevant scale which draws on the construction profile. For the river, the average water level is NAP +0.53m. There is 0.5m silex cover on the top of the tunnel, and 2.5m humic clay after relocation. See the table 4.1 and 4.2.

The POP is the difference of these two, which equal 55.85 KPa.

4.4. Calculation of theoretical settlement

The maximum settlement S of the immersed tube tunnel is composed of the maximum settlement S1 of the foundation layer (ie settlement during construction) and the maximum settlement S2 of the foundation soil

Depth	Type	Unit Weight [KN/m^3]	Stress [KN/m^2]
+0.53 - -5.5	Water	10	60.3
-5.5 - -8	Humic clay	16	40
-8 - -8.5	Silex	19	9.5
-3.2 - -6.2	Humic clay	16	48
Total (KPa)	109.8		

Table 4.2: Top load after relocation

layer (ie settlement after construction), total settlement is:

$$S = S_1 + S_2 \tag{4.1}$$

For the formula above, some premises are made:

1. The load does not change with time

2. Only the construction load and traffic load are considered, other factors such as tidal load, seismic load and water level drop are not considered, and the load is assumed to be static

3. Does not consider the secondary consolidation settlement of foundation soil

4. Assuming uniform settlement in the cross-sectional direction of the immersed tunnel

5. Simplify to the plane strain problem, take the load per meter, and use the central axis of the tube as the settlement calculation point.

4.4.1. Additional Load

When calculating the settlement, the average pressure P1 acting on the top surface of the foundation layer and the average pressure P2 on the top surface of the foundation soil layer are required. The weight of the foundation layer is P3, P3 is equal to the floating weight of the base layer times the thickness of the foundation. P1 is composed of construction load and traffic load. The construction load mainly includes the dead weight of the tube section, protective layer and backfill, and the buoyancy of the element section needs to be subtracted. Kiltunnel is a traffic tunnel, the traffic loads should be vehicle loads. The relationship between these three terms are below. And the detailed value are in table 4.3 (Wei et al., 2013).

$$P_2 = P_1 + P_3 \tag{4.2}$$

Term	P1 [Kpa]	P2 [Kpa]	P3 [Kpa]
Load	91.875	96.875	5

Table 4.3: Values for every load term

4.4.2. Foundation layer maximum settlement

The sand foundation layer is mainly composed of sand and gravel. In actual engineering, the upper part of the sand foundation layer bears less pressure, and the settlement is approximately linear with load. If the thickness of the sand foundation layer is h and the compression modulus of the sand soil is E_s, then the maximum settlement S_1 of the sand foundation layer is:

$$S_1 = \frac{h \times P_1}{E_s} \tag{4.3}$$

However, the value of E_s is uncertain and always difficult to get. According to the experimental results of Pearl River immersed tunnel (Chen et al., 1996), the settlement of pancake increases with the increase of load, and it basically changes linearly. By calculating E_s inversely through the experimental results, the result of E_s is 0.833 Mpa. While, in the Guangzhou Bio-Island-University City immersed tube tunnel experiment (Aiyuan et al., 2009), the compression test of the sand foundation found that the compression modulus E_s is in the natural state are in range 18.08 - 21.09 Mpa, and E_s in saturated state are in range 17.67 - 21.01 Mpa. There is big difference between these two experiments, and E_s is related to sand gradation, further research is needed to do for this aspect.

Under the actual engineering conditions, the sand layer is affected by buoyancy under water, thus it is difficult to be compacted to a dense state. At the same time, there are other factors to influence during construction, which lead to a large amount of compression of the sand foundation layer.

In terms of the above two experimental values, the settlement of the sand foundation layer is calculated as shown in table 4.4.

$E_s[Mpa]$	Experiment 1: 0.833	Experiment 2: 17.67
Settlement (m)	0.055	2.6e-3

Table 4.4: the settlement of the sand foundation layer for two experiments

From the table, The two results are far from each other. In terms of actual working conditions, the first one is obviously in line with the reality, while the second one is the theoretical value of the laboratory, which may have a certain disparity with the actual situation. But the specific situation still depends on the following model for analysis.

4.4.3. Theoretical consolidation settlement of foundation at time t

The maximum consolidation amount of foundation soil S_2 can be calculated by the method of layered summation. During the construction of immersed tube tunnel, the soil undergoes the process of unloading and reloading process when the upper load is received. If the settlement is calculated with soil compression modulus E_s, the settlement will be overestimated. In the next calculation, E_c will be used for calculation. E_c is a very important parameter that characterizes the unloading rebound of soil.

In Chapter 2, the consolidation settlement formula is derived in detail. Total settlement of the soil layer is in expression 4.5. Soil layers underneath the tunnel are sandy clay, fine sand and sandy clay, separately. Soft soils contributes to settlement, as a result, fine sand will be ignored in calculation.

$$S = (\frac{\Delta e}{1+e_0})H_0 = (\frac{a_{v0}\Delta\sigma_v^{'}}{1+e_0})H_0 = m_v\Delta\sigma_v^{'}H_0 \tag{4.4}$$

Using unloading reloading stiffness to estimate the settlement, the results shown in table 4.5 below are obtained.

Type	E_{ur}	m_v	k	c_v	H	T_v	U	S	s
Sandy clay	22344	4.48e-5	5e-6	1.12e-2	14	0.884	0.9	0.10094	9.08e-2
Sandy clay 1	42120	2.37e-5	5e-6	2.11e-2	23	1.93	0.82	0.19281	1.58e-1
Total (m)	0.249								

Table 4.5: Manual calculation for consolidation settlement

From the table, consolidation degree for the two sandy clay are 90% and 82%, these two values indicates that the consolidation process tends to be stable. Estimation of total settlement is 0.249m, this value is bigger than the data which displayed from monitoring system. There are two possible reason to cause this, firstly, the load is higher than actual situation. Secondly, volume compression coefficient is lower than that derived from unloading reloading stiffness, this could be possible due to the relocation of the levee.

5

Transverse PLAXIS Model

In this chapter, the calculations were performed with PLAXIS Finite Element 2D version 2020. The main goal is to verify the assumptions which presents above and get the relevant settlement data.

5.1. software

The calculations were performed with PLAXIS Finite Element 2D version 2020. PLAXIS is suitable for performing plastic and consolidation calculations and stability and deformation analyzes.

The calculation method depends on the number of elements (mesh) and the boundary conditions that are linked to this. A system of coupled normal and partial differential equations is solved for each element. The stress state and the deformation of soil can thus be accurately described.

The reliability of the results depends on the input parameters and the chosen basic model. The input parameters depend on the soil and laboratory tests carried out. Knowledge of the local specifics of the research location is of great importance for the correct determination of the input parameters. Choosing the right soil model is based on the analysis to be performed. In this case, the model is hardening soil model.

5.2. Model description

Selecting the cross section of the point 12 with the largest settlement as the research object. In PLAXIS, the model size should be 3-5 times of the tunnel size. The height of tunnel is 8.75m, and the length is 31m. Besides, the middle wall is 0.7m. Considering the value under conservative condition, length of 200m and depth of 60m were chosen. According to the profile, the thickness of sand-flow foundation underneath the tunnel is 50cm. On the two sides of the tunnel tube, the height of toe is 150cm. Concrete thickness at the bottom of the tunnel is 1.56m and total thickness with asphalt cushion is 2.29m. The walls on both sides of the tunnel are 1.1 meters thick. The high groundwater level is at NAP 0.79m, the low groundwater level is at NAP 0.27m. In the model, to get the average value is 0.53m. There is 0.5m thick silex on the top of the tunnel and then humic clay above. The distribution of soil layers is the same with Table 3.4 in Chapter 3. The interaction between the structural element and soil is modeled by means of interface, which is used to reduce the friction between structure and soil. R_{inter} could be an measurement, the value is set to be 0.65 for the soil layers that are next to the structure. Otherwise, it equals 1.

The tunnel tubes are made of concrete and linear elastic model is for this. The type of concrete is unknown. In line with the anti-floating safety factor of 1.05, the weight of concrete is 25 KN/m^3. Owing to the traffic load on the top of levee and inside of the tunnel tube, 100 KN/m/m line load and 25 KN/m/m are added to the corresponding location. In PLAXIS, plate element can be used to simulate the influence of walls, plates, shells or lining extending in z-direction. There are two methods to simulate the structure of immersed tunnel, one is to simulate the solid elastic material without pores, the other is to simulate the structure with plate element. The plate element was adopted in the tunnel tube with the advantage is that the internal force of structure can be obtained. The outer contour can be applied at the bottom and both sides of immerse tube. However, the top of immerse tube needs to be near the center line of the roof, otherwise the effective weights will be reduced after the excavation of the compartment. In order not to double the material properties, the properties are set as one thousandth of normal value to make the concrete material plays a predominant role in model. The properties of concrete and plate are indicates in table 5.1 and 5.2.

Type	γ [m/s]	e	ν	E
Concrete	25	0.03	0.2	30×10^6

Table 5.1: Properties of concrete

Type	EA [KN/m]	EI [KN m^2/m]	W [KN/m/m]
Plate	11.25	1500	0

Table 5.2: Properties of plate

The calculation consists of 7 phases. In practical construction phase, sand flow foundation will be applied after the immersion, the tunnel is temporarily supported by lifting jack between the moment of immersion and the placement of the sand flow foundation. While in PLAXIS, applied sand flow foundation have to advanced intime due to the numerical calculation, otherwise the soil body will collapse as it is not possible to model the tunnel with no connection to the soil. As a result, the finalized construction phases and their calculation types are:

1.Initial phase: plastic calculation type

2.trench dig: plastic calculation type

3.applied sand flow foundation: plastic calculation type

4.put the tunnel on the trench: plastic calculation type

5.tunnel fix (add toe): plastic calculation type

6.backfill tunnel: plastic calculation type

7.consolidation for 9125 days (until 2001): consolidation calculation type

8.leakage: consolidation calculation type

9.consolidation for 6250 days (2001 till now): consolidation calculation type

For the flow condition, boundary contours are set to be seepage. However, the clay layer boundary lines are closed and sand layer are open for consolidation calculation type in order to get better simulation. In leakage phase, the bottom line of right tube are set to be inflow, its purpose is to simulate the impact of the 2001 leak on the tunnel. The model shows in figure 5.1.

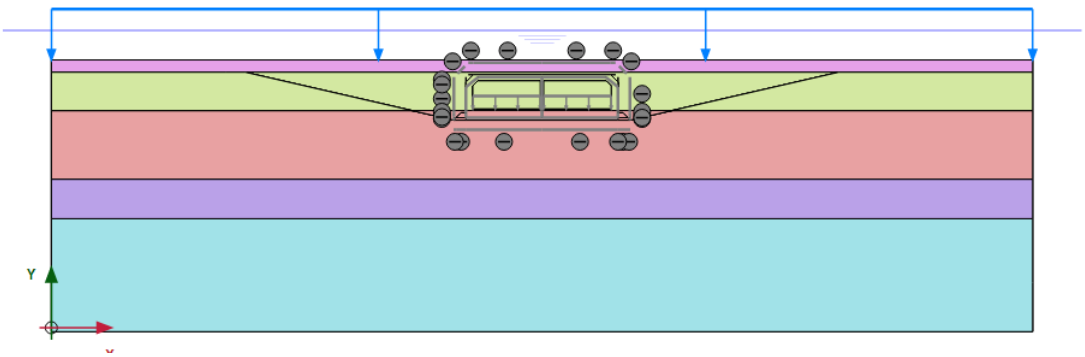

Figure 5.1: Model shape

After the construction of the tunnel was completed, the tunnel management office commissioned a professional agency to conduct long-term monitoring of the tunnel. The monitoring was interrupted from 1978 to 2001, and testing has continued since then. Total number of origin monitoring points are 50. As of November 2019, a total of 42 years of settlement monitoring has been carried out, and a large amount of data has been obtained to provide a reference for the analysis of long-term deformation of immersed tunnels. Figure 5.2 is the monitoring system arrangement. The monitoring points are set in joint positions. In the initial monitoring point setting, the odd numbers are located in the north side of the tunnel, and the even numbers are located in the south side of the tunnel. According to the trend, the largest settlement displacement is at point 12, which is also the most dangerous cross-section.

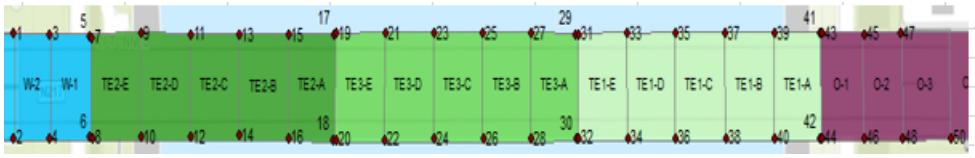

Figure 5.2: Arrangement of settlement measuring points

5.3. Python data analysis

Monitoring systems are installed to get the trend of tunnel settlement. At point 12, the settlement is the most severe. Data shows that the total settlement is 72.5mm from July 1st 1977 to 15th Nov 2019. And the settlement trend is presented in figure 5.3. However, the data was lacked from apri 78 to jul 01. The dotted line represents the approach line obtained by the logarithm of the actual settlement curve. The estimated expression is :

$$S = -12.3 \times \ln(Time) + 49.45 \tag{5.1}$$

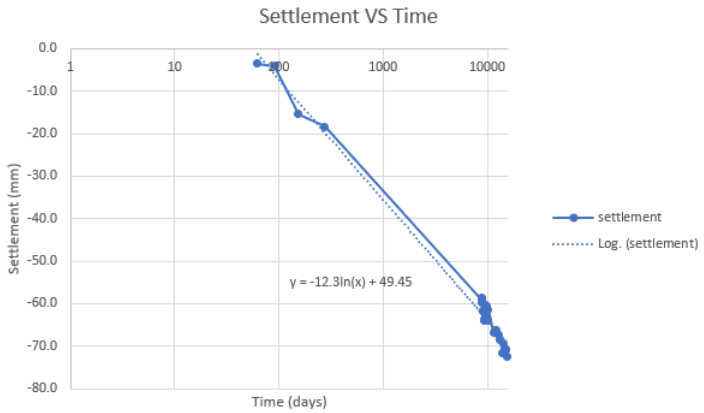

Figure 5.3: Settlement of point 12

Linear regression model and logaritmic regression model are two methods for python to do the data analysis, which is derive from the available data. This could be a method that can compare with the PLAXIS model results, do more accurate matching and predicting. In statistics, linear regression is a linear approach to modeling the relationship between a dependent variable and one or more explanatory independent variables. Logistic regression is a statistical model that in its basic form uses a logistic function to model a binary dependent variable. According to the monitoring data at point 12, linear regression analysis is performed using python, and the resulting trend graph is shown in Figure 5.4.

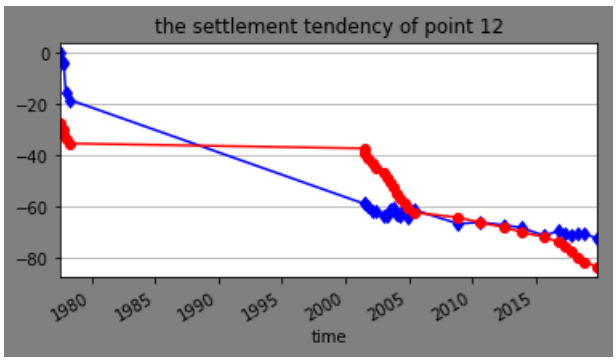

Figure 5.4: Real trend (blue) and predicted trend (red) for linear regression model

Obviously, the linear regression model is not proper, even though some parts are perfectly matched. How-

Method	10 years	20 years
Excel	-51.44	-59.97
Python	-54.29	-58.87
Error	5.24%	1.83%

Table 5.3: Results comparison between excel and python

ever, the logaritmic regression model can fit the trend of the data well, including the missing estimates which was lacking from apri 78 to jul 01. Figure 5.5 is the trend of settlement data between Jul 77 to Dec 01. At the end of the logaritmic regression model, the settlement data on 31st October is 60.2mm, the real monitoring settlement is 59.8mm, which proves the relative accuracy of the logaritmic regression model. The model shows the general formulation to estimate the settlement is:

$$S = (-15.24) * log_{10}(Time) \tag{5.2}$$

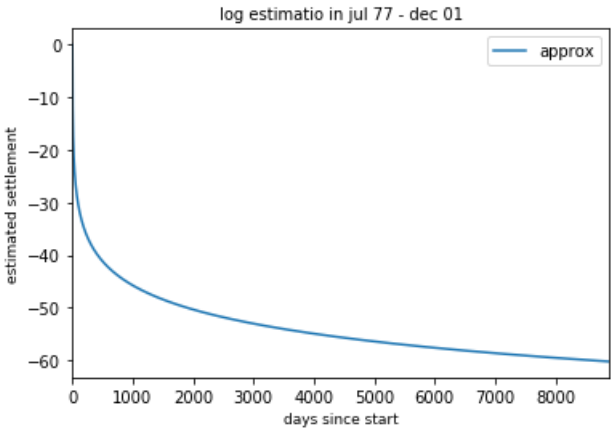

Figure 5.5: Settlement estimation from Jul 77 to Dec 01 with logistic regression model

Comparing the two expressions, using the ten and twenty years after 1st July 1977 as a reference to compare the results. From table 5.3, the errors between two methods are small, which proves the validity of python expression.

The expression is estimated by the monitoring data. However, the monitoring system started to work on 01-07-1977, the last immersed element is on 06-12-1976, there is almost half year gap. Using the above expression to retrieve data, the settlement should be 35.327mm on 01-07-1977. In other words, the monitoring data should be increased by 35.327mm, which is the real settlement data simulated by logaritmic regression. The expression becomes:

$$S = (-15.24) * log_{10}(Time) + (-35.327) \tag{5.3}$$

Even though the above expression is based on reasonable conjecture, compare it with PLAXIS to see what the difference is. The above expression is mainly based on the data of 1978 and 2001 to predict the missing period from 1978 to 2001. Therefore, the time distribution of comparison in the figure below is 1978 to 2001. The plot is shown in figure 5.6.

It is clear to check that the two curves match in the initial settlement, but as time increases, the value of the python model becomes smaller and smaller than the value of PLAXIS. Practically, this situation will exist, for two possible reasons. On the one hand, this expression estimates the values in the 1978-2001 which is a gap, the settlement changes most dramatically during this period, the consolidation curve indicates that settlement in construction phase and after stabilization of consolidation tend to be more linear rather than logaritmic. On the other hand, a constant 35.327mm might not be precisely describe the settlement between 06-12-1976 and 01-07-1977 as it is uncertain that all soil layers behave the same over this time period.

According to the experience, around 50% settlement of the total settlement will concentrate on construction phase (Wei et al., 2014).If calibrate the expression obtained by python with this empirical conclusion rather than a constant, the calculation equation should be:

$$S = 2 * (-15.24) * log_{10}(Time) \tag{5.4}$$

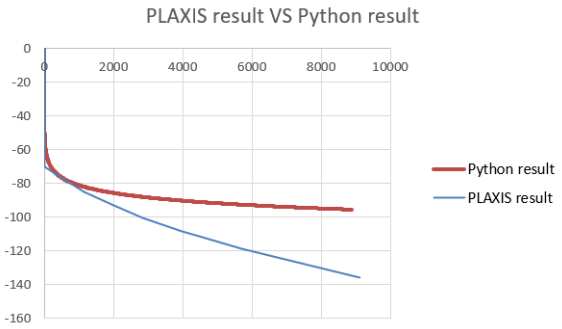

Figure 5.6: PLAXIS results VS Result under expression 5.3

Similarly, plot result derived by this expression with the PLAXIS result, the plot is indicated in figure 5.7. Compared with the previous plot, it is intuitive that this is a better match with the results of PLAXIS. Using equation 5.4 to calculate the settlement on 2019-11-15, the value is -0.128m, which is close to PLAXIS result of -0.162m, the error is approximately 20%. As a result, this equation should be more suitable rather than equation 5.3 which only follows a constant.

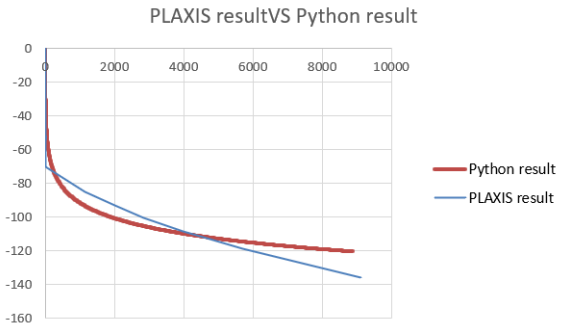

Figure 5.7: PLAXIS results VS Result under expression 5.4

5.4. Settlement

5.4.1. General final result

According to the monitoring data, the north side and the south side settlement are 67.6mm and 72.5mm. Because of the little difference of these two sides, we will assume the settlement is uniform everywhere in this cross-section.

The last immersion tube was immersed on 6th Dec 1976. However, the monitoring data started on 1st July 1977, the settlement data was set to be zero on this time. As a result, approximately 8 months time gap was brought about. Actually, the monitoring data is smaller than the real settlement data. According to experience, 50% of the total settlement will occur during the first six months after the final immsersion. This gives the estimation of total settlement of 0.145m.

Selecting three points which are at left corner, middle point and right corner of tunnel tube separately. Figure 5.8 is the indication of the settlement of cross section for the three points.

Red node 28933 is at the left corner of tunnel tube bottom which corresponds to north side, blue node 47840 is at the middle and the pink node 57757 is at the right corner which corresponds to south side. The time span is from 6th Dec 1976 to 15th Nov 2019, the total settlement of each part are -0.166m, -0.151m and -0.162m, separately.The settlement derived from python regression model has about 30% error compared with the above result. The possible reasons are already explained in above section. Comparing with the manual calculation, 0.249 is bigger than the results from PLAXIS, two possible reason for this. One is that actual compressive modulus is higher than unloading reloading stiffness, other is consolidation degree is smaller than calculated consolidation degree.

There is slightly difference between north part and south part, the north part settlement is bigger than

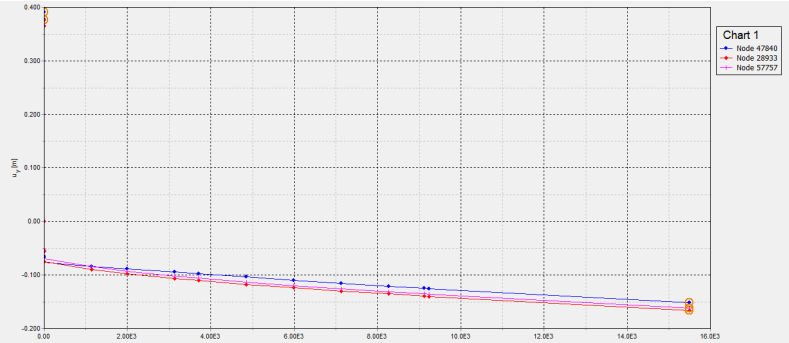

Figure 5.8: Settlement of cross section at point 12 in PLAXIS model

south part.It is obvious that the settlement accumulates rapidly at the beginning phase. The settlement of north point, middle point and south point are considerately 74mm, 76mm and 70mm after backfill. These points are the turning points of the settlement curve. Besides, the corresponding settling time is very short. Six months after the last tunnel element was immersed, the settlement values at the three points are 79.2mm, 78.9mm and 74.2mm. These values also illustrate that 50% of the total settlement will occur during the first six months after immersion.

In order to check the matching degree of PLAXIS and monitoring data, and double the monitoring settlement value, the two sets of data are plotted and compared as well. Figure 5.9 is the result. It can be seen from the plot that the results of the two methods do not match very well at the beginning, which is mainly due to two reasons. On the one hand, there is a lack of data between 1978 and 2001, so it is difficult to determine where the turning point of settlement is. This part is derived specifically in Python data analysis, but there are still uncertain factors. On the other hand, in stage construction setting of PLAXIS, the calculation type of phase 1 to phase 6 are all plastic calculation, the time interval setting does not affect any calculation result and the default value of this aspect is 1 day, as a result, the range of each scale on the x-axis is very small, this can also cause the two curves to display differently. After 2001, the settlement monitoring values are all known. If compare the values in this period, it is easy to find that the two curves are close, and the estimated error is about 15%, which is an acceptable error range. In conclusion, the validity of PLAXIS simulation is proved.

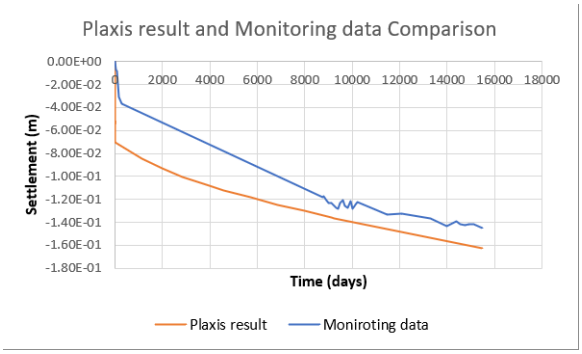

Figure 5.9: PLAXIS result and monitoring data comparison

5.4.2. Phases details

Phase 2: Trench Dig

In this phase, the vertical deformation distribution is indicated in Figure 5.10. From the vertical deformation distribution produced by PLAXIS, it clearly presents that the rebounding phenomenon happened. The middle part has the largest rebounding and the amount is 0.39m, different colour means spread from middle to outside and becomes weaken gradually. In addition to the bottom of the trench, the soil slopes on both sides of the trench also rebounded. The bottom of the trench is sandy clay, and then is fine sand below. It can be clearly seen from the figure that the distribution of the rebound displacement of the soil in the clay is curved

semicircular, while in the sand it is almost vertical, the curve distribution of the last layer and the penultimate layer of clay can be complementary.

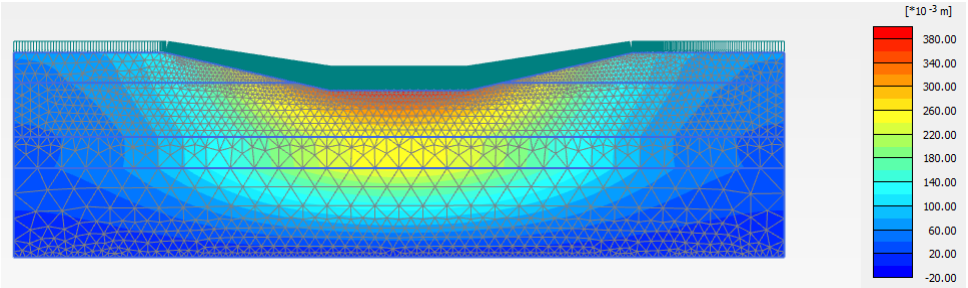

Figure 5.10: Vertical deformation in phase 2 (after trench excavation)

The effective stress distribution in this stage is on Figure 5.11. The contour still presents an inverted w shape. At the bottom of the trench, the stress is positive then becomes negative, which corresponds to the rebounding trend.

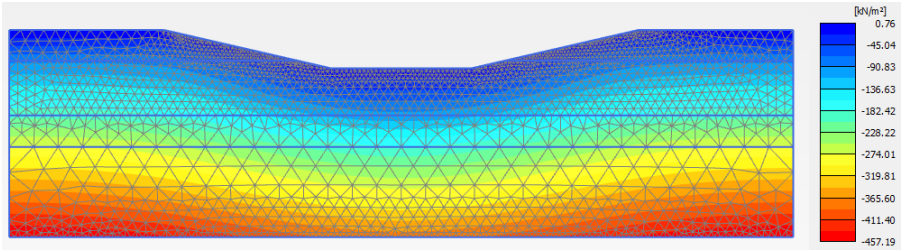

Figure 5.11: Vertical effective stress in phase 2 (after trench excavation)

Phase 3: Applied sand-flow foundation

Figure 5.12 is the vertical deformation distribution in this phase. Comparing to the last phase, rebounding amount reduced and it becomes 0.377m. Because the amount of rebounding of the lower sandy clay is too large, the foundation layer produces the same amount of rebounding. The distribution is the same with the last phase. During the construction of the sand-flow foundation, the load of the foundation is much smaller than the soil load generated by the excavation of the foundation trench. Therefore, the soil layer at the bottom of the trench continues to absorb water and rebound, but the rebound speed will slow down.

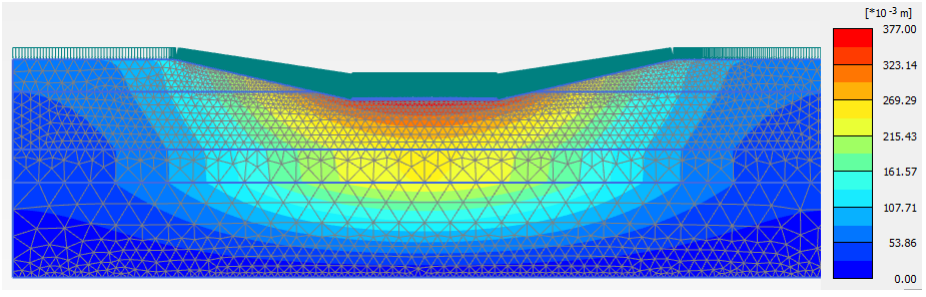

Figure 5.12: Vertical deformation in phase 3 (after sand flow foundation applied)

The effective stress distribution in this stage is the same with previous stage, the only difference between these two is the value. Due to the sand-flow foundation load, the minimum value of the effective stress reduced, nevertheless, maximum effective stress remains the same, and the maximum value is at the bottom of soil model. At the top of the foundation surface, the effective is positive which means the rebound still occurs, then value becomes negative gradually from top to bottom.

Phase 4: Put tunnel on the foundation

In this phase, the settlement distribution changes. After the tunnel pipe was installed, the vertical displacement changed from rebound to settlement due to the newly added load. The maximum settlement is 0.07m. It can be drawn from the empirical values summarized in the relevant literature that the settlement during the construction of the immersed tunnel is 20-80 mm, with an average value of 60 mm, accounting for 50% -60% of the final settlement. Maximum settlement for sand-flow foudation is 0.07m, however, from the middle to the edge, the settlement of the bottom foundation layer is reduced from 0.07m to 0.035m. At the same time, the results show that the concrete tunnel tube also have some deformations, but they are very small, so as to ignore. Besides, the range of settlement has been significantly reduced, mainly concentrated within 20m outward of the tunnel edge. Similarly, the distribution curve of clay is curved, while the sand is almost vertical.

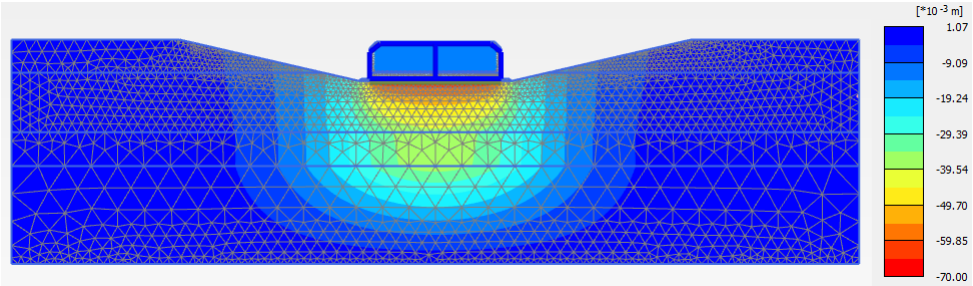

Figure 5.13: Vertical settlement in phase 4 (after tunnel placement)

After the immersion tube is placed, the effective stress increased a lot. However, most of the relative large effective stress are concentrated in concrete tunnel tube. The soil effective stress has little difference with the last stage, even for the maximum stress value. The effective stress for the sand-flow foundation increased, which is obvious for the increase of load on the top. It can be concluded from the stress distribution in the concrete that the inside of the vertical wall on both sides and in the middle of the wall of the tunnel tube are the most stressed, and in addition, the stress is greater at each corner, which may be caused by the stress concentration phenomenon. On the contrary, the outside of the walls on both sides of the tunnel tube, the stress changes from negative to positive, which means that the stress on the outside of the walls on both sides of the concrete tube is tensile rather than compressive.

Phase 5: Tunnel fix

At this stage, concrete toes are mainly poured on both sides of the tunnel in order to fix the tube. Compared with the previous stage, the settlement range is expanded, but the expanded area is not much because of the little amount of applied load. Except for the maximum settlement from 0.07m to 0.075m, other aspects almost remain the same as the previous stage.

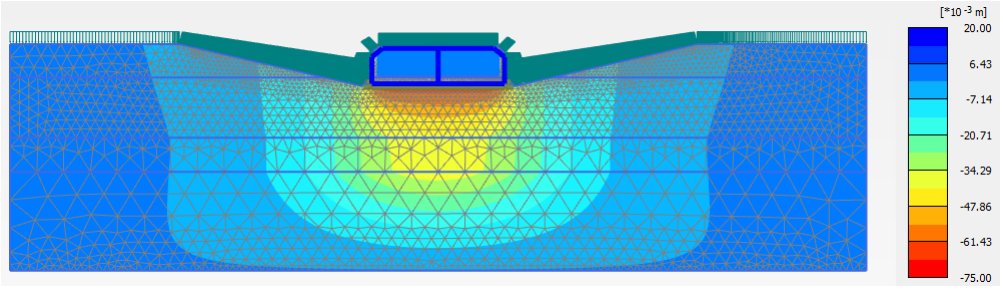

Figure 5.14: Vertical settlement in phase 5 (after adding tunnel toe)

Comparing to the past stage, the compression stress and tensile stress increased after the installation of the toes. The effective stress of the foundation layer reduced a bit, possibly because the foundation layer is drained after placing the tunnel, and the load applied at this stage is not very large. Other conclusions are consistent with the previous stage.

Phase 6: Backfill tunnel
After this stage, the tunnel construction is completed. The tunnel backfill material uses a synthetic silex, which has a larger particle size than pure sand. Then, the top layer is humic clay. The surface soil overlying the tunnel has the largest settlement and is not very uniform. The settlement range of the backfill soil on both sides of the tunnel is 0.05 to 0.17 meters. It spreads outward from both sides of the tunnel, and the settlement amount gradually decreases. Similarly, the settlement distribution curve is arc-shaped. The settlement displays in this stage is the construction settlement, which is one of the part of total settlement. The sandy clay under tunnel is from 0.049m to 0.08m. And the bottommost sandy clay is from 0m to 0.045m. For the foundation layer at the bottom of the tunnel, there is almost no change in the lateral settlement, but in the longitudinal range, the foundation layer settlement is about 0.09m to 0.077m from top to bottom. The estimation of sand flow foundation settlement is 0.055m under E_s equals 0.833MPa. This value is smaller than the result by PLAXIS. Using foundation settlement estimation formula, the compressive modulus of sand foundation is in the range of 0.51 MPa to 0.597MPa, which means the foundation is more compressible than expected. This might be caused by loose sand during the foundation layer construction. In the bottommost sandy clay, the settlement at this stage is about 5mm, which is slightly lower than the settlement at the previous stage.

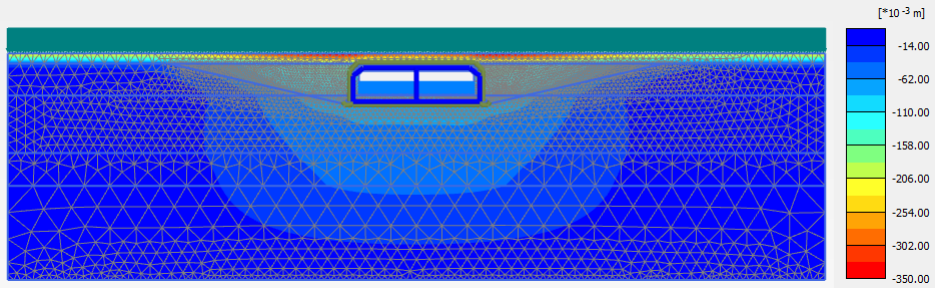

Figure 5.15: Vertical settlement in phase 6 (after backfilling trench)

After the backfill is completed, the tension on the outside of the walls on both sides of the tunnel tube increases, and at the same time, the compression stress increases significantly, which leads to the more obvious stress concentration at the corner. Backfilling causes an increase in the load on the foundation layer and the upper part of the soil, so that the effective stress increases significantly. The effective stress at the bottom of the foundation layer is about 130 kPa. Furthermore, the effective stress of the soil in the backfill area is relatively large as well.

Moreover, the excess pore water pressure starts to accumulate. Considering the characteristics of consolidation, in the flow condition at this stage, the model boundaries of all clay layers are closed, leaving only the sand layer, that is, only the sand layer is draining. Distribution shows in Figure 5.16. The maximum value 125.1 Kpa. The distribution of two sandy clay layers are consistent.

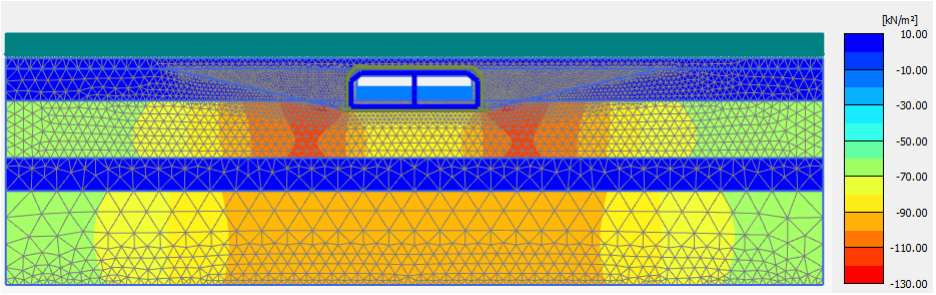

Figure 5.16: Excess pore water pressure in phase 6

Phase 7: Consolidation for 9152 days
Due to the serious leakage in 2001, the consolidation is separated to two phases. The time span of this phase is from 1976 to 2001 and the figure 5.17 indicated the condition before the serious leakage. The largest settlement still locates on the top surface of the model. Obviously, the distribution contour shape changes from

the original u-shape to an inverted w-shape. The settlement of the sand-flow foundation tends to be stable and the value is 0.14m. This value is almost twice the amount of foundation settlement in the previous stage. The settlement range of the backfill soil on both sides of the tunnel is 0.1 to 0.24 meters. In addition to the largest settlement in the middle of the model, large settlements occurred on both sides near the model boundary, as well. At this stage, the sandy clay and sand layers in the lower part of the tunnel are affected more by settlement, while the sandy clay at the bottom is less affected.

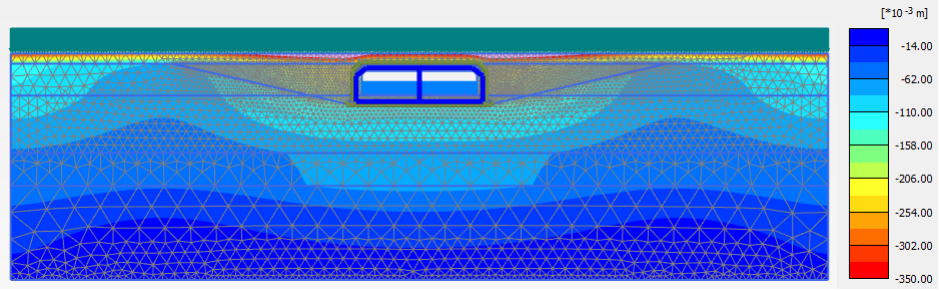

Figure 5.17: Vertical settlement in phase 7 (after consolidation of 9152 days)

Through more than 20 years of settlement, the tension on the outside of the walls on both sides of the concrete tube increases, which may be caused by settlement, while the compression stress on the inside and the corners does not change much.

Whereas the excess pore water pressure changes, the detail is in Figure 5.18. The maximum value of pore water pressure changed from 125.1kpa to 95.07kpa since the dissipation of water. Because of the length of the drainage path, the drainage is faster in the area near the model boundary, and the pore water pressure becomes 0. The closer to the middle, the greater the pore water pressure. For the sandy clay in the lower part of the tunnel, the pore water pressure dissipates more than the sandy clay at the bottom as the double-sided drainage path. It is obvious that the pore water path in the sand layer is vertical, while the clay layer is curved.

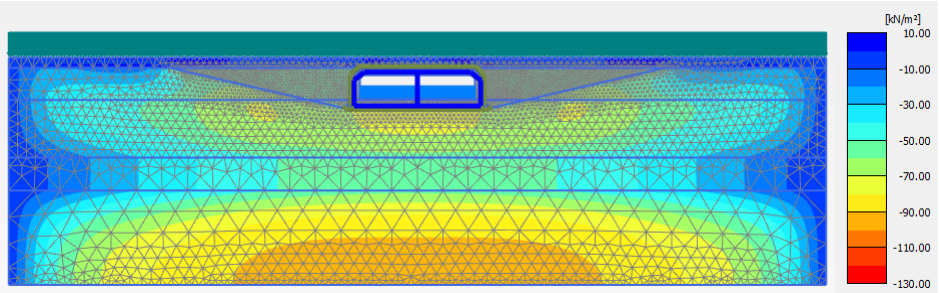

Figure 5.18: Excess pore water pressure in phase 7 (after consolidation of 9152 days)

Phase 8: Leakage

At this stage, the boundary condition in the right bottom of the tunnel is set to be inflow, the aim of this is to simulate the leakage. According to the results, there is nothing difference with the last stage and so is the contour of the settlement distribution.

Effective stress distribution and pore water pressure distribution remains the same with the last stage.

Phase 9: Consolidation for 6250 days

The time span of this phase is from 2001 to 2019 and the figure 5.20 indicated the condition after the serious leakage. Contour still shows an inverted w-shape. The settlement range of the backfill soil on both sides of the tunnel is 0.15 to 0.27 meters. Comparing to the last three stages, settlement increment of the backfill soil which is next to the tunnel is tiny, but the increment near the trench slope is larger than inside part. Apart from this, the contour slope of the distribution becomes slower, and the settlement range on both sides near the model boundary is further expanded. The settlement of the point at foundation stabilized to about 0.15m. The settlement range of sandy clay underneath the tunnel is from 0.09m to 0.18m, thus the

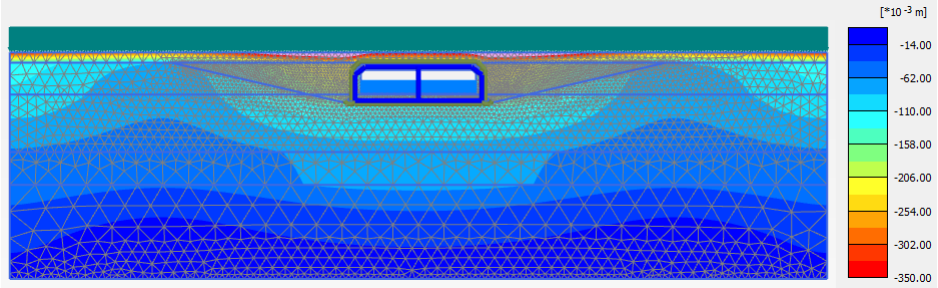

Figure 5.19: Vertical settlement in phase 8 (after leakage happen)

consolidation settlement is 0.041m to 0.1m. Besides, the bottommost sandy clay is from 0m to 0.09m, hence the consolidation settlement for this layer is in 0m to 0.045m. The manual calculation shows the settlement of these two layers are 0.0908m and 0.158m. Comparing to the results of model, sandy clay under tunnel is close for the two method, while the bottommost sandy clay is far greater than model shows, meaning the bottommost sandy clay is much more stiffer than thought.

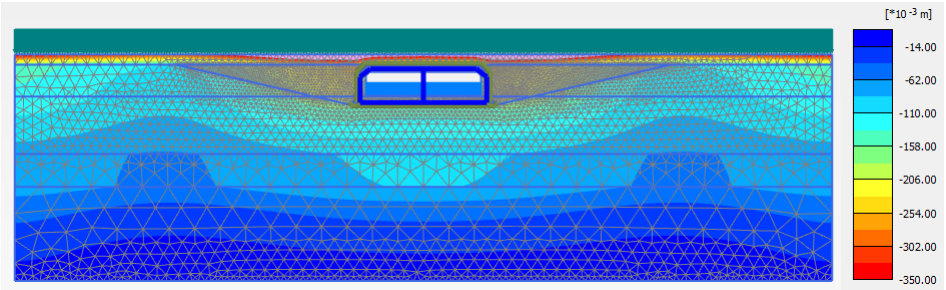

Figure 5.20: Vertical settlement in phase 9 (after consolidation for 15530 days)

Effective stress tends to be stable, the change value is very small compared with the previous stages. The distribution contour is changed from the inverted w-shape to a gentle v-shape as well. The pore water pressure is further reduced, and the pore water pressure has changed from the previous maximum 95.07kpa to 92.12kpa. The cloud map shows that the maximum value is in the bottom sandy clay layer. The relatively small difference indicates that the bottom sandy clay layer drains more slowly than the sandy layer below the tunnel. This feature is particularly evident in the dissipation of the water in the sandy clay layer below the tunnel. More pore water close to the model boundary is drained. Not only that, the pore water pressure in the backfill area is further reduced.

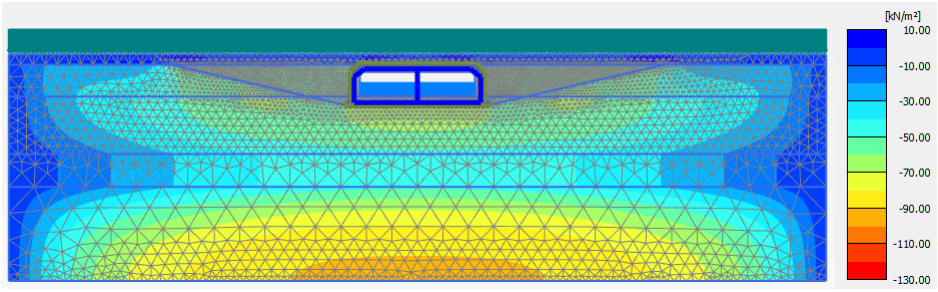

Figure 5.21: Excess pore water pressure in phase 9 (after consolidation for 15530 days)

5.5. Assumption verification

In chapter 4, two assumptions are made to explain the settlement and leakage. With the help of model data, verify in this section whether the assumptions previously proposed is correct.

Assumption 1
Sand-flow foundation settlement is one main part of total settlement. In line with the experience, immersed tunnel foundation and the treated methods of it have a significant impact on the final settlement. In Kiltunnel, the material of foundation is loose sand. The detailed properties of foundation material is in table 3.14.

In assumption 1, leakage influence was considered as a main cause of settlement. For the standard model with an inflow on the right bottom side of the tunnel,the estimated settlement of the sand-flow foundation is 0,14m, which is indicated in phase 7. Keeping other variables unchanged, increasing the value of inflow to 100 times, the settlement of the foundation still remains 0.14m. In conclusion, the leakage inflow will not impact the settlement.

Although the inflow will not affect the settlement of the tunnel, changes in the composition of the base layer itself may affect settlement. Water pressure in the crater linearly increases within the sand deposit radius. The closer to the periphery of the pancake, the greater the water pressure, which means that the sand will be washed away by the undercurrent and taken away. After the sand is washed away, the nearby clay layer may flow in, and soft soil leads to big settlement.

In assumption 1, the sand of the foundation layer was washed away by water, causing the bottom sandy clay to be mixed into the foundation layer, which led to the settlement and leakage. This is suspected. However, does the foundation layer change from sand to soft soil really affect the tunnel settlement? This question still remains. In order to answer this question, two tests are simulated in PLAXIS model.

scenario 1:

At the beginning of phase 3, the whole sand-flow foundation layer was replaced by the material of sandy clay, the settlement value between the pure sand situation and pure sandy clay situation are compared. The results are indicated in table 5.4.

Stages	Backfill Tunnel	Consolidation 1	Leakage	Consolidation 2
Settlement with pure sand	0.09 - 0.077	0.14	0.14	0.15
Settlement with pure sandy clay	0.096 - 0.08	0.147	0.147	0.165

Table 5.4: Settlement comparison with different foundation material

The data clearly presents the difference in settlement caused by the two material types. After the backfill is completed, the difference in instantaneous settlement caused by the foundation layer is not very large because of the short time. While the difference became about 7mm after more than 20 years of consolidation, which was 5% more than the clean sand foundation. Apparently, the difference in settlement further increases until the end of 2019, the settlement becomes 0.165m. Compared to the pure sand foundation layer, the settlement of the pure sand clay foundation layer is increased by 10%, which could lead to more severe leakage. Consolidation is a long-run process, the data difference between these two types from the above table clearly illustrates the impact of the soft soil foundation layer on the settlement of the tunnel. The differential settlement of the tunnel makes the tunnel cracking easier. However, even if the sand at the edge of the pancake was washed away, the lower sandy clay layer entered the base layer, and often only that part of the soil layer was mixed instead of the whole layer. Will the difference still be so large, or will it be reduced? This is a new problem in the process of verifying the Assumption. In order to answer this, new test was took to simulate in PLAXIS.

scenario 2:

In this test, the foundation layer is divided into four parts, as shown in the figure below. The number of each part is 1, 2, 3, 4 from left to right. Scour and soft clay invision is a time-dependent process. As a result, the time span of consolidation 1 is divided into two phases, one with 6125 days, another is 3000 days. The changes in material properties of various parts in pancake shows in table 5.5.

Keeping other variables the same, the results in table 5.6. It is very obvious that settlement is less than pure sandy clay in consolidation 1 and leakage phase. This should be in line with the actual situation. However, the settlement in consolidation 2 incredibly increased to 0.172, this increment reaches 22.8% of the settlement of pure sand foundation. Despite the corresponding measures taken to repair after the serious leak occurred in 2001, some report of the kiltunnel still shows that there have been several leaks, although these leaks are not very serious. Thus, this phenomenon could be used to explain such large increment in test 2. Even though the leak was stopped in 2001 and the pancake under the tunnel was remediated, The previous sand was washed away and the effect of the soft soil being mixed into the pancake may persist. The settlement will

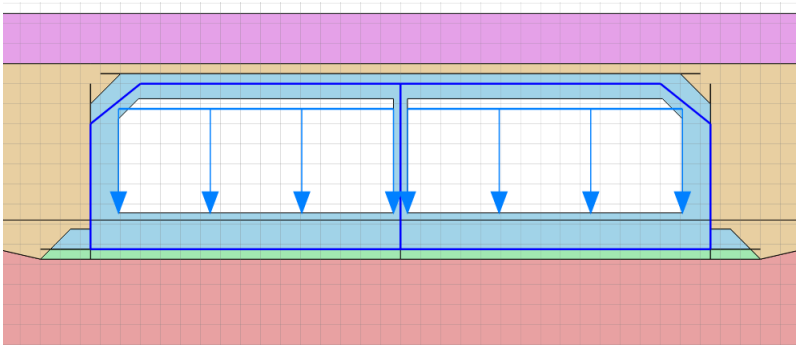

Figure 5.22: Area dividend for pancake test

Materials / Parts / Stages	1	2	3	4
Backfill Tunnel	Loose clean sand	Loose clean sand	Loose clean sand	Loose clean sand
Consolidation 1-1	Loose clean sand	Loose clean sand	Loose clean sand	Sandy Clay
Consolidation 1-2	Loose clean sand	Loose clean sand	Sandy Clay	Sandy Clay
Leakage	Loose clean sand	Loose clean sand	Sandy Clay	Sandy Clay
Consolidation 2	Loose clean sand	Loose clean sand	Loose clean sand	Loose clean sand

Table 5.5: Changes in material properties of various parts in pancake

occur again due to a long period of consolidation after the repair is completed, and may be larger than before, so that the previously repaired place is destroyed again. This could be an explanation for the increment and subsequent leak. But more reasonable data and complex plan are needed to fully verify this view. Here only as a hypothesis to support the previous data and facts.

Stages	Backfill Tunnel	Consolidation 1-1	Consolidation 1-2	Leakage	Consolidation 2
Settlement	0.09	0.1428	0.1432	0.1432	0.1722

Table 5.6: Settlement of scenario 2

Figure 5.23 displays of changes in settlement between original scenario and scenario 1 and scenario 2 more intuitively. Pink one is the original scenario data, orange one presents the scenario 1, and the blue one corresponds to scenario 2. In these three tests, except for the material variables mentioned in the above section, the other variables including the calculation stages involved are exactly the same. Owing to the different calculation time for different material, the final calculation steps between three tests which indicates on x-axis of graph look different. In the initial stage, the cohesion of sand is not as good as soft soil, so the amount of rebound is a bit larger than that of soft soil, but in the subsequent stage, the vertical displacement of the sand foundation layer is obviously smaller than the other two. And the vertical displacement of all sandy clay is larger than that of semi-sand and semi-sandy clay soil. Due to the scale, the difference in final settlement is not obvious as shown in the figure. In terms of the final settlement, from small to large, it is all-sand, all-sandy clay, semi-sand and semi-sandy clay soil. As for the phenomenon that the final settlement of semi-sand and semi-sandy clay soil is the largest, it remains to be discussed.

Through the data verification of the model, assumption 1 was proved to be a cause of settlement and leakage. The settlement data tables obtained from the model gives the hint that the difference between the foundation layers of different material types does exist, but the difference is not very large above all, hence, this is a minor factor, not the most important reason for the settlement of kitunnel.

Assumption 2

Before the construction of the tunnel, the levees on the east and west sides of the tunnel moved, which had a process of unloading and reloading the soil in the East and west directions. During the construction and operation of the immersed tunnel, it is actually the deformation process of unloading and reloading of the underlying soil layers. With the excavation of the foundation trench, the soil at the bottom of the trench will

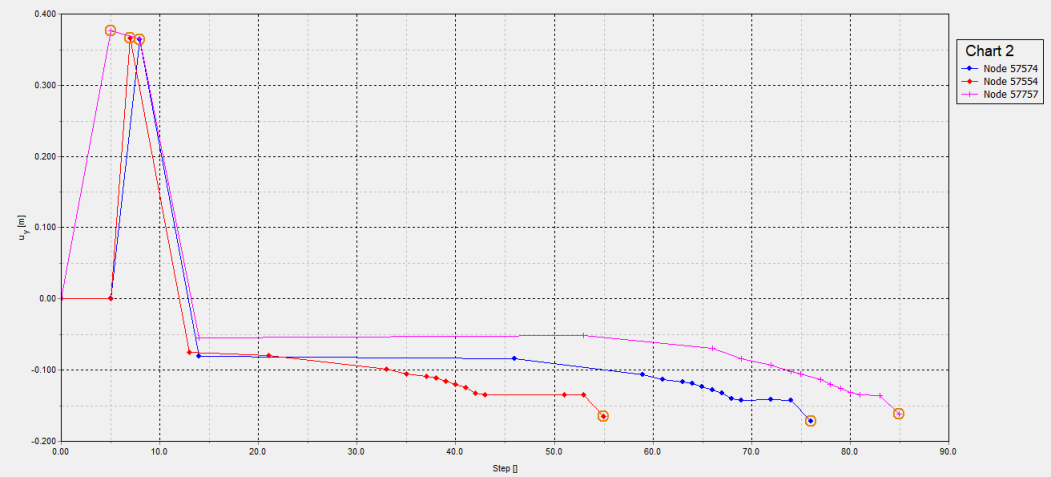

Figure 5.23: Settlement comparisn between original test (Pink) and test 1 (Orange) and test 2 (Blue)

rebound after unloading, and then the soil will be compressed again with the completion of the steps such as tunnel immersion, backfilling of foundation trench and silting. Soft soil generally has the characteristics of high water content, large void ratio, high compressibility and low bearing capacity. When unloading, it will have large rebound deformation, and when reloading, it will also have large compression deformation. Moreover, in the clay with low permeability, the rebound and compression consolidation of soil often last for a long time.

The Sensitivity Analysis and Parameter Variation facility is aim at evaluating the influence of model parameters on calculation results. The sensitivity score can be used to assess which of the parameters have a major influence and which have a minor influence. The middle point at the bottom of the tunnel is the reference point to do sensitivity analysis. The sensitivity score for the final stage is indicates in following figure.

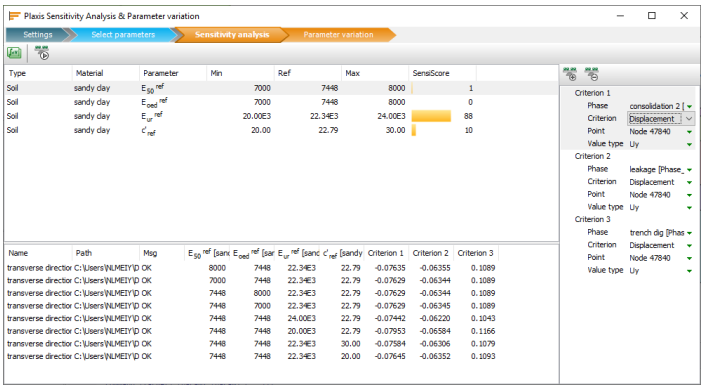

Figure 5.24: Senstivity analysis for consolidation 2 phase

From the score table, reference stiffness in unloading and reloading is the most sensitive factor and the secant stiffness from the triaxial test is the least sensitive factor.

The last stage is leakage. Whether the leakage has an effect on the final result of the sensitivity analysis is also unknown. Another sensitivity analysis which operates in leakage was tested, and the result is indicates in figure 5.25.

As the score presents, stiffness in unloading and reloading is still the most sensitive factor, and slight difference between the secant stiffness from triaxial test and tangent stiffness from oedometer test. As above mentioned, there are some process which comes to unloading reloading as well in tunnel construction. It is not enough to infer from the above two results that the influence of levee relocation on the tunnel plays the predominant role. Advance the time point for sensitivity analysis to trench dig phase, and the result is in below.

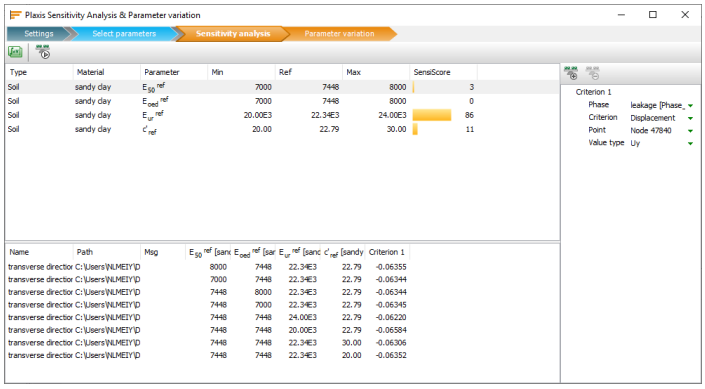

Figure 5.25: Sensitivity analysis for leakage phase

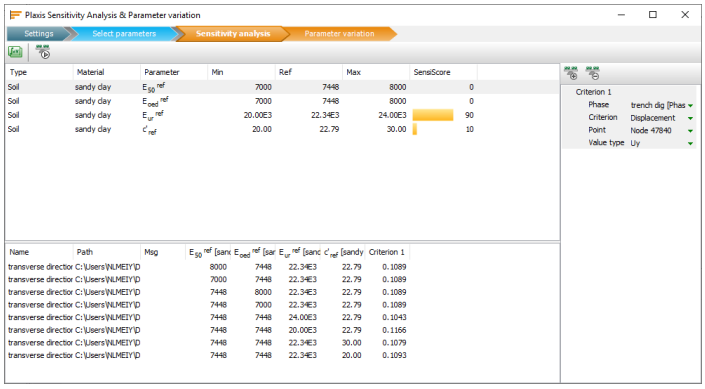

Figure 5.26: Sensitivity analysis for trench dig phase

From the above three figures, it is obvious that the soil layers which underneath the Kiltunnel is very sensitive to the stiffness in unloading and reloading, and even before the construction of tunnel. This is a strong evidence for the impact of relocation of the levee. It is the movement of the levee before the construction of the tunnel that causes the change of the parameters of the underlying soil layers then settlement during and after the tunnel construction. There are two time of unloading reloading process. On the first unloading, weight change equals to levee weight, then weight change is smaller than levee weight on first time reloading. In second time, weight removal is the trench soil weight on unloading whereas weight of reloading is tunnel weight and backfilled soil weight. The weight of the levee is the maximum stress in the history, other loads are all smaller than this. According to the unloading reloading curve, the stress change after the relocation should be linear, which means the settlement change more tends to be linear, this could be a reason to explain the settlement exceeds the expectation so much.

In conclusion, two assumptions which indicates in chapter 4 are all verified to be plausible. The main reason for the Kiltunnel settlement is the relocation of the levee, causing stress changes in the underlying sensitive soil, thus influenced subsequent tunnel construction settlement and consolidation settlement. In addition, the sand of sand flow foundation being washed away and soft soil mixed is another reason that can contribute to cause the serious settlement of Kiltunnel. Although the remediation measures were made, it might happen again for scour and cause settlement and leakage.

5.6. Tide Influence

Dordtsche Kil is located above the Kiltunnel, it is a short river in South Holland in the Netherlands and is a part of the Rhine Meuse estuary. The river is tidal and forms the connection between the Oude Maas river and the Hollands Diep. According to the geology recording, the Rhine Meuse estuary had two open connections to sea which are the Nieuwe Waterweg and the Haringvliet. Not only the water level, but also the phase and amplitude of the tide between southern and northern part were comparable. Then the Haringvlietdam was constructed, resulting in the diminishment of the tide and much larger water level difference between north and south, as well as much higher flow velocities in connecting branches. As a result, these branches show

scour hole, and one of these branches is Dordtsche Kil, figure 5.27 is the map of the Rhine-Meuse estuary (Harris et al., 2016).

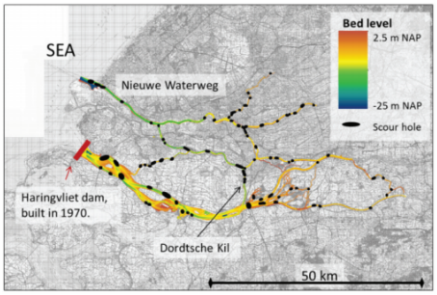

Figure 5.27: The Rhine Meuse estuary condition

The map also displays that Dordtsche Kil locates in scour hole region. Combining with the content in assumption 1, it can be explained the original cause for the change of sand-flow foundation.

Even though it mentioned that the tide is diminished, some slightly change still happens. Figure 5.28 is presented in settlement trend. From the curve, there is slightly change for settlement, concentrates in operating phase. Two main reasons are explained in this phenomenon. One reason is temperature fluctuation, the other is tidal fluctuation. In the research of Bob van Amsterdam, it has already mentioned that the initial settlement at the edges of the middle element of the Kiltunnel due to temperature fluctuation is between 0.06 and 0.08 mm and the settlement at the edges of the middle element of the Kiltunnel in 2018 is between 0.42 and 0.55 mm. The results shows a small influence on the settlement measured at these joints (van Amsterdam, 2019). Due to the influence of tide, the settlement value of immersed tunnel fluctuates to a certain extent. This fluctuation occurs in the whole operation period of immersed tunnel, does not change with time and absolute settlement of tunnel, and the value is basically unchanged (Xie et al., 2014).

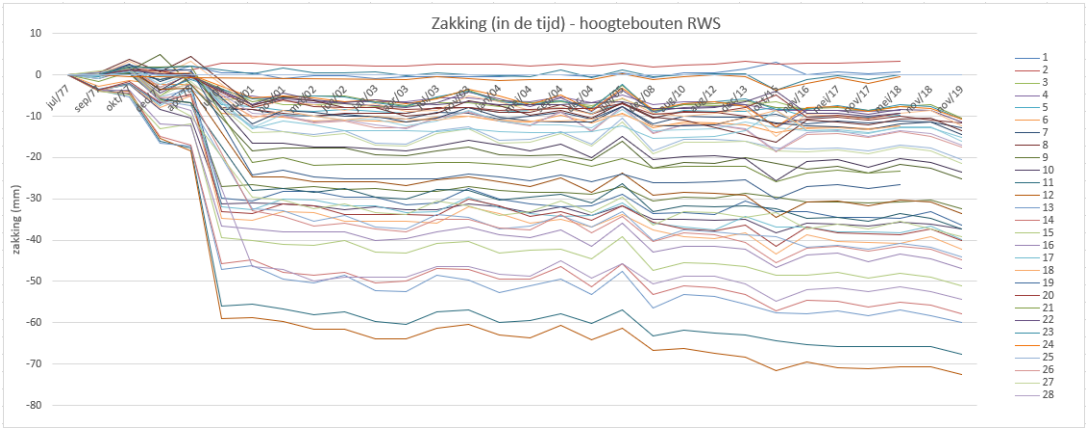

Figure 5.28: Settlement trend for different point in longitudinal direction

According to the settlement trend, the amplitude of upward and downward of tunnel obviously exceed the results derived by temperature fluctuation, therefore, the upward and downward which are shown in settlement curve is mainly originated by tidal fluctuation. The daily tidal change of Dordtsche Kil forms a cyclic load on the immersed tunnel and the underlying soil layer, and the soil layer is in the reciprocating change of compression rebound for a long time. The tunnel structure is constrained by the surrounding soil layer and changes with it, so the settlement always changes periodically. From the curves, settlement is larger in winter and the difference is around 6mm. And the soil settlement is less and soil tends to be rebound in summer, the rebound value is approximately 5mm. The comparison in these two are almost the same, which corresponds to the theory mentioned above.

Above all, tide effects indeed exists, settlement curves can be an indication for this. The fluctuation of tide makes the difference of water level between high and low tide. In addition to the self weight, the immersed tunnel element bears the pressure above the tube top and water pressure. The water level is variable, that is to say, the pressure on the immersed tube is dynamic, there is no pile foundation under the kiltunnel element,

and most of the soil layer underneath the tunnel is soft soil, as a result the settlement of the underwater tunnel segments is dynamic, as well. The data shows that the seasonal tide changes make the settlement of the tunnel fluctuate about 6mm, accounting for 6% to 9% of the final settlement, and the fluctuation of the settlement occurs in the whole tunnel operation period, which does not convert into the permanent settlement of the tunnel.

5.7. Prediction

5.7.1. Final condition

The future settlement trend is another focus besides the current settlement study. Taking ten years as a time, the settlement after 50 years is predicted by PLAXIS simulation which is given in figure 5.29.

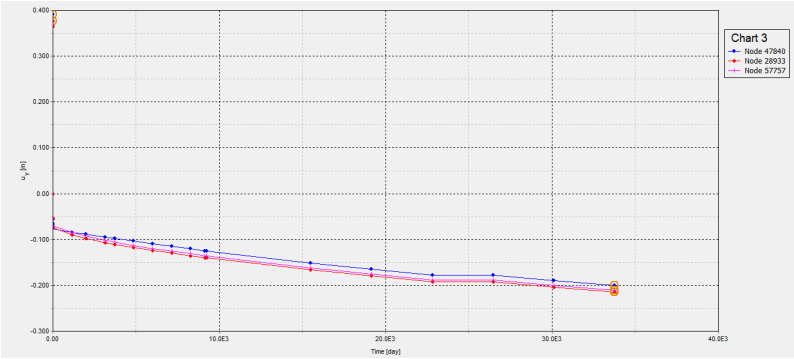

Figure 5.29: Prediction settlement for in next 50 years

The following table is an assemble for the settlement in different time at different point.

settlement \ time / point	10 years	20 years	30 years	40 years	50 years
Node 57757(South)	-0.176	-0.188	-0.188	-0.2	-0.211
Node 47840(Middle)	-0.165	-0.178	-0.178	-0.189	-0.2
Node 28933(North)	-0.179	-0.192	-0.192	-0.204	-0.215

Table 5.7: Settlement in different time at different point.

The data in table displays that the settlement is very slight comparing to the previous stages. Table 5.8 is the combination of settlement rate for every ten years. When the time node becomes 30 years, the settlement rate is 0, this might caused by numerical error, but after that, the data returns to normal, so the impact of this error is not significant. In the next 50 years, the rate of settlement change is in 0-7% every ten years. It can be concluded that from the table that the settlement in the north is slightly larger than that in the south, and that in the middle is the smallest, but all increase with time. And the settlement rate for each part seems stable, which illustrates that the change of settlement is linear with time. During the whole 50 year prediction period, the settlement growth rates of each part from north to south are 20.1%, 21.2% and 19.8% respectively.

settlement rate \ time / point	10 years	20 years	30 years	40 years	50 years
Node 57757(South)	8.64%	6.83%	0%	6.38%	5.5%
Node 47840(Middle)	9.27%	7.88%	0%	6.18%	5.82%
Node 28933(North)	10.49%	7.26%	0%	6.25%	5.39%

Table 5.8: Settlement rate in different time at different point.

5.7.2. Phase details

Phase 10: consolidation for 10 years
This is the prediction after 10 years from now. The consolidation settlement distribution is given in figure 5.30. In this phase, the distribution is almost the same with last stage except the value becomes larger. Among them, the settlement of backfill soil on both sides of the top of the tunnel is the largest, reaching 0.28m. The settlement range at the left and right boundary of the model is also slightly expanded.

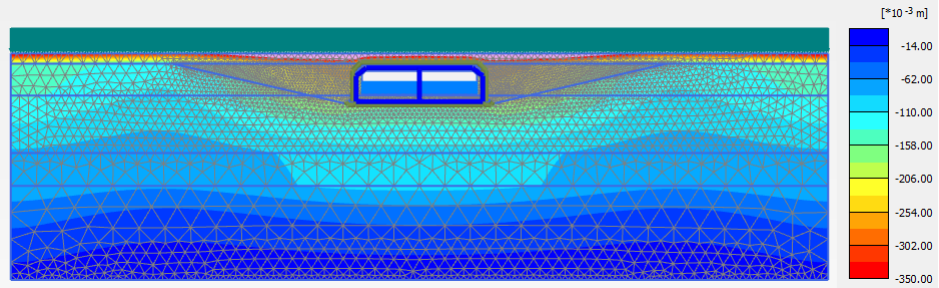

Figure 5.30: Settlement prediction for 10 years

In addition to consolidation settlement, excess pore water pressure is another important term as the consolidation process of soil is the process of excess pore water pressure dissipation and effective stress growth. The excess pore water pressure is shown in figure 5.31.

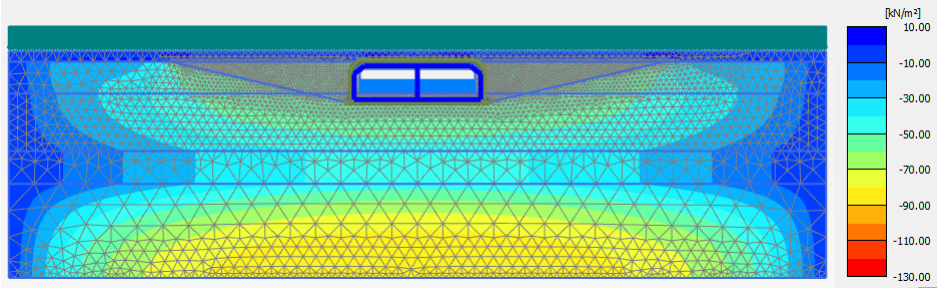

Figure 5.31: Excess pore water pressure in phase 10

In phase 9, the maximum excess pore water pressure is 92.12 KN/m^2, while it turned to be 89.81 KN/m^2. The area of pore water dissipation is slightly smaller than before, which means some part completed dissipation and most concentrated next to model boundary, this trend is uniform with previous stages.

Phase 11: consolidation for 20 years
The settlement distribution over the whole model keeps the same, only value becomes larger. The backfill soil near the top of the tunnel reaches 0.3m.

The excess pore water pressure displays in figure 5.32. The maximum value is 87.1 KN/m^2, dissipation rate of excess pore water pressure in ten years is 3%. Water dissipates more to the boundary part. Sandy clay layer which is at bottom becomes smaller. The change of excess pore water pressure can be seen from the fine sand layer as well.

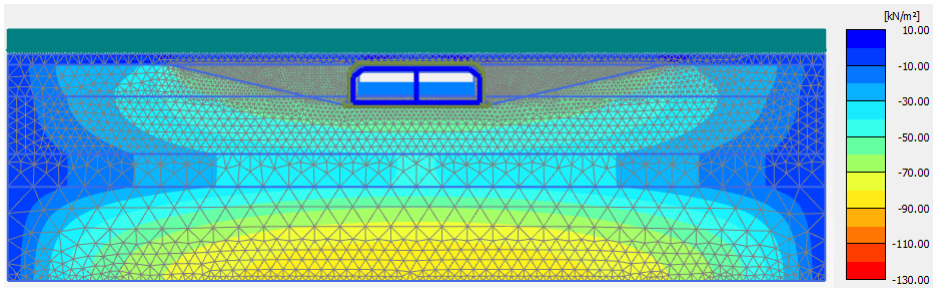

Figure 5.32: Excess pore water pressure in phase 11

Phase 12: consolidation for 30 years
In table 5.7, the settlement after 20 years is basically the same as that after 30 years, which is also applicable to the settlement distribution of the whole model, even for the backfill region, the settlement keeps the same. Consolidation process is relatively stable.

As for excess pore water pressure, consolidation settlement is caused by dissipation of excess pore water pressure, slight settlement change means slight excess pore water pressure change, which is displayed in following figure. The maximum value dropped a little to 86.9 KN/m^2.

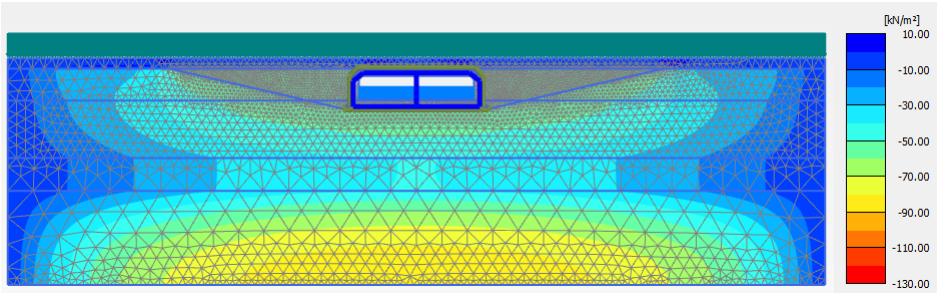

Figure 5.33: Excess pore water pressure in phase 12

Phase 13: consolidation for 40 years
At this stage, the settlement further increases. The settlement of the middle part below the bottom of the tunnel is greater than that of both sides. The settlement of backfill region increases to 0.33m. Others remain the same.

The maximum value of excess pore water pressure dropped to 84.11 KN/m^2. Although the distribution keeps uniform with last stage, the value changes, especially in fine sand layer, the excess pore water pressure drops from 50 KN/m^2 to 40 KN/m^2. As well as weak silty sand layer, the pressure reduced which indicates in the reduction in yellow part.

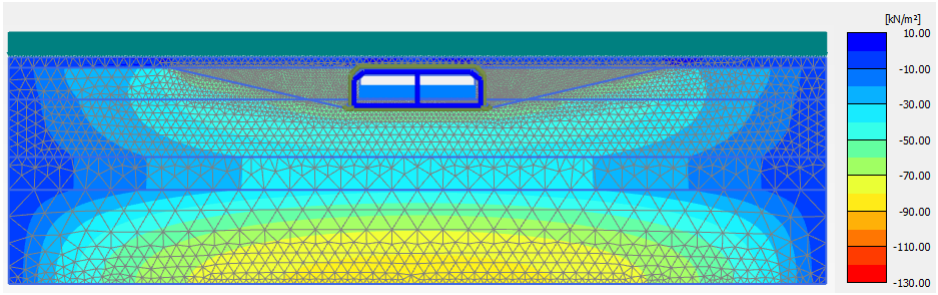

Figure 5.34: Excess pore water pressure in phase 13

Phase 14: consolidation for 50 years
At the last stage, the backfill soil on both sides of the top of the tunnel further settled to 0.35m. The settlement distribution at the bottom part has slight change.

The excess pore water pressure dissipates more

Through the consolidation of more 50 years, total settlement range of sandy clay under tunnel is from 0.12m to 0.25m, the settlement caused by consolidation is 0.043m to 0.16m. The consolidation settlement of bottommost sandy clay is 0m to 0.085m, considerably. Combining with the manual calculation and PLAXIS simulation, the sandy clay layer under tunnel contributes more settlement than bottommost sandy clay, and the consolidation process has not been finished. The deformation change may more like linear due to the unloading reloading under current loads. The bottommost sandy clay is very stiff derived from the data perspective.

The estimation of python expression presents the settlement is 0.104m. Obviously, there is 50% error comparing with results of PLAXIS, hence, it is not proper to predict the next 50 years settlement. One explanation is python estimation is logistic regression model, logarithmic function curve shows the further the

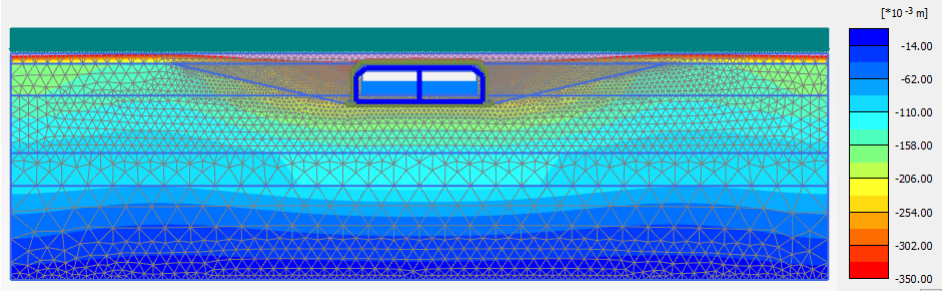

Figure 5.35: Settlement prediction for 50 years

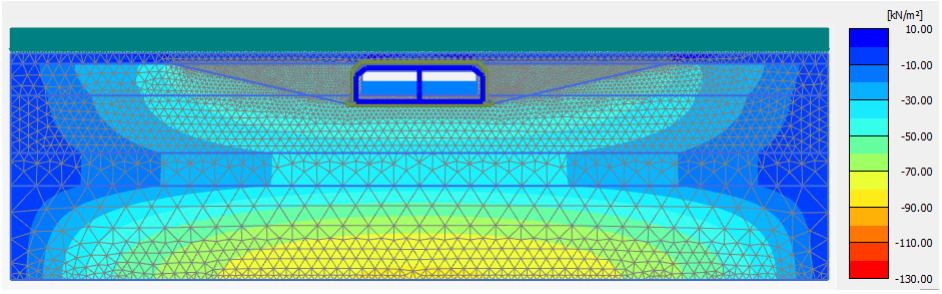

Figure 5.36: Excess pore water pressure in phase 14

calculation, the smaller the difference, if the time span is long. The gap of 0.1m also indirectly confirms that the subsequent consolidation settlement of the soil layer under the tunnel is more likely to be linear relationship between stress and deformation rather than logarithmic relationship, and explained the reason for such a large settlement. In conclusion, the relocation of the levee indeed influence a lot to the subsoil condition.

6

Longitudinal PLAXIS model

In this chapter, the longitudinal direction model will be elaborated. Settlement analysis and prediction will applied from longitudinal direction.

6.1. Model description

The soil model is 1000m long and 60m deep for soil body. Ground surface is at NAP 0 and the middle soil surface is at NAP -8.5m. The top of element 2 and element 1 starts at NAP -5.36m then connect with of element 3 that the top is at NAP -10.4m. From longitudinal profile, the whole tunnel consists of fives parts which are entrance, element 1, element 2, element 3 and exit. The length of per element is 111.5m. Actually, one element contains five sections but it will not be presented in this longitudinal model. Sand flow foundation and backfilled silex are 0.5m thickness, distribute from the leftmost element 2 to rightmost element 1. The ramp of the entrance and exit is 10.89m deep and 252.05m long, the length of connection segment which link entrance and exit to tunnel element is 31m long. The concrete roof is 1.1m thick, and the concrete floor is 1.56m thick, The thickness of asphalt is uneven in the tunnel, it is thicker at the element joint than element inside, as a result, take 0.73m as the average value. The total thickness of the bottom of the tunnel is 2.29m. The soil layer distribution is indicates in chapter 3. In transverse model, to model the interaction between the structural element and soil, an interface is applied. However, in the longitudinal model, using an interface will lead to poor quality meshing, resulting in unstable and failing calculation, therefore, the interface is not taken in longitudinal model. The R_{inter} keeps the same, the value is 0.65 for the soil layers which is next to the tunnel and others remain to 1.

The levees locate on the two sides of the tunnel, the top is at NAP +4.5m. The toe of the levee is at NAP -8.5m. Material of clay is assigned to levee. The material of levee is on table 6.1. In this model, the levee is not the target of simulation, thus, the dike is expected to keep stable and without landslide during the whole numerical simulation period. One method is to increase and other is to increase cohesion to a value large enough.

Type	Material Model	γ [KN/m^3]	e	E [KN/m^2]
Clay	Morh-Coulomb	21	0.5	100×10^3

Table 6.1: Properties of clay

In construction report of Kiltunnel, the levee contains plate. As a result,plate is applied as well. Triangular is a good shape to keep stable, hence, triangular plate structure is assigned under tunnel to prevent the soil slide. Details see figure 6.1. The results in transverse direction can be used to calculate the properties of plate. According to the transverse direction model, the inner force of tunnel tube is around 7000 KN/m^2, and the corresponding deformation is 0.1m, therefore the bending rigidity is available, then plate strength and moment of inertia are available as well. Similarly, the aim of plate is to prevent slide for levee, the properties of it should be stiff enough. The properties of plate is on table 6.2.

In the 3D model, the tunnel can be supported by three-dimensional space easily. However, in the 2D model, longitudinal cross-section is chosen, and the middle of the tunnel is hollow. How to support the tunnel so that the model does not collapse is the first key point in this case. Using simple plate is a solution but it

Type	EA [KN/m]	EI [KN m^2/m]	W [KN/m/m]
Plate	505.7E3	3.045E6	25

Table 6.2: Properties of plate

requires a lot of plates due to the heavy load on top. The special concrete material is applied to support the whole tunnel. For the tunnel structure itself, the concrete properties keep the same with transverse direction. Besides, the other two new concrete types are defined (see table 6.3). Concrete 1 will assign to the tube sections under the river, while concrete 2 will assign to the ramp part of entrance and exit. The stiffness of these two are not the same, because there are levee and river on the top, the load is heavy thus the stiffness is higher.

Type	Model Type	Drainage Type	γ [KN/m^2]	ν	E [KN/m^2]
Concrete 1	Linear Elastic	Undrained	10	0.2	15×10^6
Concrete 2	Linear Elastic	Non-porous	10	0.2	15×10^5

Table 6.3: Properties of new concrete type

Figure 6.1: Longitudinal model profile

The construction phase and the corresponding calculation type are below:
1. Initial phase: K0 procedure
2. Excavate exit and entrance: Plastic
3. Trench dig: Plastic
4. Applied sand flow foundation: Plastic
5. Put element 1 on the foundation: Plastic
6. Put element 3 on the foundation: Plastic
7. Put element 2 on the foundation: Plastic
8. Backfill tunnel: Plastic
9. Consolidation for 9152 days: Consolidation
10: Leakage: Consolidation
11. Consolidation for 6250 days: Consolidation

The water level for the ground soil is assumed to be at NAP 0, but it increased to NAP 0.53m between two sides of levee. The flow condition is defined to be open at the beginning, the ramp and 31m connection segment are changed to be dry when in excavate entrance and exit, 3 elements always keep open. The aim of this definition is to make sure the water can flow from top to bottom, and the excess pore water pressure will be accumulates, which is crucial to consolidation phase. Otherwise, the water flow in levee and that of river are stuck in top part and cannot transport into bottom soil. The clay layer boundaries are closed during consolidation phase and only sand layer boundaries are open.

In addition, the focus of this model is the behaviours of underlying soil, and according to records, the severe settlement points are not located in immersion joint, as a result, the immersion joint will not be presented in longitudinal direction.

6.2. Settlement

6.2.1. Final results

In terms of the monitoring data, longitudinal direction settlement is presented below. Longitudinal settlement trend shows settlement are generally larger at the element 1 and element 2, the middle is the smallest. The difference between middle part and western part or eastern part is very large, the value in the middle is 3.4 times of that in the West and 2.54 times of that in the east. The maximum settlement point for west remains the same with transverse direction, and the value is 72.5mm. Maximum settlement of middle part is 21.4mm which is under element 3c-3d. As for east, settlement has the largest value of 54.4mm and under

element 1A-1B. The same method is used to retrieve the settlement as the transverse model, they should be 0.145m for west, 0.042m for east and 0.108m for middle.

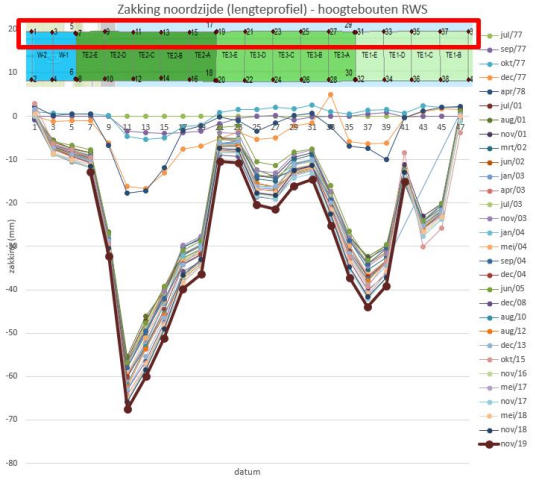

Figure 6.2: North settlement in longitudinal direction

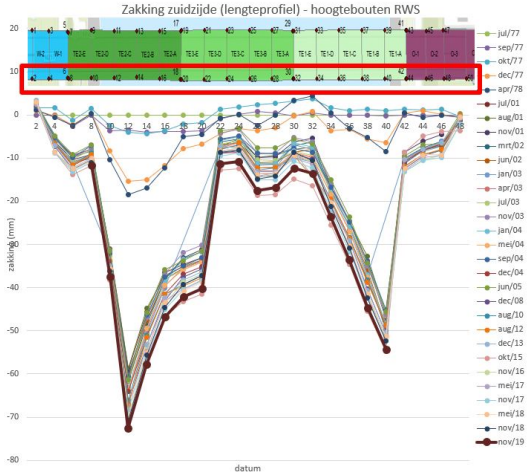

Figure 6.3: South settlement in longitudinal direction

Load is a crucial part in the model. There are two roads on the levee, thus, traffic load will be added to the levee. The load distribution in transverse direction is applied in longitudinal model. Through comparison, the following load sequence is proved to be most realistic.

Phase	Western levee	element 2	element 3	element 1	Eastern levee
Initial Phase	0	125	0	0	0
Excavate exit and entrance	0	0	0	0	0
trench dig	0	0	0	0	0
Applied sand flow foundation	0	0	0	0	0
Put element 1 on the foundation	0	0	0	0	0
Put element 3 on the foundation	0	0	0	0	0
Put element 2 on the foundation	0	0	0	0	0
Backfill tunnel on the foundation	50	125	25	100	50
Consolidation for 9152 days	50	125	25	100	50
Leakage	50	125	25	100	50
Consolidation for 6250 days	50	125	25	100	50

Table 6.4: Load distribution in longitudinal direction

In the model, the reference point on the east side is below the south side of the section joint of element 1A-1B. The reference point of middle is located on north of tunnel and under the element 3c-3d. And reference point of west is still on the south side of tunnel and is underneath element 2c-2d. The curves in figure 6.4 shows the settlement trend of these three reference points. Pink line is for eastern point, the final settlement is 0.103m. Blue line is for western point and the value is 0.145m, orange line represents middle points with final result of 0.027m. The error between east west and middle are 5%, 0% and 35%. The results are close to the actual estimation.

6.2.2. Monitoring Data Analysis

According to the monitoring data, the trend of each reference point are available. There will not display trend of point 12 as it has already been give in chapter 5. Figure 6.5 and 6.6 are the derivation of other two reference points over operation phase. The corresponding approach lines for point 27 and point 40 are:

$$S = -3.173 \times \ln(Time) + 13.213 \tag{6.1}$$

$$S = -10.12 \times \ln(Time) + 45.023 \tag{6.2}$$

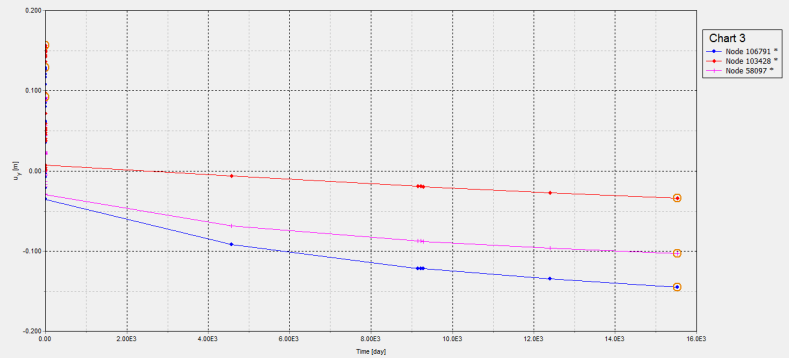

Figure 6.4: Final settlement for longitudinal direction

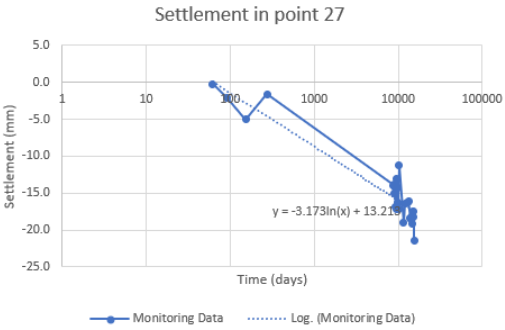

Figure 6.5: Monitored settlement in point 27

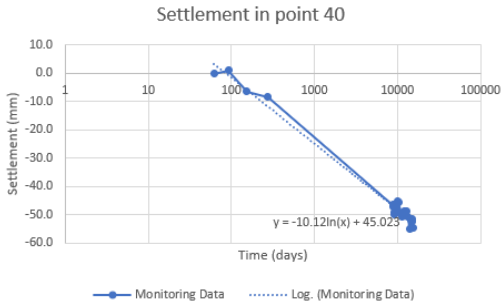

Figure 6.6: Monitored settlement in point 40

The settlement that has already happened in the time gap of 8 months isn't included in the data which is given by the expression. If calculated according to the trend line, the settlements at points 27 and 40 within the eight months after immersion are 3.8mm and 9.23mm, respectively. Using these two constants to calibrate the expressions, they should be:

$$S = -3.173 \times \ln(Time) + 9.413 \tag{6.3}$$

$$S = -10.12 \times \ln(Time) + 35.793 \tag{6.4}$$

Using the same method like transverse model, in order to check the validity of longitudinal model and monitoring data, double the monitoring settlement value, the two sets of data are plotted and compared as well. Figure 6.7 and figure 6.8 are the comparison. It can be seen from the plot that the results of the two points matches very well, espicially for point 40. After 2001, the settlement monitoring values are available. Focusing on this part, it is easy to find that the two curves are close enough on both two points, and the estimated error for point 27 is approximately 30%, as for point 40, the estimated error is almost zero. In conclusion, the validity of longitudinal model simulation is proved.

Not only for the separated point, but also for the whole trends of monitoring data and PLAXIS result are made. Applying experience to back-calculated the monitoring displacement, which means the monitoring data will times 2, the specific results is shown in figure 6.9. In figure, x-axis means the number of each monitoring point, y-axis is the settlement. Due to the data lack in record, it can be seen that there are no settlement in point 2, 4, 42(44), 46 and 48. But on the whole, the overall settlement trend in the two situations is very consistent, that is, the east-west settlement is larger, and the central settlement is smaller. Overall, the difference in settlement is approximately 20%, but there are some unusual values as well, which are due to some limitations of PLAXIS 2D for longitudinal direction simulation, like the flow condition of water from river to bottom. Further study can achieve in PLAXIS 3D if needed.

6.2.3. Phases details

Phase 2 : Excavate exit and entrance

In this phase, concrete 2 will be assigned to ramp. In order not to make levee slide, two sides are assigned simultaneously. The maximum displacement in vertical direction is 0.1599m while the minimum value is

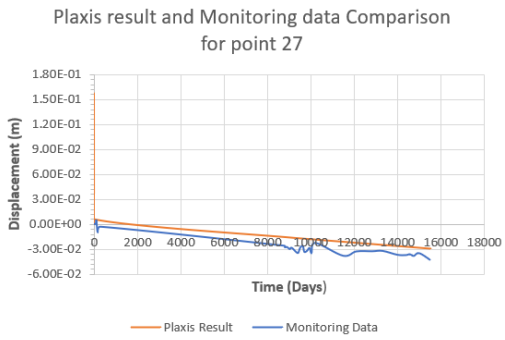

Figure 6.7: Plaxis result and monitoring data comparison of point 27

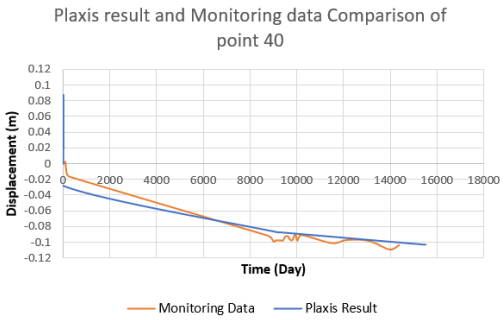

Figure 6.8: Plaxis result and monitoring data comparison of point 40

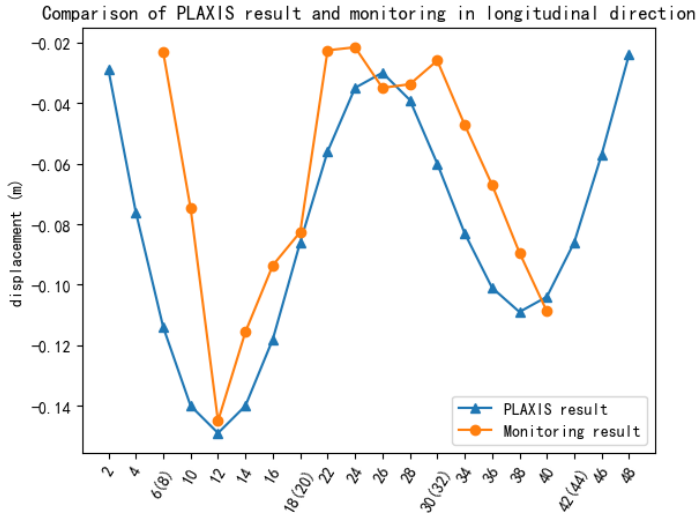

Figure 6.9: Comparison of PLAXIS result and monitoring data in longitudinal direction

-0.1094m. The displacement distribution is on figure 6.10. In this stage, the two sides of the model are symmetrical and the difference between results are small, so half of the model is taken.

The figure displays that the phenomenon of unloading and rebound occurred in the ramp with the maximum displacement of eastern side. The displacement contour is semicircle, and from top to bottom, the rebound amount is reduced, the rebound phenomenon is weakened. When reaching the bottom sandy clay layer, the rebound is about 40mm. At the same time, levee settlement occurred with maximum value of 0.1094m.

The distribution of effective stress in this phase presents 'M' shape. Maximum effective stress is 563.7 KN/m^2 and the minimum value is -985.2 KN/m^2. However, these two extreme value concentrates on the corner which link the entrance and ramp, hence, there is a great possibility that these two values are the results of numerical error. The effective stress in bottom sandy clay is around -500 KN/m^2. The effective stress of soil under eastern and western levee is larger than that of other parts.

Phase 3: Trench dig

In this stage, rebound is more obvious to observe. The maximum displacement is 0.1570m and the range of reboundare across from entrance to exit but most are concentrate on element 3. The displacement of the sandy clay layer which is under tunnel is from 0.15m to 0.09m from top to bottom. The upper part of levee changes from settlement which indicates in the last stage to rebound because of compression, and the rebound value is around 50mm.

In transverse direction model, the reboundamount is 0.39m for the sandy clay which is under tunnel, while the maximum rebound amount in longitudinal direction model is 0.15m for the same position. The

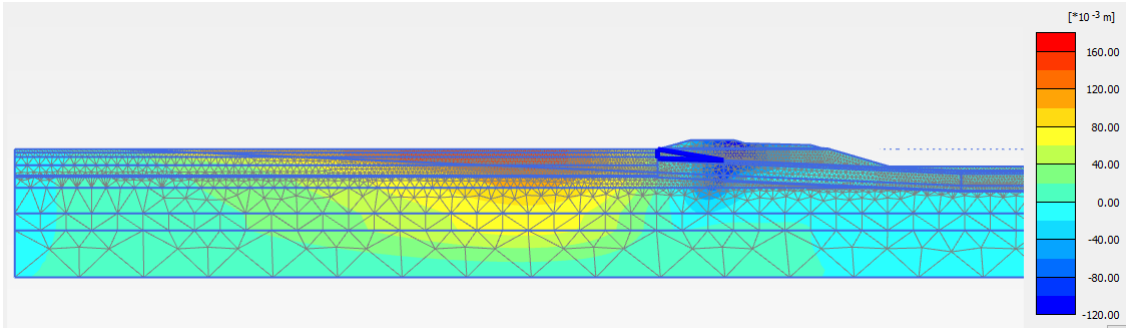

Figure 6.10: Settlement in excavate entrance and exit phase

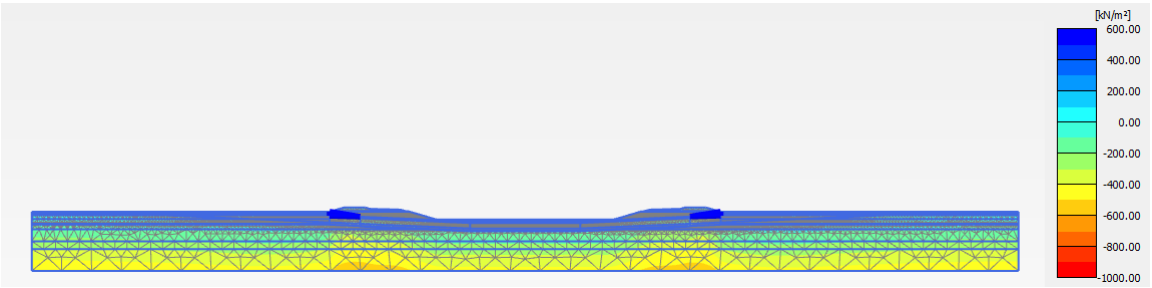

Figure 6.11: Effective stress in excavate entrance and exit

reason to cause this difference is the change of model simulation. In transverse direction, there is nothing above the excavation surface. However, a special concrete type is assigned to support the tunnel space with unit weight of 10 KN/m^2. Besides, clay is on the top of tunnel space which is a type of load as well. Considering both aspects, more load is applied to constrain the rebound.

At this stage, the effective stress distribution is still 'M' shape, the maximum value changes to 636.9 KN/m^2 and the minimum effective stress changes to -1009 KN/m^2. But these two are still raised by numerical error. The value for the bottom sandy clay increased to approximately -600 KN/m^2. Effective stress increased about 100 KN/m^2 when compare with last stage In addition, the effective stress under levee is larger than other parts at the same depth.

Phase 4: Applied sand flow foundation
The displacement range in this stage is from 0.1487m to 0m. After applying sand flow foundation, displacement is reduced from 0.1570m to 0.1487m, reducing rate is around 5.29%. The foundation weight is not heavy, result in little difference. The distribution of displacement is the same with last stage. The levee is in rebound situation, with rebound value is 50mm.

In the output results, the distribution of the whole effective stress has no change from the previous stage. The maximum effective stress is 647.4 KN/m^2 and the minimum is -975.8 KN/m^2. The maximum value and minimum value are still in the corner, and there is a big gap between these extreme value and next range value. Removing the two extreme values, effective stress should be in the range of 0 - (-600) KN/m^2. And the -600 KN/m^2 is on the bottom of the whole model. Comparing to last stage, effective stress is very stable and almost without change.

Phase 5: Put element 1 on the foundation
The displacement range in this stage is from 0.1457m to 0. From the figure below, the rebound phenomenon around element 1 reduced a lot. The maximum value in this part is 0.08m which locates at the element joint between element 1 and element 3. After putting element 1 on the foundation, it is obvious for PLAXIS to indicate the immediate displacement change, then, the maximum displacement is reduced around 2% when comparing with last stage, but the range still keep the same. However, levee has gone from rebound phenomenon to a small settlement, the settlement value is -6.79mm. Because in the previous step, the space required for the tunnel is regarded as a whole, and the concrete material is assigned. Due to the application of the tunnel load, the rebound of the preset tunnel space is weakened, so the upper levee follows the lower soil layer from the previous rebound to the settlement.

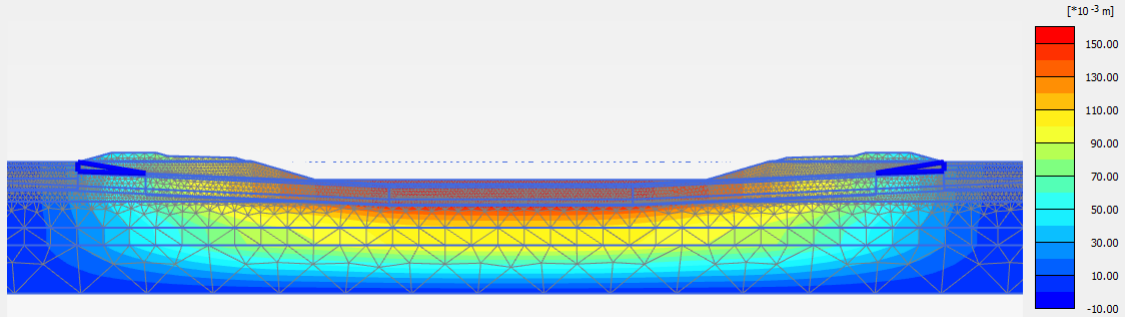

Figure 6.12: Settlement in trench dig phase

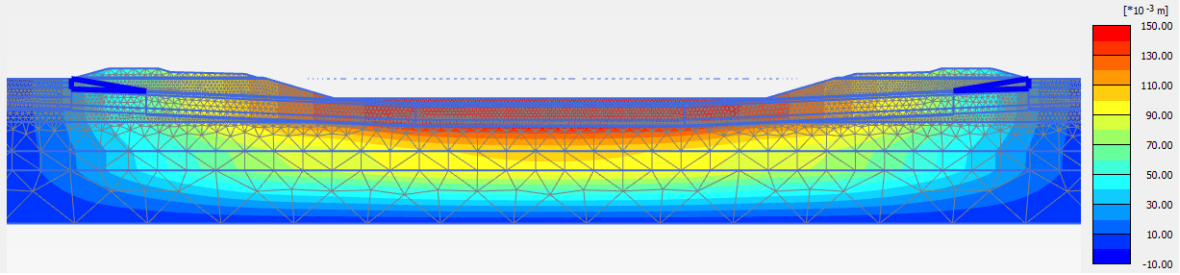

Figure 6.13: Settlement in applied sand flow foundation phase

The effective stress in this stage range from 539.4 KN/m^2 to -976.2 KN/m^2. Getting rid of the two abnormal stresses, the effective stress should be in 0 - (-600) KN/m^2. The effective stress still keeps stable comparing to last two stages although the two extreme values change. The effective stress of the soil under levee is larger than other parts. And the maximum effective stress is in the bottom sandy clay layer under levee.

Phase 6: Put element 3 on the foundation
Depending on the order in which the tunnel is actually placed, the third element should be placed before the second. Compared with phase 5, this phase shows the change of displacement more intuitively. The specific displacement distribution is shown in the figure 6.15. The displacement range changes to 0.1085m - (-0.0063m). The maximum displacement concentrates on element 2, and is still rebound, but the rebound is reduced by 25.5%. The displacement in eastern levee has not changed.

The effective stress range changes to 390.6 KN/m^2 - -951.7 KN/m^2, the shape is like 'M'. While except extreme value, the range of effective stress is quite stable like last phase, the same for the place with largest effective stress.

Phase 7: Put element 2 on the foundation
The last immersion element is element 2. After the immsersion of element 2, the whole tunnel is completed. The range of displacement in this phase is 37.92mm - (-6.63mm). The rebound of sandy clay under the tunnel becomes 37.5mm to 22.5mm. Comparing to 0.15m to 0.09m in trench dig phase, the value reduces a lot.

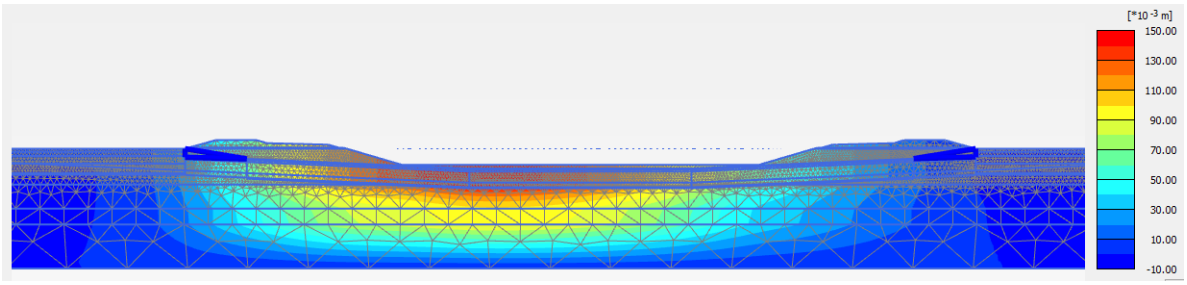

Figure 6.14: Settlement in applied sand flow foundation phase

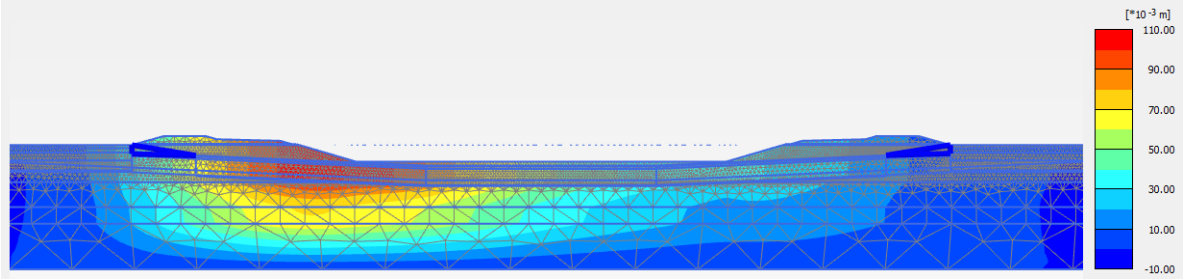

Figure 6.15: Settlement in put element 3 on the foundation

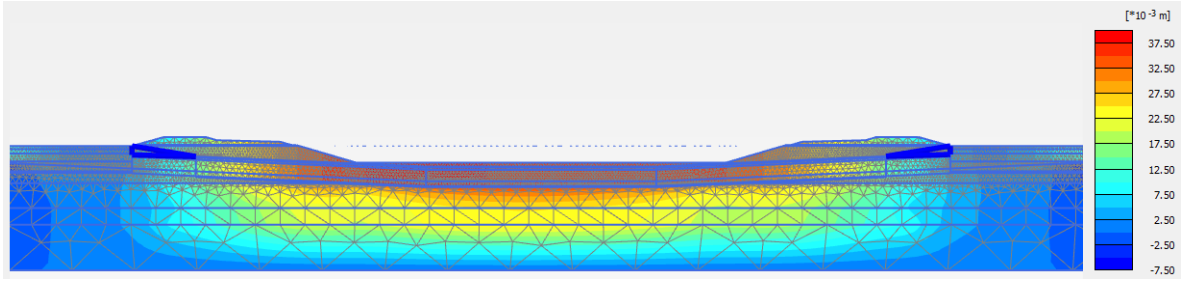

Figure 6.16: Settlement in put element 2 on the foundation

The distribution of effective stress in this phase is 'M' shape.However, the value changes. Specific distribution is shown on figure 6.17. The minimum extreme value disappears, and the normal minimum effective stress is at the bottom sandy clay with -600 KN/m^2. Whereas the maximum value is 417.9 KN/m^2, this is due to numerical error as well, the normal one is at the top of model with effective stress 0 KN/m^2.

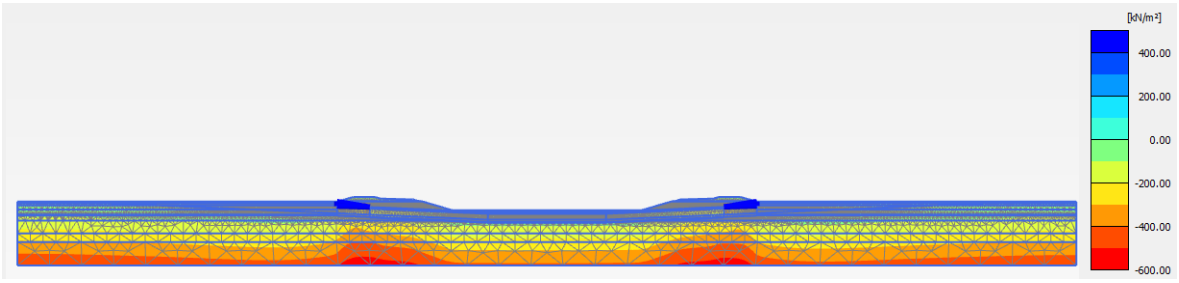

Figure 6.17: Effective stress in put element 2 on the foundation

Phase 8: Backfill tunnel
In this phase, line loads are added, as a result, western and eastern displacement changes to settlement. Except the western and eastern part, the displacement of other parts are rebound. Owing to the calculation type of plastic, and the interval time is 1 day,these two settings limit the settlement caused by load application, making the result value of this phase relatively small. The maximum settlement of western part is -0.04203m whereas the it of eastern part is -0.032m. The rebound of middle part is 0.012m. From the following distribution figure, the displacement of each part is very intuitive. In transverse model, the settlement of sandy clay layer under tunnel in ppoint 14 is 0.049m to 0.08m. And in longitudinal model, the range of it is 0.032m to 0.036m in the same phase. The settlement in longitudinal model is smaller than transverse settlement in the same point, the main reason to cause this difference is that construction method changes.

The distribution of effective stress has no change compared with that of the previous stage, and it still presents the shape of 'm', but the value range of normal effective stress is in 0 KN/m^2 - (-643.2) KN/m^2. The maximum value rises slightly in this phase, but the effective stress is counts to be stable in general.

At this phase, the excess pore water pressure is applied. Figure 6.19 indicates the excess pore water pressure distribution in the whole model, and figure 6.20 indicates the details of excess pore water pressure across the whole tunnel. The maximum excess pore pressure is 294.6 KN/m^2, and spreads on the bottom of element

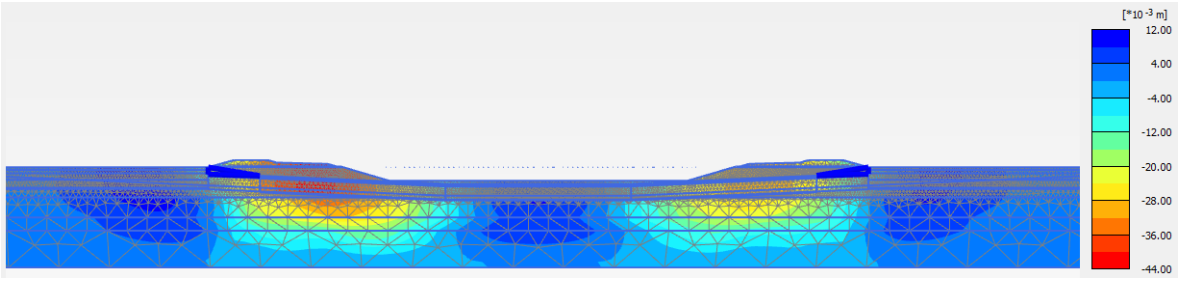

Figure 6.18: Settlement in backfill tunnel

2. For the soil, the minimum excess pore pressure is around -160 KN/m^2 and spreads on the sandy clay layer. In addition, it can be perceived that the excess pore water pressure distribution of two sandy clay layers under the tunnel is continuous.

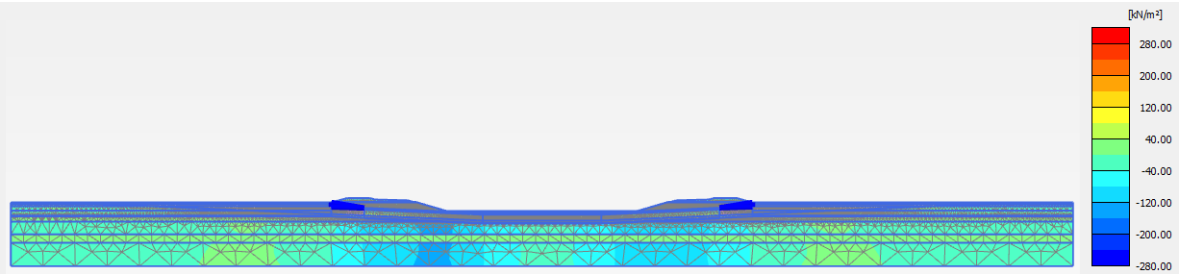

Figure 6.19: Excess pore water pressure in backfill tunnel phase

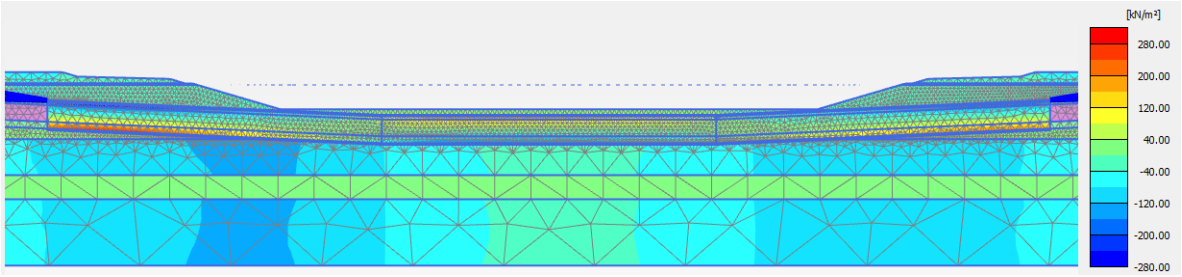

Figure 6.20: Detailed excess pore water pressure in backfill tunnel

Phase 9: Consolidation for 9152 days
Time span in this phase is from 1976 to 2001, which keeps the same with last phase, then the settlement occurs. Figure 6.21 displays the situation of settlement in the model. The maximum settlement of western part is -0.1271m, and the maximum settlement of eastern part is -0.1m, while the maximum settlement in middle part is -0.03m. The soil around ramp has slightly rebound with value of 0.24m. At the same point 12, the settlement in transverse direction is 0.14m, however, it is 0.1271m in longitudinal direction, these is 9% error between these two model, which is acceptable. Calculating the settlement with two estimated expression which mentioned in monitoring data analysis, the results of middle reference point 27 and eastern reference point 40 are -19.53mm and -56.52mm. Obviously, the data is different in PLAXIS model and approach line, errors exceeds half, especially for middle one. But the monitoring data on 2001-08-01 for middle and east are 13.9mm and 46.4mm. Through the comparison of these data, the PLAXIS result of middle point 27 is not correct, it is too small, but it can be calibrate through the load. As for east, if judge it with experience, the 50% settlement will happen in construction time, and 2001-08-01 is in operating time, so estimation settlement under this experience should be 92.8mm, the error between this value and PLAXIS result is 7.2%, which is acceptable. The difference between the approach line and the numerical simulation results may be caused by the distribution of the logarithmic curve. In the logarithmic curve, the larger the number of the horizontal axis, the smaller the change of the vertical axis.

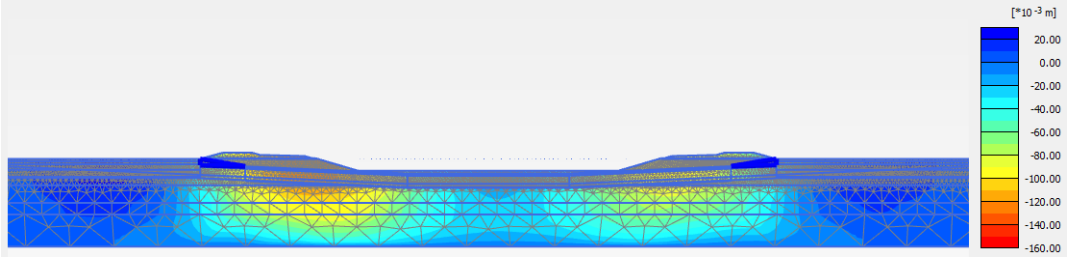

Figure 6.21: Settlement in consolidation for 9152 days

The range of effective stress in this phase is 0 - (-786.3) KN/m^2. The distribution is still like 'M' with the maximum effective stress spreads on bottom sandy clay layer. Except the bottom sandy clay layer, the other parts which has relatively large effective stress are at the bottom of element 1 and element 2.

Figure 6.22 is the excess pore water pressure distribution after 9152 days' consolidation. The positive stress concentrates on the tunnel structure, the maximum value is 595.9 KN/m^2, which is distributed at the bottom of element1 and 2. For the soil, it can be concluded from the figure that the excess pore water pressure is relatively large under element 2, and the value is about 180.55 KN/m^2. This value is almost twice as the excess pore water pressure in transverse model, mainly due to the difference of flow condition settings. In addition, the water dissipation path in the last three soil layer is clearly reflected in the figure. The water in the two sandy clay layers below the tunnel is discharged from the middle fine sand layer, this can be indicated on the different colour.

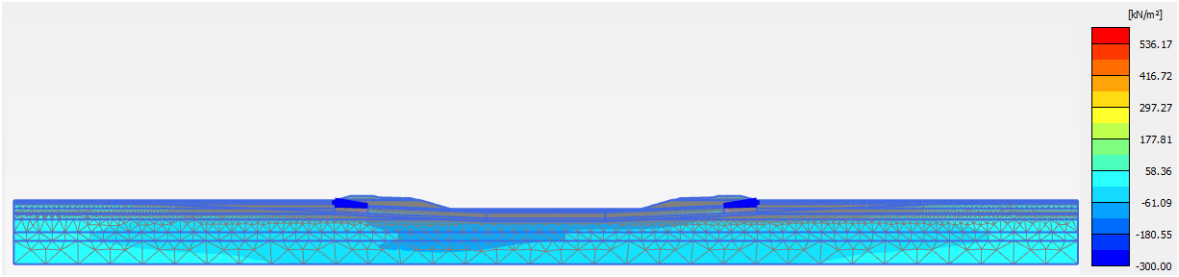

Figure 6.22: Excess pore water pressure in consolidation 1

Phase 10: Leakage

In this phase, the inflow was added to the bottom of element 2 to simulate leakage. The leakage amount and point keep the same with transverse model. After applying inflow, the settlement of western part increased to -0.1274m, with increase rate of 0.24% which shows little influence for inflow to leakage. The rebound occurs in the ramp area, with value of 0.024m, which is the same with last phase. The maximum settlement in eastern part is -0.1m, and the average settlement in middle part is 0.035m. For element 3, the settlement near the west is greater than that near the east. As a whole, the settlement value of this stage has not changed much compared with that of the consolidation 1 phase, and it is generally stable.

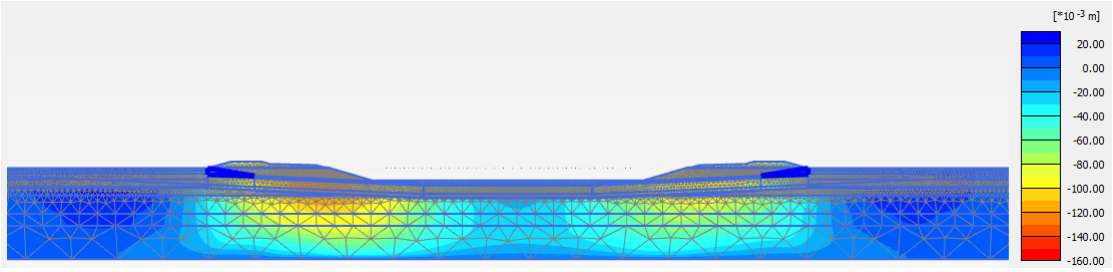

Figure 6.23: Settlement in leakage

For effective stress, there is no difference from the result and distribution of the last phase in general.

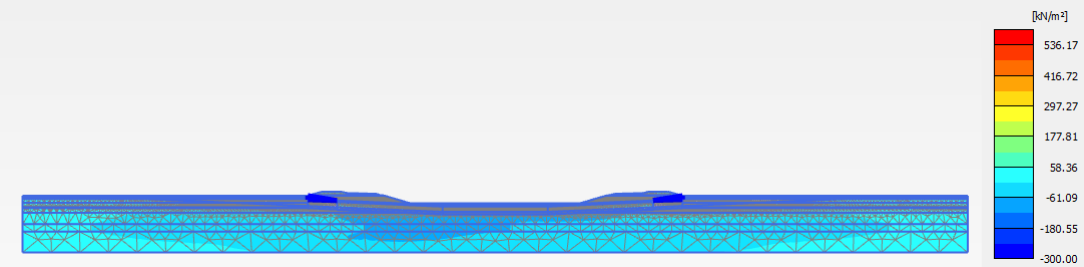

Figure 6.24: Excess pore water pressure in leakage

In this stage, the diffusion of excess pore water pressure in fine sand soil layer is more than that in the previous stage, but in general, the value does not change, only the path is a little diffusion.

Phase 11: Consolidation for 6250 days
After consolidation for 6250 days, the settlement of tunnel west increases to -0.1502m, and the tunnel east is -0.103m, and settlement of the tunnel middle is -0.027m. The settlement in transverse model is 0.15m, the error between these two model is almost 0, which proves the effectiveness of the model and its result. On the whole, the settlement in the west is the largest, followed by that in the East, and the settlement in the middle of the tunnel is the smallest. The trend of monitoring data is very consistent. The settlement values in the middle and the east obtained by the model are 0% and 5% different from those predicted by the monitoring data. Using approach line to estimate settlement, the value for point 27 and point 40 are 21.21mm and 61.9mm, and real monitoring data on 2019-11-15 are 21.4mm and 54.4mm. Despite the adjustments made to the previous approach line, the difference between the calculated value at this stage and the actual monitored value is not large, so it seems that the result of the approach line is still too conservative, and is not very consistent with the empirical trend derived the actual situation, therefore, the results of numerical simulation are more inclined.

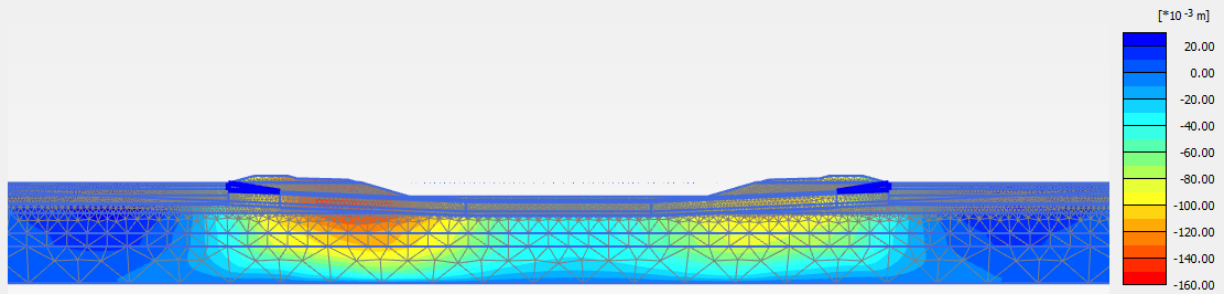

Figure 6.25: Settlement in consolidation for 6250 days

The effective stress range is still 0 - (-700) KN/m^2, which is quite stable from phase 9, and equally for the specific distribution. As for excess pore water pressure, compared with the diffusion of the excess pore water pressure in the last phase, the excess pore water pressure in the bottom sandy clay layer dissipated a lot, while the excess pore water pressure in the sandy clay layer under the tunnel dissipated more at the boundary with the lower layer of fine sand, and the water is drained by fine sand, but the excess pore water pressure near the interface of the tunnel is still large, about - 60 KN/m^2, which means it still needs time to be drained.

If the data of the west reference point is extracted and compared with the transverse model, the result is shown in the curve below. Node 106791 is the node of Longitudinal model and the node 57757 is the node of transverse model. Two trend are close, the difference between these two is around 20mm, the error of it is approximately 14%, which proves the effectiveness of the two models.

6.3. Prediction

For predicting the future trend, five steps are added to calculate, the phase details are:
- Consolidation for next 10 years: consolidation calculation type, 3650 days
- Consolidation for next 20 years: consolidation calculation type, 3650 days

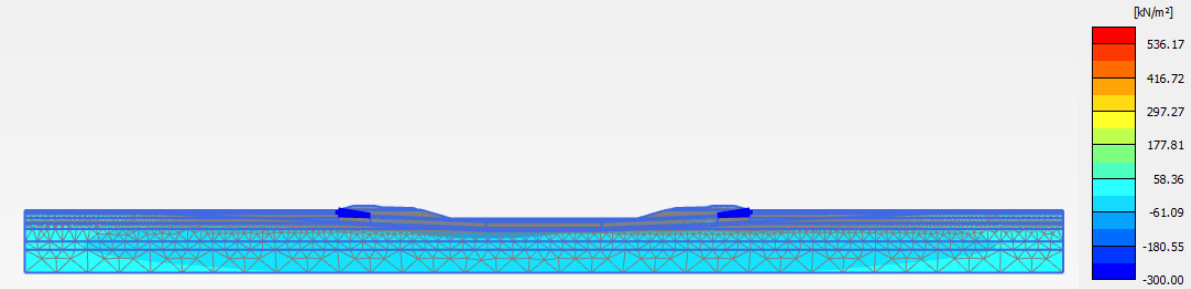

Figure 6.26: Excess pore water pressure in consolidation for 6250 days

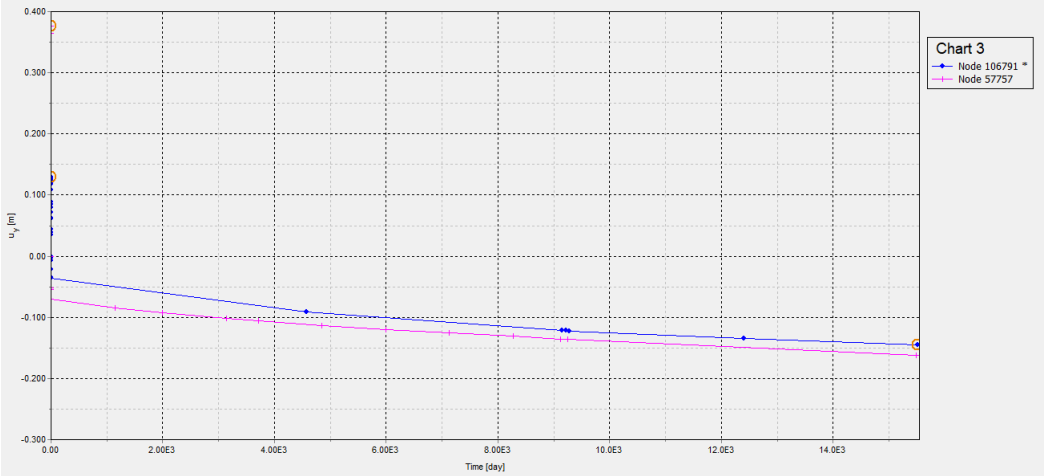

Figure 6.27: Settlement comparison between longitudinal direction and transverse direction in point 12

- Consolidation for next 30 years: consolidation calculation type, 3650 days
- Consolidation for next 40 years: consolidation calculation type, 3650 days
- Consolidation for next 50 years: consolidation calculation type, 3650 days

Table 6.5 shows the settlement set of three reference points in the west, middle and east of the tunnel in the next 50 years, and table 6.6 is the settlement increase rate every ten years. The cloud image of the tunnel distribution in the previous stage has not changed, but the settlement value is increasing, and the rebound value of ramp is kept at 0.03m. For the same reference point in the west, the settlement of the longitudinal model is smaller than that of the transverse model. According to the table 6.6, the average settlement rate of west is 4.29%, and that of middle and east are 12.58% (except the extreme value) and 4.32%. As a result, the settlement rate of the middle part is the largest, but the settlement value of the middle part itself is not very large, so the risk of tunnel damage due to uneven settlement is relatively small. The settlement in the west is similar to the average settlement rate in the east, but because the concrete around the reference point in the West has been damaged, resulting in settlement, according to the predicted settlement rate, this failure point still needs to be paid attention to, and it is necessary to prevent cracking due to uneven settlement again after repair. The largest settlement point in the east also needs to be monitored to prevent cracking although it is safe now.

settlement \ time / point	10 years	20 years	30 years	40 years	50 years
Node 106791(West)	-0.155	-0.164	-0.172	-0.175	-0.185
Node 58097(Middle)	-0.043	-0.05	-0.057	-0.063	-0.069
Node 103428(East)	-0.11	-0.116	-0.121	-0.125	-0.127

Table 6.5: Settlement in different time at different point.

Figure 6.28 is the settlement prediction curves for these 3 points. It can be seen from the figure that in

settlement rate / time / point	10 years	20 years	30 years	40 years	50 years
Node 106791(West)	3.33%	5.81%	4.88%	1.74%	5.7%
Node 58097(Middle)	59.26%	16.28%	14%	10.53%	9.52%
Node 103428(East)	6.80%	5.45%	4.31%	3.31%	1.75%

Table 6.6: Settlement increase rate in reference point

the initial stage of settlement, the settlement is relatively large, showing a logarithmic distribution, but the further back, the settlement tends to be more linear. This is consistent with the conjecture of the impact of the unloading and reloading in the previous chapter.

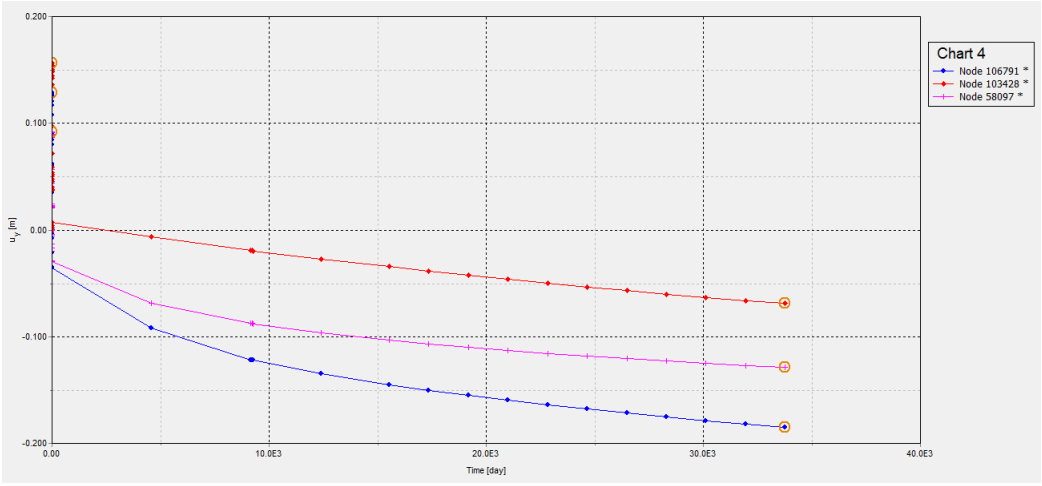

Figure 6.28: Future trend for next 50 years in longitudinal direction

Figure 6.29 is the curve comparison between two models, transverse model result is indicated by sky blue, longitudinal model is in navy blue, and it is pretty obvious that the overall trend is similar except the initial value of the transverse model is 0.07m but the longitudinal model is 0.036m at the beginning. There may be two reasons for this, on the one hand, the loading method is different, on the other hand, the setting of the excavation method is different. Afterwards, the trends of the two models are consistent and the values are similar. Table 6.7 is the settlement comparison and error between transverse model and longitudinal model in the point 12. It can be obtained from the table that the average error is around 11%, which shows the validity of the data between the two models, and matches the actual monitored data as well.

settlement rate / time / point	10 years	20 years	30 years	40 years	50 years
Node 106791(West)	-0.155	-0.164	-0.172	-0.175	-0.185
Node 57757(West)	-0.176	-0.188	-0.188	-0.2	-0.211
Error	11.93%	12.77%	8.51%	12.5%	12.32%

Table 6.7: Settlement increase rate in reference point

6.4. Longitudinal structure analysis

When loading immersed tunnels vertically, there is mainly the chance of failure of immersion joints between tunnel elements and / or of the failure of expansion joints between two connecting tunnel sections. Failure then occurs if watertightness is not guaranteed. The reason for this is the difference in settlement undergone by the tunnel elements and the tunnel sections. From the results presented above, the differential settlement is obvious in longitudinal direction.

In construction phase, in order to be able to absorb differential displacement, dowels are placed in the

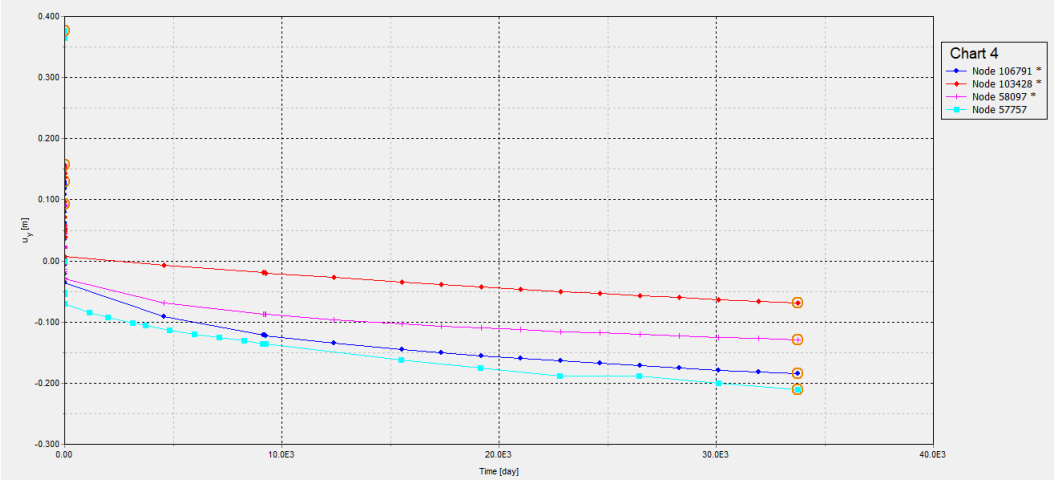

Figure 6.29: Comparison between transverse model and longitudinal model

expansion joints in the immersed tunnels that transmit vertical transverse force. These dowels form a collar construction over the entire cross-section of the tunnel. The watertightness of the tunnel is realized by means of rubber joint profiles; steel-rubber joint strips, so-called W9U or W9Ui profile (old names W9A, W9B and W9C, depending on the dimensions), are applied over the entire circumference of segment joints, which is poured into the concrete. Figure 6.30 indicates the specific profile(Benhaddou, 2013).

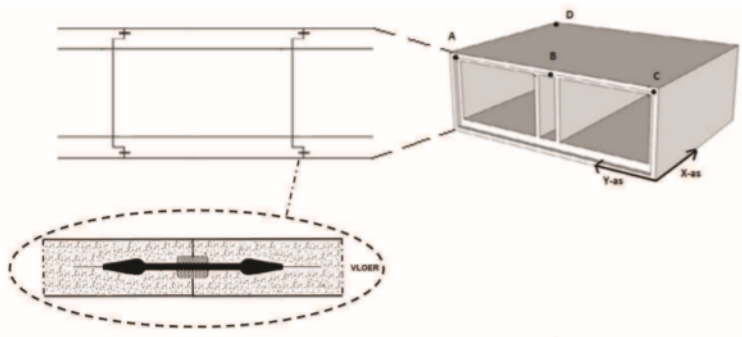

Figure 6.30: Tunnel section profile

According to the result in PLAXIS, the structural damage mechanism was deducted as below. Differential displacement in a vertical direction can occur both within a section and between two consecutive sections. If two points within a segment (for example point A and point C in figure 6.30) move differently, this results in a rotation of the segment. If three points within a segment (point A, B and C) move differently, bending or torsion of the segment occurs. However, this situation did not occur in Kiltunnel in terms of the monitoring settlement in north and south direction. If two adjacent sections show a differential displacement, this results in a deformation that is pretty harmful. The resulting force is absorbed by the collar construction in the roof or floor, depending on the direction of displacement. As long as the collar construction does not collapse, the sealing profile does not experience vertical shearing as a result. See figure 6.31.

Two consecutive sections can rotate about the X axis that are not equal to each other. This results in a rotation of the segment joint about the X axis and creates a compression and a tensile zone in the joint. However, the tensile zone is fictional since the section joint (with collar construction and sealing profile) is unable to transmit tensile forces,resulting in additional compression in the roof of the collar construction (see figure 6.31). In Kiltunnel, at point 12, the damage mechanism to the leakage is largely consistent with this explanation. Excessive differential settlement makes the floor of the tunnel partially cracked. And the concrete has a stronger compressive capacity, hence the roof area did not show cracking. Similarly, expansion joint 1A-1B is still under risk of cracking like 2C-2D according to longitudinal result profile.

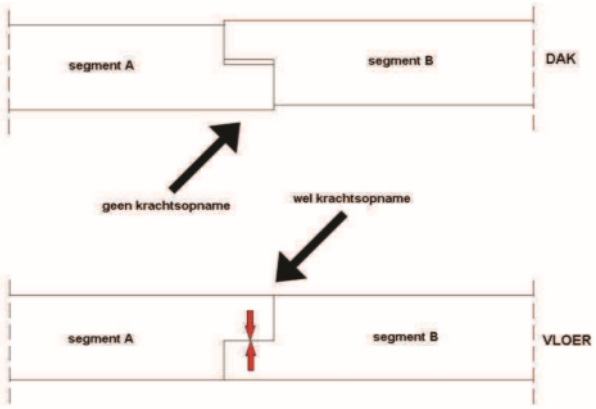

Figure 6.31: Expansion joint force mechanism(Benhaddou, 2013)

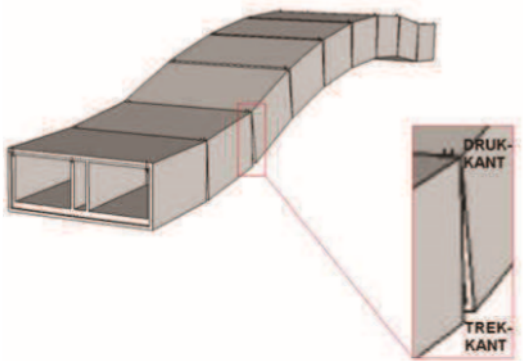

Figure 6.32: Sketch rotation of tunnel sections(Benhaddou, 2013)

7

Conclusion and Recommendation

7.1. Conclusions

The conclusions that drawn from the result of this project can be discussed in three sections: the conclusion for the soil profile, the conclusion for the transverse cross-section with the most serious settlement and the conclusion for the longitudinal cross-section.

The conclusions for the soil profile are:

1. The most common two ways to interpret soil properties are Table 2b from NEN9997 and Roberson's method. But Robertson's method requires more available information, the two methods can be combined when the known parameters are missing. The results are conservative and when they are input to model. The obtained parameters are more conservative and can be used as the initial reference level, and then can be adjusted in the model until the most suitable state.

2. Pre-overburden Pressure have to be derived for each soil layer when input the parameters in model, if the maximum stress state is different with current stress state, especially in the deep soil layers. The impact of POP on the settlements results is large, especially since the levees were relocated during the tunnel construction period.

3. The type of soil layer that appears most under the tunnel is sandy clay. But the properties of the soil corresponding to sandy clay at different depths are completely different. According to the calculated results, the deeper the sandy clay, the stiffer it is, which means that the contribution on the consolidation settlement is less, although it belongs to soft soil.

The conclusions of the transverse model are:

1. The monitoring data was interrupted between 1978 and 2001. In order to figure out the settlement of the tunnel during this period, two methods are used simultaneously, excel was used to estimate the trend line through the scatter plot while the Python regression analysis model was used to do linearly regression and logaritmic regression with the monitoring data, the related expressions are obtained. The results show that the settlements calculated by the two methods between 1978 and 2001 are very close, which proves the validity of python logaritmic model. However, since the starting point of the monitoring data is not after the immersion, but eight months gap after immersion, which means it has caused a part of the settlement before monitoring. The experience in the literature sums up that 50% of the settlement usually occurs during the construction period of the tunnel, thus the actual settlement value of the kiltunnel may be twice the monitoring data. Next, compare the result of the expression obtained by python with the result of numerical simulation and find that the previous python expression multiplied by two is very consistent with the result of PLAXIS. On the one hand, it proves the empirical conclusion, on the other hand, it obtains the credible actual settlement of the tunnel as well.

2. The most serious settlement of the tunnel obtained currently which corresponds to monitoring point 12, has a total settlement value of 0.162m. For the tunnel settlement, the difference between north and south in this cross-section is not large, but the settlement difference between the other two adjacent expansion joints and point 12 is very large, the difference in point 10 and point 12 and that in point 12 and point 14 are 36.1mm and 12.5mm separately. As so for the tunnel structure itself, at point 12, the external concrete wall is under tremendous tension and the internal concrete wall is under compression, which eventually leads to cracking at point 12 then cause leakage.

3. There are two main reasons for the large settlement at point 12. The most important reason is that the relocation of the western and eastern levee caused a process of loading, unloading and reloading to the soil layers before the construction of the tunnel, which affected the characteristics of the soil layers. And the weight of the levee is the historical maximum weight, the subsequent loads are less than this value, making the settlement change of the soil linear. The secondary reason is that the pancake under the tunnel is relatively loose, and the scour of the undercurrent causes the sand to be washed away, and the soft sandy clay may be mixed into the pancake and cause more settlement.

4. Prediction of the settlement at point 12, the settlement value will reach about 0.2m in 50 years. Calculating the settlement rate every ten years found that the settlement rate remained at a relatively stable value and was not too large, indicating that the settlement of the Kiltunnel has been relatively stable, and from the settlement rate it can be seen that the settlement tends to change linearly.

The conclusions of longitudinal model are:

1. The most serious settlement points indicated by the monitoring data are taken as reference points for the western and eastern sides and the middle part respectively, and the settlement values are 0.145m, 0.027m and 0.108m, respectively. The difference between the settlement value obtained by the longitudinal tunnel and the settlement value obtained by the transverse model at the same time point is about 10%. However, in the initial settlement after the completion of the construction, PLAXIS obtained the settlement value in the middle part of the tunnel is not accurate, which is related to the loading method and can be adjusted by the load.

2. In the settlement prediction, the settlement prediction values of the eastern and western and central regions in the next 50 years are 0.185m, 0.127m and 0.069m, respectively. The difference between the western subsidence prediction and the lateral model prediction is about 7%. As far as the settlement rate is concerned, the settlement rate in the center is greater than that in the east,

7.2. Recommendations

For some problems found in the simulation process of the whole project, some suggestions are summarized as follows:

1. Performing CPT measurements for understanding actual soil condition, which will include cone resistance, friction ratio and pore water pressure, this is beneficial for evaluation of consolidation condition. And make sure it as close to the tunnel as possible because it can provide more accurate information and the backfilled soil may be involved into.

2. There are some limitations for PLAXIS 2D in longitudinal direction, cause the flow condition can not be presented precisely. PLAXIS 3D will solve this problem well, as a result, PLAXIS 3D could be another option for longitudinal simulation.

3. Injection of polyurethane can be used to refill any voids in the sand below and next to the tunnel, densify the sand, and thereby reduce the settlement rate. This is may help in reducing future damage near monitoring point 12. Besides, some measurements can be took to repair the pancake below and reduce the settlement rate.

4. From the longitudinal model, in addition to 2c-2d cracking due to excessive uneven settlement, 1a-1b is also likely to be cracked due to uneven settlement. The numerical simulation results show that this point is between the left and right adjacent points The settlement difference is about 10mm and 30mm respectively. Such uneven settlement is also likely to cause damage to the tunnel, which requires close monitoring.

Bibliography

ZHENG Aiyuan, TAN Zhongsheng, and LI Zhiguo. Simulation experiment of pumped sand on immersed tunnel. *Engineering Sciences*, 11(7):81–85, 2009.

N Benhaddou. Invloed van getijdewerking op de stabiliteit van de vlaketunnel. 2013.

Bentely. *LAXIS CONNECT Edition V20 / Material Models Manual*. 2019.

Ronald Brinkgreve. *Behaviour of soils and rocks Lecture Notes*, chapter 10. 2018a.

Ronald Brinkgreve. *Behaviour of soils and rocks Lecture Notes*, chapter 16. 2018b.

Shaozhang Chen, Xiaosi Ren, and Yue Chen. Foundation treatment technology of pearl river immersed tunnel. *World tunnel*, 6:34–39, 1996.

Cui, Yu-Jun, Nguyen Xuan-Phu, Tang, Anh Minh, and Li Xiang-Ling. An insight into the unloading/reloading loops on the compression curve of natural stiff clays. *Applied clay science*, 83:343–348, 2013.

Baiyong Fu and Yan Jiang. Discussion on the main steps and precautions of the settlement analysis of immersed tunnel by plaxis2d.

Wei Gang, Qiu Hui Jie, and Wei Xinjiang. *Analysis of Settlement Reasons and Mechanism in Immersed Tunnel*, volume 238, pages 803–807. 2012.

Grantz and Walter C. Immersed tunnel settlements. part 1: nature of settlements. *Tunnelling and Underground Space Technology*, 16(3):195–201, 2001.

Farzad Habibbeygi and Hamid Nikraz. The effect of unloading and reloading on the compression behaviour of reconstituted clays. *International Journal of GEOMATE*, 15(51):53–59, 2018.

John Harris, Richard Whitehouse, and Sarah Moxon. *Scour and Erosion: Proceedings of the 8th International Conference on Scour and Erosion (Oxford, UK, 12-15 September 2016)*. CRC Press, 2016.

Dym Clive L, Shames Irving Herman, et al. *Solid mechanics*. Springer, 1973.

Yanfeng Liu. Research and analysis on key technologies of immersed tube tunnel project. 2017.

Junjiang Shao and Yongsheng Li. Settlement analysis of immersed tunnel. *Transport Technology of Zhe Jiang Province*, (2):41–43, 2005.

Ying Tang, Minxing Guan, and Xiaoyan Wan. *Theoretical analysis and research of immersed tunnel joint*. PhD thesis, 2002.

Bob van Amsterdam. Probabilistic analysis of immersed tunnel settlement using cpt and masw. 2019.

Gang Wei, Xinguang Zhu, and Qinwei Su. Calculation method and distribution study of vertical uneven settlement of immersed tunnel. *Modern tunnel technology*, 50(6):58–65, 2013.

Gang Wei, Huijie Qiu, Zhi Ding, Xinjiang Wei, Jianjian Xin, et al. Settlement measurement and calculation analysis caused by construction of subsea immersed tube tunnel. *Modern Tunnelling Technology*, (2014-05):121–128, 2014.

XY Xie, P Wang, YS Li, JH Niu, and H Tan. Monitoring data and finite element analysis of long term settlement of yongjiang immersed tunnel. *Rock Soil Mech*, 35(8):2314–2324, 2014.